

AWARD NUMBER: W81XWH-13-1-0489

TITLE: Combination Therapies for the Mitigation of Musculoskeletal Pathologic Damage in a Novel Model of Severe Injury and Disuse

PRINCIPAL INVESTIGATOR: Charles E. Wade, PhD

CONTRACTING ORGANIZATION: The University of Texas Health Science Center- Houston
Houston, TX 77030

REPORT DATE: December 2018

TYPE OF REPORT: Final

PREPARED FOR: U.S. Army Medical Research and Materiel Command Fort Detrick,
Maryland 21702-5012

DISTRIBUTION STATEMENT: Approved for Public Release; Distribution Unlimited

The views, opinions and/or findings contained in this report are those of the author(s) and should not be construed as an official Department of the Army position, policy or decision unless so designated by other documentation.

REPORT DOCUMENTATION PAGE

Form Approved
OMB No. 0704-0188

Public reporting burden for this collection of information is estimated to average 1 hour per response, including the time for reviewing instructions, searching existing data sources, gathering and maintaining the data needed, and completing and reviewing this collection of information. Send comments regarding this burden estimate or any other aspect of this collection of information, including suggestions for reducing this burden to Department of Defense, Washington Headquarters Services, Directorate for Information Operations and Reports (0704-0188), 1215 Jefferson Davis Highway, Suite 1204, Arlington, VA 22202-4302. Respondents should be aware that notwithstanding any other provision of law, no person shall be subject to any penalty for failing to comply with a collection of information if it does not display a currently valid OMB control number. **PLEASE DO NOT RETURN YOUR FORM TO THE ABOVE ADDRESS.**

1. REPORT DATE December 2018			2. REPORT TYPE Final		3. DATES COVERED 30 Sept 2013-29 Sept 2018	
4. TITLE AND SUBTITLE Combination Therapies for the Mitigation of Musculoskeletal Pathologic Damage in a Novel Model of Severe Injury and Disuse					5a. CONTRACT NUMBER	
					5b. GRANT NUMBER W81XWH-13-1-0489	
					5c. PROGRAM ELEMENT NUMBER	
6. AUTHOR(S) Charles E. Wade, PhD E-Mail: Charles.e.Wade@uth.tmc.edu					5d. PROJECT NUMBER	
					5e. TASK NUMBER	
					5f. WORK UNIT NUMBER	
7. PERFORMING ORGANIZATION NAME(S) AND ADDRESS(ES) University of Texas Health Science Center-Houston 6431 Fannin St, MSB 5.204 Houston, TX 77030					8. PERFORMING ORGANIZATION REPORT NUMBER	
9. SPONSORING / MONITORING AGENCY NAME(S) AND ADDRESS(ES) U.S. Army Medical Research and Materiel Command Fort Detrick, Maryland 21702-5012					10. SPONSOR/MONITOR'S ACRONYM(S)	
					11. SPONSOR/MONITOR'S REPORT NUMBER(S)	
12. DISTRIBUTION / AVAILABILITY STATEMENT Approved for Public Release; Distribution Unlimited						
13. SUPPLEMENTARY NOTES						
14. ABSTRACT Severe injury in patients results in adverse physiologic and musculoskeletal changes that are immediate and long lasting. In response to injury, metabolic and physiologic responses determine length of hospitalization and subsequent activity limitations. Reduced mobility from bed rest and injury severity affect muscle and bone health and are detrimental to rehabilitative success. Therefore, means to counteract adverse effects on muscle and bone after injury and disuse are needed. Pharmacologic (i.e. insulin or oxandrolone), nonpharmacologic (i.e. exercise) and nutritional interventions have been used independently with limited success [17]. The combination of pharmacological interventions and exercise has not been systematically investigated. We propose to determine if the administration of pharmacologic agents combined with exercise attenuates muscle atrophy and bone degradation following severe injury, disuse and re-ambulation. The current proposal is for mitigation of musculoskeletal pathologic change in polytrauma patients.						
15. SUBJECT TERMS						
16. SECURITY CLASSIFICATION OF:				17. LIMITATION OF ABSTRACT	18. NUMBER OF PAGES	19a. NAME OF RESPONSIBLE PERSON USAMRMC
a. REPORT Unclassified	b. ABSTRACT Unclassified	c. THIS PAGE Unclassified	19b. TELEPHONE NUMBER (include area code)			

Table of Contents

	<u>Page</u>
1. Introduction.....	4
2. Keywords.....	4
3. Overall Project Summary.....	4
4. Key Research Accomplishments.....	20
5. Conclusion.....	22
6. Publications, Abstracts, Manuscripts.....	23
7. Inventions, Patents, Licenses.....	26
8. Reportable Outcomes.....	26
9. Other Achievements.....	26
10. References	27
11. Appendices.....	28

1. INTRODUCTION

Background: Severe injury results in physiologic and musculoskeletal changes to the patient that are immediate and long lasting. Reduced mobility from bed rest and injury severity affect muscle and bone health and are detrimental to rehabilitative success. We propose to determine if the combination of exercise and the use of insulin or oxandrolone will further improve muscle and bone strength and subsequent function for improved quality of life. The specific aims of this study are to: 1) Characterize the effect of resistance exercise on muscle and bone health in a validated model of burn and disuse. 2) Evaluate the effect of resistance exercise in combination with currently used pharmacological therapies (insulin or oxandrolone) on muscle and bone health in a validated model of burn and disuse. 3) Determine the interrelationship between muscle and bone after re-ambulation following pharmacological interventions and exercise. To accomplish these aims we will use our established rat model of burn and disuse for a 14 day period. Rats will be assigned to vehicle or drug treatment and will be further randomized into either exercise or no exercise groups. After 14 days, additional studies will examine the effects of re-ambulation. Analysis will be completed on blood, tissues, and bones of the study animals. This proposed project will delineate the synergistic effects of current therapy that will be directly translational to the clinical care of military polytrauma victims.

2. KEYWORDS

- Rats
- Burn
- Hindlimb Unloading
- Exercise
- Disuse
- Insulin
- Oxandrolone

3. OVERALL PROJECT SUMMARY

Specific Aim 1 was to characterize the effect of resistance exercise on muscle and bone health in a validated model of burn and disuse. The milestones for Year 1 of the project, included beginning and completing experiments for Aim 1, including animal, assay work and data analysis. There were eight major tasks associated with this milestone.

Specific Aim 2 was to evaluate the effect of resistance exercise in combination with currently used pharmacological therapies (insulin or oxandrolone) on muscle and bone health in a validated model of burn and disuse. The milestone for Year 2 of the project was to begin and complete experiments for Aim 2, including animal assay work and data analysis. There were six major tasks associated with this milestone.

Specific Aim 3 was to evaluate the effect of resistance exercise in combination with currently used pharmacological therapies (insulin) on muscle and bone health in a validated model of burn and disuse and then continuing with re-ambulation. The milestone for

Year 3 of the project was to begin and complete experiments for Aim 3, however, due to unforeseen circumstances and delays in getting IACUC renewal in place, a no-cost extension was requested and granted to be able to complete AIM 3 in FY17. Aim 3 experiments were completed in Year 4.

Results (Wade):

Specific Aim 1:

All local Institutional Animal Care and Use Committee and USAMRMC ACURO approvals were obtained prior to initiation of the study (**YEAR 1, TASK 1**). Male, Sprague-Dawley rats were randomized into four groups: Sham Ambulatory (SA), Burn Ambulatory (BA), Sham/Hindlimb unloaded (SH) and Burn/Hindlimb unloaded (BH), with daily resistance exercise (EX) or no exercise (NEX) (N=6/group). Rats were introduced to resistance exercise by adding weight to each tail during repetitive ladder climbing ten days prior to injury. Rats were then weight-matched into treatment groups, either daily exercise or no-exercise. Daily resistance exercise was completed on a 1m ladder at 85° incline. Each rat completed 5 climbs 2x/day. At the conclusion of the experimental period, samples were collected for further analysis (**YEAR 1, TASKS 2-6**). Statistical analysis using ANOVA with significance at p<0.05 was used.

Body mass during Aim 1 showed a similar response as seen during our previous work (Wade et al, 2013). There were no differences in initial body mass between treatment groups, however, differences were apparent by day 14 (**TABLE 1**).

BA and SH showed similar reductions in body mass, and BH had the most dramatic decrease over time, accentuated by an additive effect when burn and disuse were combined. At day 14, NEX-SA and NEX-BA body mass were significantly greater than EX-SA and EX-BA, but there were no differences in SH or BH. BH rats were significantly smaller than other treatment groups. Compared to other treatment groups, there was a significant increase in average kcals consumed over the last 5 days in BH, irrespective of exercise. No other differences in food intake between NEX and EX within each treatment group were observed. Percent body mass decrease over time was the greatest in BH rats at day 14 (p<0.001). There was an exercise effect in body mass in all treatment groups (**FIGURE 1**). No differences in body mass were observed between any groups at the time of injury. Fat mass was significantly reduced in the disuse groups, with an additive effect of burn with disuse (p<0.001).

	SA	BA	SH	BH
D14 Body Mass (g)				
NEX	336±7	307±7	305±6	282±4 [¥]
EX	319±6*	287±5*	294±7	278±4 [¥]
Caloric Intake (kcal/100g BM/day)				
NEX	20.5±0.8	21.3±0.4	21.7±0.6	22.1±0.9 [¥]
EX	19.7±0.4	21.0±0.6	20.2±0.5	23.0±0.9 [¥]

*p<0.05 from NEX; ¥ p<0.05 from SA

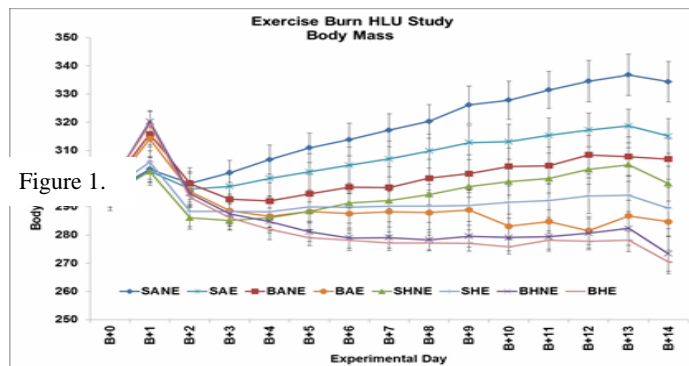


Figure 1.

Plasma interleukin-6 (IL-6) was significantly elevated in the burn groups, irrespective of exercise ($p>0.03$).

Free Fatty Acids (FFA) was significantly reduced in the burn groups, irrespective of exercise ($p>0.03$).

Bone strength parameters, including peak force, ultimate stiffness, bending failure energy and ultimate bending stress were measured (**YEAR 1, TASK 7**). We found that there was a disuse effect, irrespective of exercise, in peak force and ultimate bending stress ($p>0.05$).

Results (Wolf):

Specific Aim 1:

Muscle tissue wet weight from hind limb muscle including tibialis anterior (TA), extensor digitorum longus (EDL), plantaris (Plant), soleus (SL), gastrocnemius medialis (GM), gastrocnemius lateralis (GL) were weighed (**YEAR 1, TASKS 2-5**). Tissue weight was further normalized by body mass (per 100g) to eliminate individual variation.

Table 3. Animal body mass and muscle tissue wet weight in right hind limb (g)

	Mean	Body Mass	TA	TA per 100g	EDL	EDL per 100g	PL	PL per 100g	SL	SL per 100g	GM	GM per 100g	GL	GL per 100g
SA	NX	334.4	0.639	0.191	0.181	0.055	0.394	0.117	0.142	0.043	0.916	0.274	1.088	0.326
SH	NX	298.2	0.597	0.201	0.129	0.043	0.290	0.098	0.069	0.023	0.652	0.218	0.824	0.276
BA	NX	306.9	0.642	0.210	0.131	0.043	0.365	0.119	0.122	0.040	0.826	0.269	0.989	0.322
BH	NX	273.3	0.537	0.196	0.120	0.044	0.289	0.106	0.078	0.028	0.616	0.225	0.722	0.265
SA	EX	315.1	0.651	0.207	0.164	0.052	0.408	0.130	0.147	0.047	0.881	0.279	1.131	0.359
SH	EX	289.5	0.617	0.213	0.122	0.042	0.294	0.102	0.084	0.029	0.673	0.233	0.815	0.282
BA	EX	284.7	0.609	0.214	0.129	0.045	0.349	0.123	0.143	0.050	0.795	0.280	0.976	0.343
BH	EX	270.5	0.560	0.207	0.125	0.046	0.296	0.109	0.086	0.032	0.666	0.247	0.760	0.281
	SEM	Body Mass	TA	TA per 100g	EDL	EDL per 100g	PL	PL per 100g	SL	SL per 100g	GM	GM per 100g	GL	GL per 100g
SA	NX	7.15	0.036	0.010	0.039	0.014	0.025	0.007	0.005	0.002	0.026	0.009	0.032	0.012
SH	NX	6.14	0.022	0.008	0.012	0.003	0.014	0.006	0.005	0.002	0.028	0.008	0.054	0.014
BA	NX	7.20	0.035	0.014	0.008	0.003	0.017	0.004	0.007	0.002	0.025	0.006	0.050	0.013
BH	NX	3.45	0.014	0.005	0.016	0.006	0.009	0.003	0.007	0.003	0.036	0.011	0.025	0.011
SA	EX	6.14	0.006	0.003	0.007	0.003	0.016	0.006	0.009	0.002	0.031	0.006	0.029	0.006
SH	EX	7.24	0.028	0.009	0.007	0.003	0.009	0.002	0.002	0.001	0.018	0.008	0.018	0.007
BA	EX	5.55	0.026	0.008	0.007	0.002	0.013	0.005	0.007	0.002	0.023	0.013	0.014	0.008
BH	EX	4.13	0.013	0.006	0.004	0.002	0.010	0.004	0.004	0.002	0.026	0.012	0.041	0.014
	Mean	Body Mass	TA	TA per 100g	EDL	EDL per 100g	PL	PL per 100g	SL	SL per 100g	GM	GM per 100g	GL	GL per 100g
SA	NX	334.4	0.639	0.191	0.181	0.055	0.394	0.117	0.142	0.043	0.916	0.274	1.088	0.326
SH	NX	298.2	0.597	0.201	0.129	0.043	0.290	0.098	0.069	0.023	0.652	0.218	0.824	0.276
BA	NX	306.9	0.642	0.210	0.131	0.043	0.365	0.119	0.122	0.040	0.826	0.269	0.989	0.322
BH	NX	273.3	0.537	0.196	0.120	0.044	0.289	0.106	0.078	0.028	0.616	0.225	0.722	0.265
SA	EX	315.1	0.651	0.207	0.164	0.052	0.408	0.130	0.147	0.047	0.881	0.279	1.131	0.359
SH	EX	289.5	0.617	0.213	0.122	0.042	0.294	0.102	0.084	0.029	0.673	0.233	0.815	0.282
BA	EX	284.7	0.609	0.214	0.129	0.045	0.349	0.123	0.143	0.050	0.795	0.280	0.976	0.343
BH	EX	270.5	0.560	0.207	0.125	0.046	0.296	0.109	0.086	0.032	0.666	0.247	0.760	0.281
	SEM	Body Mass	TA	TA per 100g	EDL	EDL per 100g	PL	PL per 100g	SL	SL per 100g	GM	GM per 100g	GL	GL per 100g

Tissue wet weight decreased significantly in TA, EDL, SL, GM, GL under HLU condition. There were significant changes of wet tissue weight in TA, PL, GL and GM after burn. There was not a significant change in tissue wet weight of all muscle. After normalized with body mass (BM), we still observed that the ratio values still significantly decreased in PL, SL, GL and GM after HLU, and values in soleus and GL increased with exercise treatment (Almost all of means increased after exercise by looking the table above, **TABLE 3**).

Muscle dry tissue weight decreased significantly in GM and GL under HLU condition, burn decreased dry weight only in GL. No significant changes were observed in SL and PL.

Muscle Isometric Force Measurement

Isometric force was measured from the left side of plantaris (PLANT) and soleus (SL) muscle. Results showed that twitch force (Pt) decreased in both SL and PLANT in HLU group. No significant difference was observed in Pt between exercise and no exercise.

In rat soleus, tetanic (Po) and specific Po (sPo) force were also significantly lower in the HLU group (p<0.001). The burn/hind limb (B/H) group had a significantly higher Pt in the exercise group (p=0.04). Burn/ambulatory (B/A) rats had a lower tetanic force in the exercise group versus no exercise (p=0.02). sPo in the B/H group was significantly higher in exercise (p<0.01).

Fatigue index was significantly lower in the ambulatory (55%) and exercise (52%) groups versus hindlimb (69%) and no exercise (73%) groups (p=0.03, p=0.002 respectively) (**TABLE 4**).

Soleus Weight and Isometric Contractile Function								
Table 4	No Exercise				Exercise			
	BA	BH	SA	SH	BA	BH	SA	SH
Muscle Weight (mg)	200 (10)	170 (40)	210 (20)	140 (40)	190 (10)	110 (10)	190 (10)	120 (4)
Twitch Force (g)	36 (4.4)	8 (2.0)	31 (2.8)	14 (2.1)	27 (2.0)	14 (2.1)	30 (2.6)	11 (0.6)
Tetanic Force (g)	165 (9)	42 (5)	159 (18)	56 (4)	118 (14)	54 (5)	150 (16)	66 (8)
Specific Force (N/cm ²)	25 (2)	7 (1)	25 (3)	12 (2)	20 (2)	14 (2)	23 (2)	17 (2)
Fatigue Index (%)	69 (6)	76 (3)	66 (6)	82 (11)	37 (11)	58 (13)	52 (11)	63 (6)
Data are expressed as mean (SEM)								
BA: Burn Ambulatory; BH: Burn Hindlimb; SA: Sham Ambulatory; SH: Sham Hindlimb								
Specific Force calculated from maximum tetanic force (N)/ physiological cross sectional area (cm ²)								
Fatigue Index: (minimum force at 4 minutes/maximum force) x 100								

Skeletal Muscle Protein Content

Muscle proteins were extracted from rat gastrocnemius media (GM), soleus (SL) and plantaris (PL) following T-PER Tissue protein extraction procedure (Thermo Fisher Scientific). Protein concentration was measured with DC Protein Assay (Bio-Rad Laboratories Inc.). There was significant protein content loss in SL in rats with HLU (p=0.001), and protein yield in GM significantly increased in rats with exercise training (p=0.003).

Skeletal Muscle Histology and Myofiber Type Change

Morphology of soleus in H&E staining: the area of single myofiber decreased under hind limb unloading significantly; exercise increased myofiber size significantly (**FIGURE 2**). No change was observed in rat soleus 14 days after burn.

Myofiber type in soleus: by counting 5 random microscopic views under 10x magnifications, the positive stained myofiber with fast twitch myosin antibody. (**FIGURE 3**).

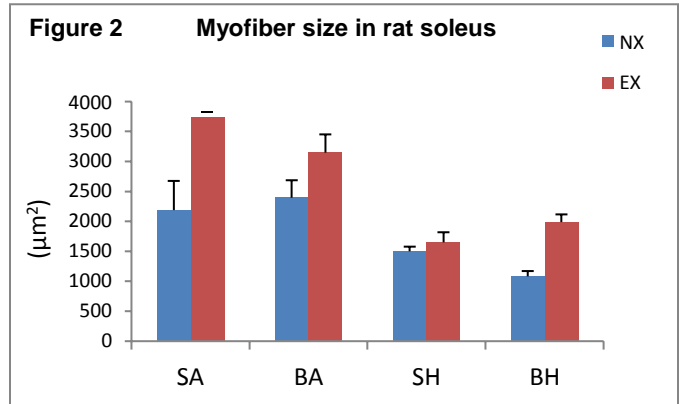
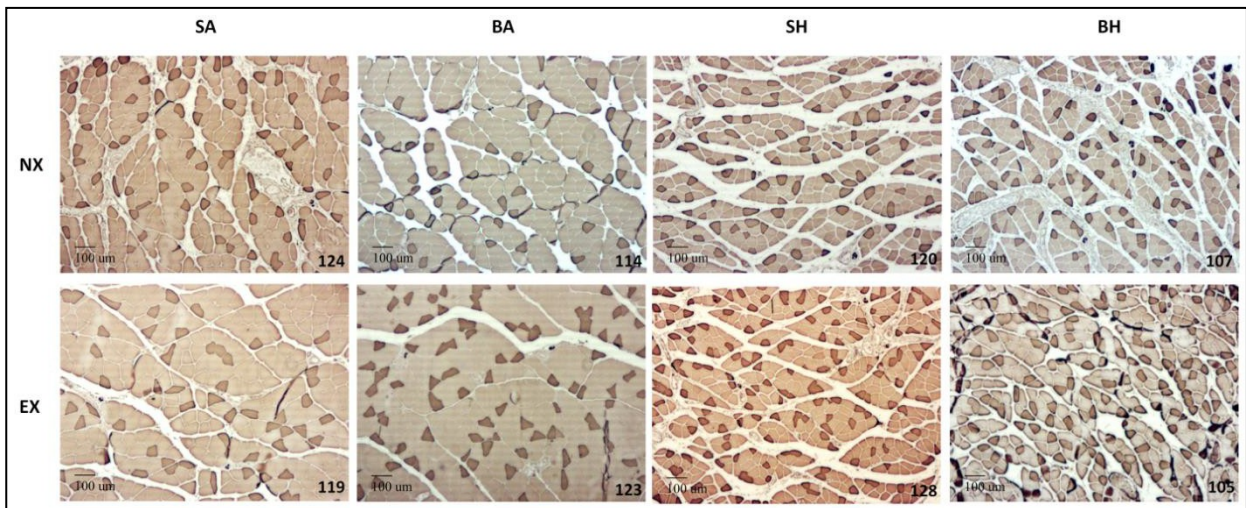


Figure 3



The following table showed the number of muscle cell stained with fast twitch myosin antibody and the percentage of positive cells increased in HLU group (**TABLE 5**). The total number of myofiber was less in exercised group. Value presented as Mean \pm SEM.

TABLE 5	Total Cell #		Positive Cell #		% Positive Cells	
	Non-exercise	Exercise	Non-exercise	Exercise	Non-exercise	Exercise
SA	314 \pm 28	273 \pm 9	37 \pm 12	33 \pm 11	11.4 \pm 3.1	11.8 \pm 3.6
BA	274 \pm 26	306 \pm 7	27 \pm 11	30 \pm 19	9.1 \pm 3.5	10.3 \pm 4.5
SH	392 \pm 30	316 \pm 32	89 \pm 4	69 \pm 23	23.2 \pm 2.7	21.5 \pm 3.8
BH	400 \pm 17	238 \pm 84	76 \pm 16	71 \pm 35	19.3 \pm 4.5	24.6 \pm 10.7

Results (Wade):

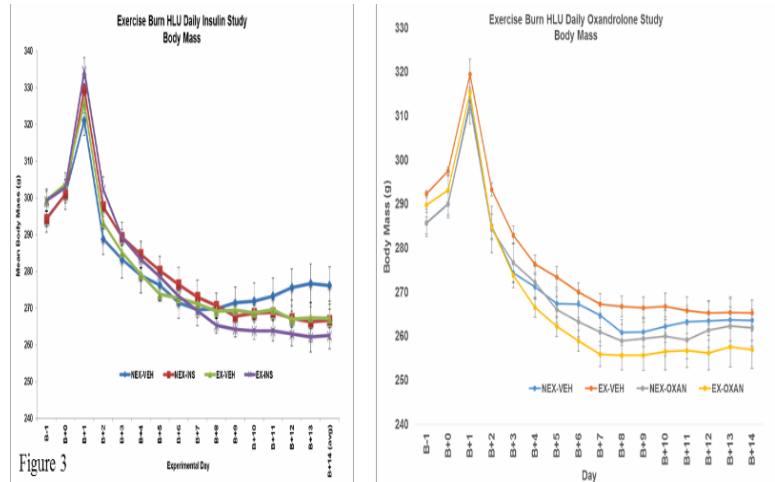
Specific Aim 2:

All supplies were ordered for Aim 2, including disposable, assays and controlled substances. (**YEAR 2 TASK 1**). Each experiment (Insulin and Oxandrolone) were run independently. For each experiment, male, Sprague-Dawley rats were randomized into four groups: Burn/Hindlimb unloaded-Vehicle (BHV), Burn/Hindlimb unloaded-Treated (INS or OXAN) with daily resistance exercise (EX) or no exercise (NEX) (N=6/group). Rats were introduced to resistance exercise by adding weight to each tail during repetitive ladder climbing ten days prior to injury. Rats were then weight-matched into treatment groups, either daily exercise or no-exercise. Following injury, rats were administered daily subcutaneous (SQ) doses of either the vehicle or drug. In addition, daily resistance exercise was completed on a 1m ladder at 85° incline. Each rat completed 5 climbs 2x/day. At the conclusion of the experimental period, samples were collected for further analysis (**YEAR 2 TASKS 2-6**). Statistical analysis using ANOVA with significance at $p < 0.05$ was used.

Body mass during Aim 2 for both the insulin study and oxandrolone study showed a similar response as seen during our previous work looking specifically at the burn/hindlimb unloading groups (Wade et al, 2013). There were no differences in initial body mass between treatment groups, however, we did observe differences by day 14 as a result of exercise or treatment. (FIGURE 4/TABLE 6).

In both studies, at day 14, exercise and drug treatment body mass were significantly reduced compared to the other treatment groups. Compared to other treatment groups, there was an increase in average food consumed over the last 5 days in the exercise groups, irrespective of treatment.

Fat mass was significantly reduced in the disuse groups, with an additive effect of burn with disuse ($p < 0.001$).



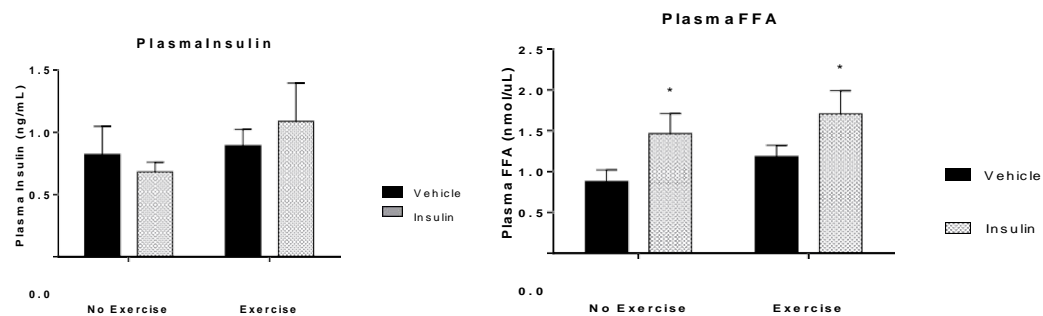
Insulin Study:

Plasma insulin was not different between groups, irrespective of treatment or exercise. Insulin dosing was discontinued 36 hours prior to blood collection to avoid hypoglycemia during fasting. Circulating insulin has a half-life of approximately 24 hours, which may be contributing to no differences being observed.

Table 6	BH-VEH	BH-INS
D14 Body Mass (g) (n=63)		
NEX	270±3	271±4
EX	273±3	262±6
Food Intake (Last 5 days-g/100g BM/day) (n=63)		
NEX	7.2±0.1	7.3±0.2
minEX	7.4±0.1*	7.8±0.2*
Fat Mass (per 100g BM) (n=63)		
NEX	0.62±0.03	0.69±0.04
EX	0.66±0.03	0.65±0.05
Total Hindlimb Muscle Mass (per 100g BM) (n=63)		
NEX	0.88±0.01	0.90±0.02*
EX	0.95±0.01*	0.99±0.02* ^{xy}

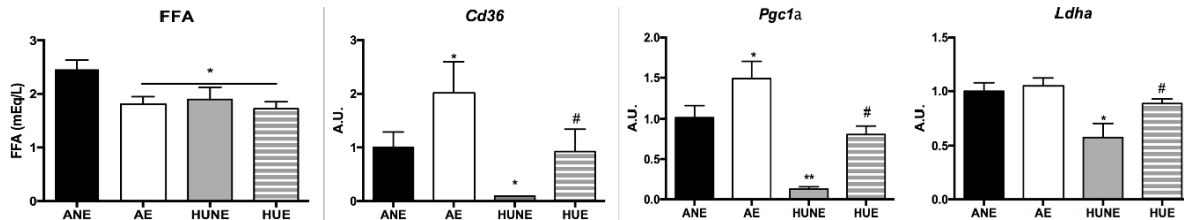
Free Fatty Acids (FFA) was significantly increased in EX-INS as compared to NEX-VEH. We found no differences between the other groups ($p > 0.05$) (FIGURE 5).

Figure 5



When we looked at gene expression in subcutaneous white adipose tissue (scWAT) for fatty acid metabolism and mitochondrial activity (FFA, Cd36, Pgc1a and Ldha), in the hindlimb unloading, exercise vs no exercise, we found that exercise restored these genes in the fat ($p < 0.05$) (**FIGURE 6**).

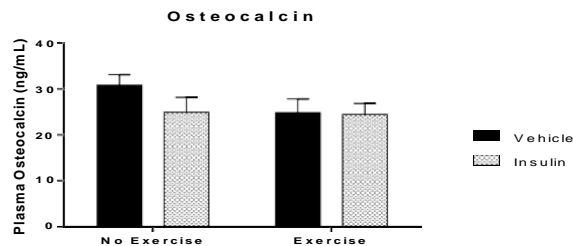
Figure 6



No differences were found in body mass between groups, irrespective of treatment. Food intake was significantly increased as a function of exercise, but was not affected by pharmacological treatment (**TABLE 6**).

Plasma Osteocalcin was increased in NEX-VEH as compared to the other groups ($p = 0.09$) (**FIGURE 7**).

Figure 7



Bone strength parameters, including peak force, ultimate stiffness, bending failure energy and ultimate bending stress were measured (**YEAR 2, TASK 5**). We found that there was a disuse effect, irrespective of exercise, in peak force and ultimate bending stress ($p > 0.05$) (**TABLE 7**). In addition, we measured mineral content in ashed bone. We found no significant changes in Ca, P, Mg or Zn.

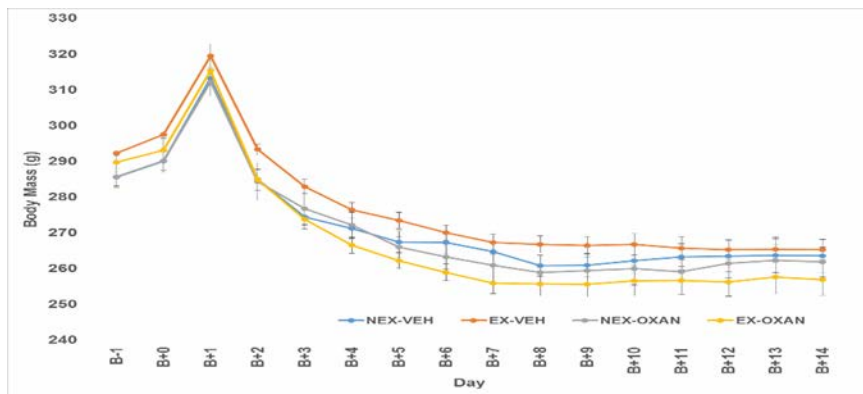
Table 7

	Vehicle	Insulin
Ca (mg/mg bone)		
NEX	215.9±6.8	213.9±6.3
EX	228.3±13.9	223.4±4.3
P (mg/mg bone)		
NEX	97.5±3.1	98.4±2.5
EX	100.7±2.3	102.0±1.4
Mg (mg/mg bone)		
NEX	4.4±0.1	4.4±0.2
EX	4.3±0.1	4.4±0.1
Zn (mg/mg bone)		
NEX	0.19±0.01	0.18±0.01
EX	0.21±0.02	0.20±0.02

Oxandrolone Study:

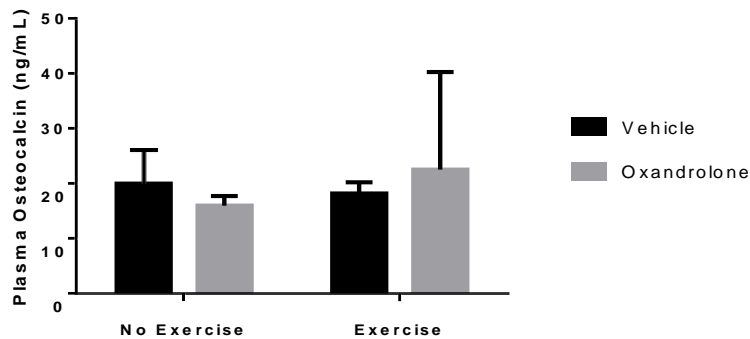
Sample analysis continuing.

Body mass during Aim 2 for the oxandrolone study showed a similar response as seen during our previous work looking specifically at the burn/hindlimb unloading groups (Wade et al, 2013). There were no differences in initial body mass between treatment groups, however, we did observed differences by day 14 as a result of exercise or treatment.



Plasma Osteocalcin was increased, but not significantly different in EX-OXAN as compared to the other groups (**FIGURE 8**).

Figure 8



Oxandrolone is a derivative of testosterone, so plasma testosterone was measured to determine circulating testosterone at the conclusion of the study. No significant differences were observed in plasma testosterone, however NEX-OXAN was increased as compared to the other treatment groups.

Bone strength parameters, including peak force, ultimate stiffness, bending failure energy and ultimate bending stress were measured (**YEAR 2, TASK 8**). We found that there was a disuse effect, irrespective of exercise, in peak force, bending failure and ultimate bending stress ($p > 0.05$) (**FIGURE 9**). In addition, we measured mineral content in ashed bone, including Ca, P, Mg, and Zn. No significant differences were observed in any measured bone minerals (**TABLE 8**).

Figure 9.

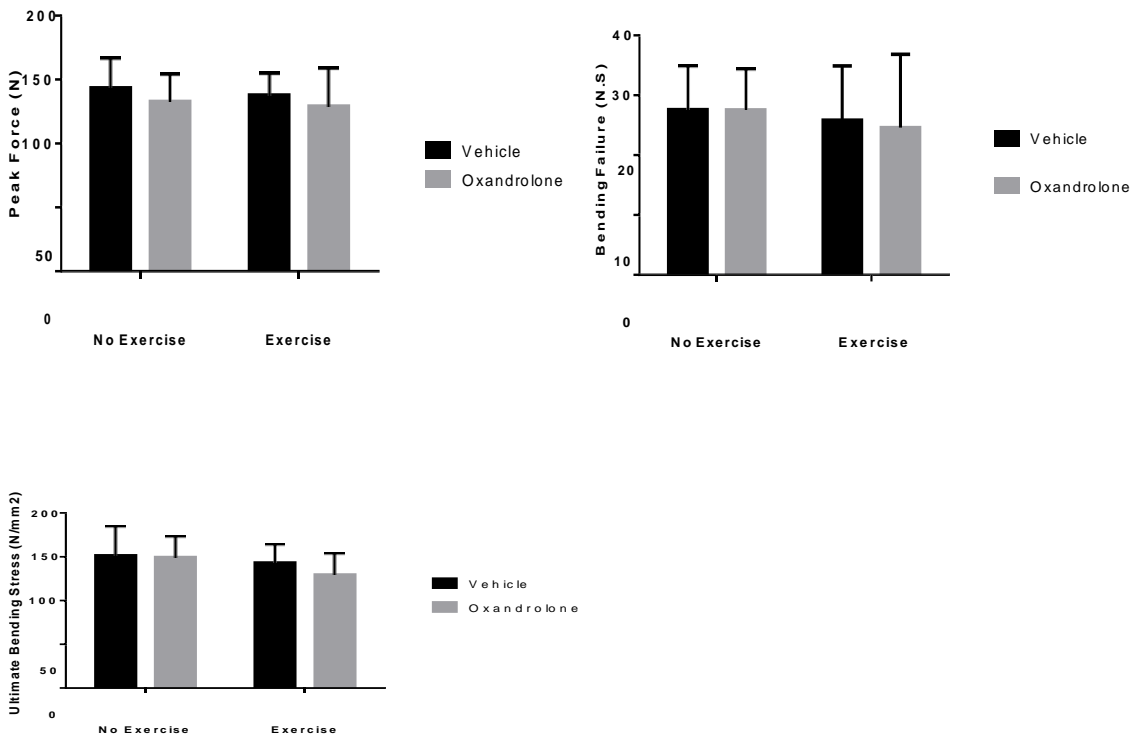


Table 8

	Mean±SEM	Vehicle	Oxandrolone
Ca (mg/mg bone)			
NEX		199.6±2.5	186.6±12.1
EX		193.4±5.0	202.2±5.6
P (mg/mg bone)			
NEX		87.1±1.0	83.7±5.5
EX		87.5±1.5	89.1±1.2
Mg (mg/mg bone)			
NEX		3.8±0.1	4.1±0.6
EX		3.9±0.1	3.9±0.1
Zn (mg/mg bone)			
NEX		0.13±0.02	0.12±0.01
EX		0.15±0.02	0.14±0.01

Results (Wolf):

Specific Aim 2:

The reversal effect of exercise training on muscle genomic profile in rats with burn and hind limb

Micro RNA (miRNA) is a class of non-coding RNA that regulates gene expression by silencing messenger RNA. We pooled 3 animal muscle samples from each treatment group for RNA extraction. We measured miRNA expression by using Affymetrix miRNA 4.0 Arrays and gene expression by using Affymetrix rat gene 2.0 chips.

MiRNAs and gene profiles are distinguished in response to burn, hindlimb unloading and exercise respectively. There are 1,218 rat splice miRNAs in a total 36,222 miRNAs detected in each group. We identified 703 (57.7%) up-regulated miRNAs and 515 (42.3%) down-regulated miRNAs in the burn group compared to sham. Thirty-five up-regulated and 12 down-regulated genes after burn in rat plantaris. 623 miRNAs were upregulated and 587 were down regulated with exercise. Forty-one gene transcript probes were identified including 40 down-regulated and 1 up- regulated between the exercise or non-exercise in BH rats.

Burn and hind limb unloading contribute respectively. However, there are overlaps in both miRNA and transcript gene levels between burn and hindlimb unloading. MiR-182 increased 12.81 fold in burn, 23.82 fold in hindlimb unloading respectively, and increased 35.35 fold in burn and hindlimb unloading group. Nr4a3 gene expression increased 2.45 in burn and 3.59 fold in hindlimb unloading respectively, and increased 6.31 fold in BH rats.

One targeted gene could be regulated by a group of miRNAs. For instance, miR-409a-3p was the most down-regulated miRNA in response to burn (-2.95 fold change). It functions with up-regulated miRNA-182 to inhibit muscle Col1a2 gene expression after burn. Gene-related

pathways are activated after a burn, such as inflammation response, oxidative stress, cell cycle, cell apoptosis, calcium regulation, and striated muscle contraction.

The effect of exercise alleviated miRNA and gene expression in BH rats. miR-182 decreased -7.04 fold in BH rats with exercise training; gene expressions of Fgl2 in blood clotting cascade and Colla1 in inflammatory response pathway decreased in response to exercise training as well. In summary, miRNAs and transcript gene profiles were affected in burn and hindlimb unloading, those changes are associated with muscle pathophysiological changes, including muscle mass loss and function impairment. The muscle improvement with exercise training were also observed in gene levels with miRNA alterations.

The improvement of exercise and insulin pharmacological combination in rat muscle

Twenty Four animals received burn and hindlimb unloading procedure (as previous experiment) and were randomly assigned (n=6) to vehicle without exercise (V/N), insulin (pro zinc 40U daily) without exercise (I/N), vehicle with exercise (V/E), or insulin with exercise (I/E). On day 14 muscle functions were tested and tissue collected.

In summary, we observed that muscle functions including tetanic (Po) and twitch (Pt) were significantly elevated in both plantaris and soleus with insulin and exercise combined treatment. No function improvement with solely insulin treatment was found. (Data values presented as mean ±SEM listed the following table).

Muscle Dimensions and Isometric Muscle Function

Parameter		Plantaris				Soleus			
		No Exercise		Exercise		No Exercise		Exercise	
Group		Vehicle	Insulin	Vehicle	Insulin	Vehicle	Insulin	Vehicle	Insulin
Muscle	Wet weight (mg)	332 ± 18	329 ± 9	348 ± 6.3	354 ± 14	119 ± 2	143 ± 23	151 ± 32	131 ± 7
	Lo (mm)	35 ± 2	31 ± 0.3	32 ± 1	32 ± 1	33 ± 1.4	29 ± 0.4	31 ± 0.9	30 ± 0.4
	PCSA (mm ²)	27 ± 3	30 ± 2	30 ± 2	#31 ± 2	5.0 ± 0.2	6.9 ± 2.3	6.7 ± 1.3	6.0 ± 0.3
Twitch Force Pt (g)		89 ± 9	85 ± 3	92 ± 2	†102 ± 8	10 ± 2	10 ± 2	14 ± 2	*18 ± 1
Tetanic Force Po (g)		430 ± 31	459 ± 12	508 ± 14	†522 ± 17	38 ± 8	38 ± 9	59 ± 5	*69 ± 5
Po/CSA (N/cm ²)		16 ± 2	15 ± 2	16 ± 1	17 ± 1	7.4 ± 2	7.0 ± 1	10 ± 2	†12 ± 1
Pt/Po (%)		21 ± 1	19 ± 1	18 ± 0.4	20 ± 1	26 ± 1	24 ± 2	24 ± 2	26 ± 2
Fatigue	Maximum (g)	—	—	—	—	33 ± 6	34 ± 9	53 ± 4	*64 ± 4
	Minimum (g)	—	—	—	—	27 ± 6	27 ± 6	†46 ± 4	*54 ± 4
	Index (%)	—	—	—	—	81 ± 7	84 ± 5	87 ± 5	84 ± 5

Lo = optimal muscle length

PCSA = Physiological Cross Sectional Area

Po/CSA = Tetanic force normalized to PCSA

Pt/Po (%) = Ratio of twitch to tetanic force

Fatigue Index = Ratio of fatigue minimum to maximum

* vs. No Exercise (ANOVA, p<0.05)

† vs. Vehicle No Exercise (ANOVA, p<0.05)

vs. Vehicle No Exercise (one-tailed t-test p<0.05)

‡ vs. Other groups combined (two-tailed t-test, p=0.05)

The effect of exercise and oxandrolone pharmacological combination in rat muscle function

Twenty Four animals received burn and hindlimb unloading procedure (as previous experiment) and were randomly assigned (n=6) to vehicle without exercise (V/N), oxandrolone (daily) without exercise (O/N), vehicle with exercise (V/E), or insulin with exercise (O/E). On day 14 muscle functions were tested and tissue collected.

Two way ANOVA statistical analysis showed that there is a significant decrease in fatigue index (FI) with exercise training, like we observed in previous study. There is no significant changes with oxandrolone treatment. (Data values presented as mean \pm SD listed the following table).

Plantaris	NX		E X		Soleus	NX		EX	
	VEH	OXD	VEH	OXD		VEH	OXD	VEH	OXD
Tissue weight(g)	0.33034 \pm 0.018	0.312 \pm 0.028	0.331 \pm 0.042	0.300 \pm 0.033	Tissue weight(g)	0.109 \pm 0.015	0.100 \pm 0.031	0.102 \pm 0.014	0.110 \pm 0.016
Lo(mm)	22.2 \pm 1.8	22.2 \pm 2.5	22.3 \pm 1.1	22.3 \pm 1.2	Lo(mm)	21.8 \pm 2.4	22.0 \pm 3.0	21.4 \pm 3.4	20.8 \pm 0.8
1/2 RT(s)	0.0166 \pm 0.001	0.0169 \pm 0.001	0.0187 \pm 0.001	0.0165 \pm 0.001	Pt(g)	47.80 \pm 29.44	52.30 \pm 14.13	64.95 \pm 39.77	48.82 \pm 11.19
Pt(g)	98.00 \pm 13.39	115.85 \pm 27.13	112.40 \pm 22.47	105.86 \pm 11.51	Po(g)	113.49 \pm 69.89	126.02 \pm 49.97	106.30 \pm 18.62	124.09 \pm 17.81
Po(g)	426.67 \pm 137.64	469.08 \pm 47.16	489.74 \pm 58.13	555.44 \pm 45.41	FI	26.43 \pm 11.79%	27.24 \pm 13.02%	15.56 \pm 7.75%	16.08 \pm 6.36%
Po/Pt	4.29 \pm 1.01	4.17 \pm 0.70	4.48 \pm 0.94	5.31 \pm 0.55	Fatigue (max)(g)	79.89 \pm 45.63	95.075 \pm 36.44	100.25 \pm 13.55	104.71 \pm 11.34
sPt(N/cm2)	6.787 \pm 0.804	8.969 \pm 2.974	7.853 \pm 1.449	8.187 \pm 1.020	sPt(N/cm2)	9.693 \pm 5.549	10.814 \pm 4.504	14.055 \pm 8.328	9.521 \pm 1.741
sPo(N/cm2)	29.686 \pm 10.058	35.212 \pm 7.434	34.733 \pm 6.979	38.251 \pm 11.784	sPo(N/cm2)	22.671 \pm 14.044	29.082 \pm 13.787	23.413 \pm 6.091	24.459 \pm 4.136

CONCLUSIONS (WOLF):

- Immobilization significantly decreases muscle mass and strength in both burned and non-burned conditions
- Burn has less effect on decreasing muscle mass and strength than immobilization in the current animal model
- Exercise improves muscle size and strength after burn and immobilization, primarily in slow twitch muscles
- Insulin and exercise have additive effects of muscle function improvement in the current burn and hindlimb unloading animal model.

Aim 3 Methods:

Twenty Four rats received 40% TBSA burn and hindlimb unloading (HLU) as described previously. All rats were pre-trained 10 days prior to injury. Immediately following injury, all rats were put into HLU, and continued exercise training for 14 days. Rats were divided into 2 treatment groups, either daily subcutaneous injections of pro zinc insulin 5U/kg or vehicle saline injection. At day 14, all rats were removed from HLU, and all injections stopped. Rats within each treatment group were separated into exercise (EX)/no exercise (NEX) (n=6) for an additional 14 days.

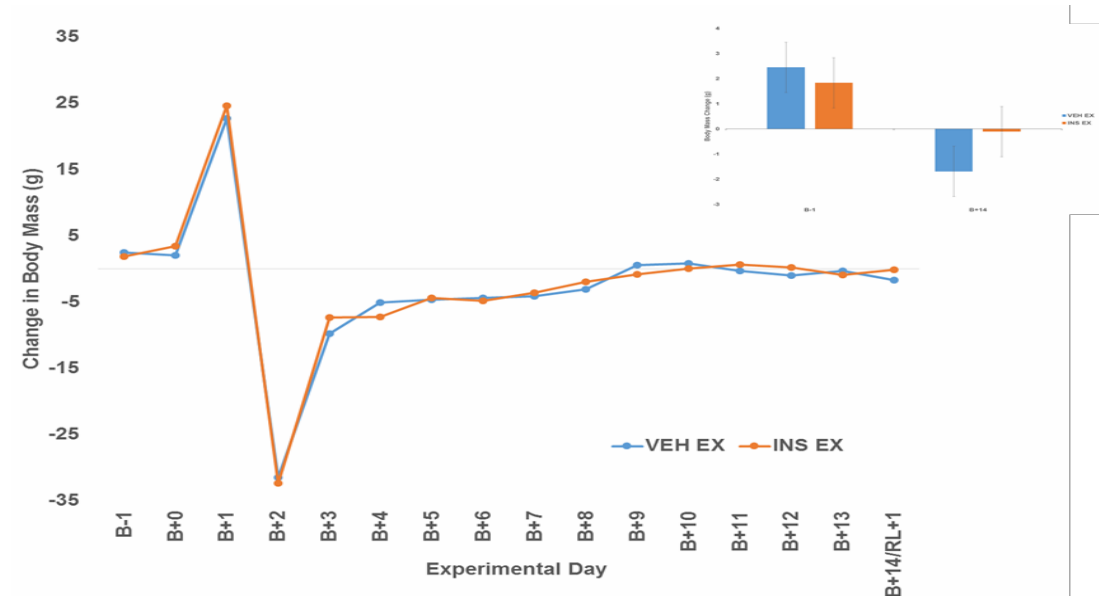
At the conclusion of the reloading period, muscle function testing was completed, blood was collected and selected tissues were removed and stored for further analysis.

Results (Wade):

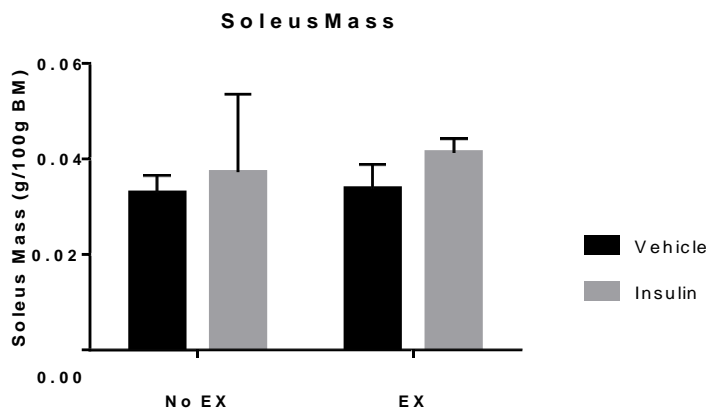
Specific Aim 3:

Body mass during unloading/daily injection and exercise period.

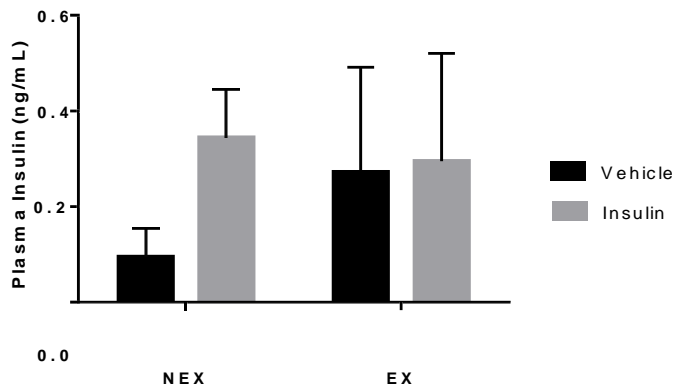
During the unloading period, there were no differences in body mass between the saline vehicle injection plus exercise group, and the insulin injection plus exercise group until day 14. The change in body mass is illustrated in the graph insert below.



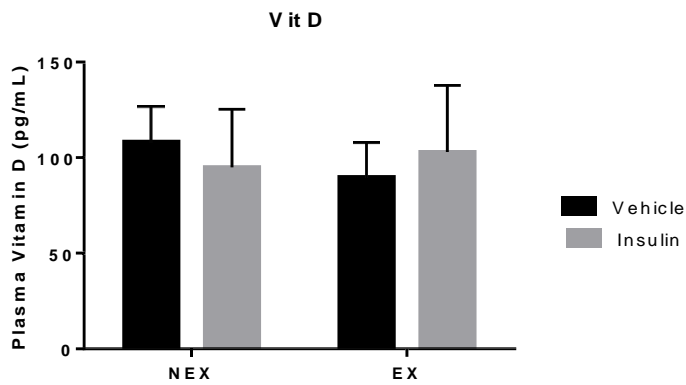
Soleus mass on Day 28. Insulin injections throughout the unloading period with exercise had an effect during the reloading period, irrespective of exercise.



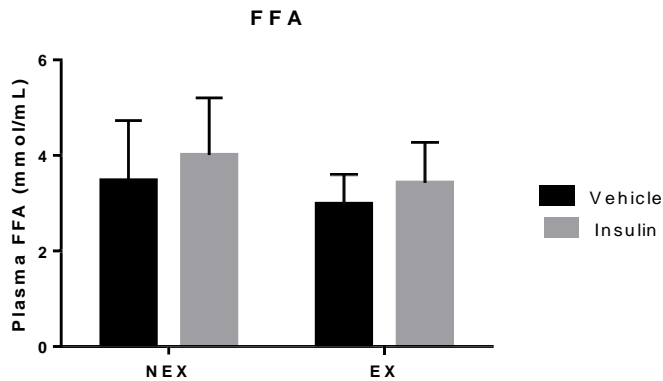
Plasma insulin on Day 28. Insulin injections had an effect throughout the unloading period primarily in the no exercise group. Exercise has a slight effect.



Plasma Vitamin D on Day 28. Vitamin D was not different between groups at the end of the unloading period.



Plasma Free Fatty Acids on Day 28. FFA showed a slight increase between groups at the end of the unloading period, but were not significantly different.



Preliminary plasma analysis shows that at the conclusion of the reloading period, daily insulin

injections with exercise, the reloading plus exercise had minimal effect on various indices.

Though exercising resulted in a persistent reduction in body mass measurements of bone function, morphology and mineral composition demonstrated no significant differences between treatment groups.

4. KEY RESEARCH ACCOMPLISHMENTS

The milestone for Year 1 was the completion of Aim 1. There were 8 major tasks associated with this aim. See **Appendix 1** for project timeline. The tasks and completion status are included below:

- Major Task 1 was to obtain protocol approval from the University of Texas Health Science Center at Houston. This task was *completed* before any associated animal work could be completed (Wade).
- Major Tasks 2 and 3 included training personnel, acquiring any equipment needed for the experiments associated with Aim 1 and setting up for the animal testing. These tasks were *completed* prior to any work being done. Coordination with investigators from the other institutions was initiated and timelines were able to be generated experiment completion (Wade/Wolf).
- Major task 4 includes starting and completing Aim 1 experiments. All pre-training and experimental procedures were *completed* according to the timeline. Samples were collected and stored appropriately for further analysis (Wade/Wolf).
- Major task 5 was *completed* at the conclusion of each experiment. Muscle function was completed on all animals in all groups for Aim 1. Plasma and tissue were collected and stored for processing at a later time (Wade). Muscle function testing was completed (Wolf).
- Major task 6 is *complete*. Specific ELISA kits were ordered and assays have been completed. Additional ELISA kits were purchased for repeating of data and were *completed* (Wade). Muscle tissue weight measurement *completed*. Muscle protein extraction, histology and immunohistology staining of muscle tissue, muscle tissue protein electrophoresis and analysis of these data are *complete*. Muscle tissue RNA extraction, genomic profile analysis are *complete* (Wolf).
- Major task 7 bone analysis is *complete*. Bone strength and mechanical testing has been *completed* on all bones collected during this aim. Microcomputer topography (μ CT) is *complete*. Data analysis of μ CT scans is *complete* (Wade).
- Major task 8 is *complete*. Six abstracts have been submitted to professional scientific meetings detailing this work to-date. Three manuscripts have been published in a peer-reviewed journal detailing this work to-date (Wade/Wolf).

The milestone for Year 2 was the completion of Aim 2. There were 6 major tasks associated with this aim. See **Appendix 1** for project timeline. The tasks and completion status are included below:

- Major Task 1 was to order supplies, animals and set-up for the completion of Aim 2 experiments. Coordination with investigators from the other institutions was initiated and timelines were able to be generated experiment completion. This task was *completed* prior to the start of the two separate experiments (Wade/Wolf).
- Major task 2 includes starting and completing all Aim 2 experiments. All pre-training and experimental procedures were *completed* according to the timeline. Samples were collected, and stored appropriately for further analysis (Wade/Wolf).
- Major task 3 was *completed* at the conclusion of each experiment. Muscle function was *completed* on all animals in all groups for Aim 2. Plasma and tissue were collected and stored for processing at a later time (Wade). Muscle function testing was *completed* (Wolf).
- Major task 4 is *complete*. Specific ELISA kits were ordered, and assays have been *completed*. Muscle tissue weight measurement *completed*. Muscle protein extraction, histology and immunohistology staining of muscle tissue, muscle tissue protein electrophoresis, and analysis of these data are *complete*. Muscle tissue RNA extraction, genomic profile analysis are *complete* (Wolf).
- Major task 5 bone analysis is *complete*. Bone strength and mechanical testing has been *completed* on all bones collected during this aim. Microcomputer topography (μ CT) is *complete*. Data analysis of μ CT scans is *complete* (Wade).
- Major task 6 is *complete*. Two abstracts have been submitted to professional scientific meetings detailing this work to-date (Wade/Wolf).

The milestone for Year 3 was the continuation of analyzing data from Aim1 and Aim 2, as well as completion of the animal experiment and sample collection for Aim 3. There were 6 major tasks associated with this aim, and major tasks 1-3 were completed in Year 2. See **Appendix 1** for project timeline. The tasks and completion status are included below:

- Major task 4 is *complete*. Specific ELISA kits were ordered and have been *completed*. Muscle tissue weight measurement *completed*. Muscle protein extraction, histology and immunohistology staining of muscle tissue, muscle tissue protein electrophoresis, and analysis of these data are *complete*. Muscle tissue RNA extraction, genomic profile analysis are *complete* (Wolf).

- Major task 5 bone analysis is *complete*. Bone strength and mechanical testing has been *completed* on all bones collected during this aim. Microcomputer topography (μ CT) is *complete*. Data analysis of μ CT scans is *complete*. A delay occurred with the departure of the primary individual tasked for conducting all of the μ CT measurements. A compatible source has been identified and analysis has been *completed* (Wade).
- Major task 6 is currently *on-going*. Nine abstracts have been submitted to professional scientific meetings detailing this work to-date (Wade/Wolf).
- Major task 8 is currently *on-going*. Twelve abstracts have been submitted to professional scientific meetings detailing this work to-date. Three manuscripts have been published in a peer-reviewed journal detailing this work to-date (Wade/Wolf).

5. CONCLUSION

Both Aim 1 and Aim 2 used our validated rodent model of burn and disuse, with a daily resistance exercise regimen started before injury and continuing for the duration of the experimental period. Aim 2 focused on the addition of daily doses of either vehicle or a pharmacological agent (insulin or oxandrolone), in unison with the daily resistance exercise regimen. For both aims, all rats were able to complete the exercise program after injury, and no rats were excluded from the experiment at any time. Data presented, irrespective of resistance exercise and daily dosing, are comparable to previous studies. Daily resistance exercise resulted in a significant decrease in body mass, which can be attributed to the reduction in fat mass. The changes in muscle and bone support our previous research. Bone was affected primarily by the disuse component. Exercise alone did not seem to contribute to the overall changes. Muscle changes, however, were a result of the addition of resistance exercise. All eight major tasks for Year 1 have been completed. All six major tasks for Year 2 have been completed.

In both Aim 1 and Aim 2, μ CT analysis is complete despite change in personnel and availability of the equipment to complete the scanning and analysis of the bones. In both Aim 1 and Aim 2, abstract and manuscript submissions are currently *on-going* as they are actively being drafted and submitted.

The animal experiment portion of Aim 3 was completed and data analysis is *complete*. The primary focus will be determining the interrelationship between muscle and bone following re-ambulation following pharmacological interventions and exercise. Assay work and data analysis is *on-going* and abstracts/manuscripts are actively being prepared for submittal.

6. PUBLICATIONS, ABSTRACTS AND PRESENTATIONS

a. All publications resulting from this project

(1) Lay Press: Not applicable

(2) Peer-Reviewed Scientific Journals:

Threlkeld MRS, Wolf SE, Song J. Muscle function improved in injured mice with a biological de-cellularized matrix application. Submitted to J. Surgical Res in 2018 March.

Hernandez P, Buller D, Mitchell T, Wright J, Liang H, Manchanda K, Welch T, Huebinger RM, Carlson DL, Wolf SE, Song J. Severe Burn-Induced Inflammation and Remodeling of Achilles Tendon in a Rat Model. *Shock*. 2018 Sep;50(3):346-350. doi: 10.1097/SHK.0000000000001037. PMID: 29065066; PMCID: PMC6072366.

Song J, Saeman MR, Baer LA, Cai AR, Wade CE, Wolf SE. Exercise Altered the Skeletal Muscle MicroRNAs and Gene Expression Profiles in Burn Rats With Hindlimb Unloading. *J Burn Care Res*. 2017 Jan/Feb;38(1):11-19. doi: 10.1097/BCR.0000000000000444. PMID: 27753701; PMCID: PMC5179292.

Saeman MR, DeSpain K, Liu MM, Carlson BA, Song J, Baer LA, Wade CE, Wolf SE. Effects of exercise on soleus in severe burn and muscle disuse atrophy. *J Surg Res*. 2015 Sep;198(1):19-26. doi: 10.1016/j.jss.2015.05.038. Epub 2015 Jun 12. PMID: 26104324; PMCID: PMC4542145.

(3) Invited articles: Not applicable

(4) Abstracts:

Baer LA, Song J, Wolf SE, Wade CE. Effects of resistance exercise on caloric intake and body mass in rats following burn and disuse. Poster presented at: 47th American Burn Association (ABA) Annual Meeting; 2015 Apr 21-24; Chicago, IL.

Carlson BA, Song J, Saeman MR, DeSpain K, Baer LA, Wade CE, Wolf SE. Exercise alleviates skeletal muscle protein loss after severe burn and hindlimb disuse. Poster presented at: 47th American Burn Association (ABA) Annual Meeting; 2015 Apr 21-24; Chicago, IL.

Song J, Baer LA, Saeman MR, Liu MM, Carlson B, Wolf HE, DeSpain K, Wade CE, Wolf SE. Skeletal muscle fiber type changes in severe burn rats with muscle disuse atrophy. Poster presented at: 47th American Burn Association (ABA) Annual Meeting; 2015 Apr 21-24; Chicago, IL.

Saeman MR, DeSpain K, Liu M, Carlson B, Baer LA, Song J, Wade CE, Wolf SE. The effects of exercise on soleus function in severe burn with muscle disuse atrophy. Poster presented at: 10th Annual Academic Surgical Congress Meeting; 2015 Feb 3-5; Las Vegas, NV.*

Saeman MR, Song J, Baer LA, DeSpain K, Wade CE, Wolf SE. Plantaris miRNA and target gene profile after exercise training in an animal model of hindlimb unloading and severe burn. Poster presented at: 38th Annual Shock Society Conference; 2015 Jun 6-9; Denver, CO.

Saeman MR, Song J, Baer LA, DeSpain K, Wade CE, Wolf SE. Plantaris microRNA and target gene profile after exercise training in an animal model of bed rest and severe burn. Poster presented at: 38th Annual Shock Society Conference; 2015 Jun 6-9; Denver, CO.

Song J, Saeman MR, DeSpain K, Baer LA, Wade CE, Wolf SE. Muscle microRNA profile alteration following severe burn. Poster presented at: 38th Annual Shock Society Conference; 2015 Jun 6-9; Denver, CO.

Baer LA, Song J, Stanford KI, Wolf SE, Wade CE. Burn and disuse with resistance exercise effects on fibroblast growth factor-21 and eNOS in rats. Poster presented at: Cell Symposia Exercise Metabolism Annual Meeting; 2015 Jul 12-14; Amsterdam, Netherlands.

Baer LA, Song J, Wolf SE, Wade CE. Effects of resistance exercise and daily insulin on body mass, food intake, fat mass and total hindlimb muscle mass in rats following burn and disuse. Poster presented at: 48th American Burn Association (ABA) Annual Meeting; 2016 May 3-6; Las Vegas, NV.

Cai A, Song J, Kumar P, Sehat A, Saeman MR, Baer LA, Wade CE, Wolf SE. Exercise treatment reversed micro RNA profile in burn rats with hindlimb unloading. Poster presented at: 48th American Burn Association (ABA) Annual Meeting; 2016 May 3-6; Las Vegas, NV.

Song J, DeSpain K, Baer L, Wade CE, Wolf SE. Combined effects of oxandrolone and exercise on muscle function recovery in rats with severe burn and hindlimb unloading. Poster presented at: 39th Annual Shock Society Conference; 2016 Jun 11-14; Austin, TX.

Saeman MR, DeSpain K, Song J, Baer LA, Wade CE, Wolf SE. Combined effects of insulin and exercise on muscle function in severe burn. Poster presented at: 11th Annual Academic Surgical Congress; 2016 Feb 2-4; Jacksonville, FL.

Baer LA, Stanford KI, Song J, Wolf SE, Wade CE. Resistance exercise effects on body mass, free fatty acid concentration and fatty acid metabolism in sqWAT following burn and disuse in rats. 49th American Burn Association (ABA) Annual Meeting; 2017 Mar 21-24; Boston, MA.

Baer LA, Harris J, Sindeldecker D, Song J, Wolf SE, Stanford KI, Wade CE. Moderate resistance exercise improved the metabolic profile of adipose tissue in a model of disuse. Poster presented at: 49th American Burn Association (ABA) Annual Meeting; 2017 Mar 21-24; Boston, MA.

Baer LA, Harris J, Sindeldecker D, Song J, Wolf SE, Stanford KI, Wade CE. Moderate resistance exercise improved the metabolic profile of adipose tissue in a model of disuse. Poster presented at: Experimental Biology Annual Meeting; 2017 Apr 22-26; Chicago, IL.

Song J, Baer L, Saeman M, Wade CE, Wolf SE. Transcriptomic profile alterations in burn/hindlimb unloaded rats with insulin and exercise combination treatment. Poster presented at: 40th Annual Shock Society Conference; 2017 Jun 3-6; Fort Lauderdale, FL.

b. Presentations made during the last year

Baer LA, Nutall K, Burchfield J, Vincent S, Stanford KI, Song J, Wolf SE, Wade CE. Effects of the combination of daily insulin plus resistance exercise during the unloading and reloading phases following burn and disuse in rats on body mass, food intake and fat mass. Poster presented at: 50th American Burn Association (ABA) Annual Meeting; 2018 Apr 10-13; Chicago, IL.

Geng CX, Karbhari N, Song J, Baer L, Wolf SE, Wade C. Insulin and exercise combination therapy recovers muscle function in a burn and disuse rat model by activating protein synthesis and inhibiting proteolysis. Oral presentation presented at: 50th American Burn Association (ABA) Annual Meeting; 2018 Apr 10-13; Chicago, IL.

Song J, DeSpain K, Baer L, Burchfield J, Nutall K, Vincent S, Wade C, Wolf SE. A long-term of resistant exercise decreased rat muscle function in fast twitch myofiber dominated plantaris. Poster presented at: 50th American Burn Association (ABA) Annual Meeting; 2018 Apr 10-13; Chicago, IL.

Hernandez P, Fa A, Mitchell T, Buller D, Huebinger R, Van Hal M, Wolf SE, Song J. Molecular and structural changes in Intervertebral Discs following Severe Burn in Rats. Poster presented at: 50th American Burn Association (ABA) Annual Meeting; 2018 Apr 10-13; Chicago, IL.

DeSpain K, Song J, Rosenfeld CR, Wolf S. Vascular smooth muscle dysfunction after burn. Poster presented at: 50th American Burn Association (ABA) Annual Meeting; 2018 Apr 10-13; Chicago, IL.

7. INVENTIONS, PATENTS AND LICENSES

Nothing to report.

8. REPORTABLE OUTCOMES

Nothing to report.

9. OTHER ACHIEVEMENTS

Nothing to report.

10. REFERENCES

1. Herndon DN, Tompkins RG. Support of the metabolic response to burn injury. *Lancet* 2004;363: 1895-902.
2. Jeschke MG, Kraft R, Song J, Gauglitz GG, Cox RA, Brooks NC, Finnerty CC, Kulp GA, Herndon DN, Boehning D. Insulin protects against hepatic damage postburn. *Mol Med* 2011;17: 516-22.
3. de Lateur BJ, Magyar-Russell G, Bresnick MG, Bernier FA, Ober MS, Krabak BJ, Ware L, Hayes MP, Fauerbach JA. Augmented exercise in the treatment of deconditioning from major burn injury. *Arch Phys Med Rehabil* 2007;88: S18-23.
4. Wolf SE, Edelman LS, Kemalyan N, Donison L, Cross J, Underwood M, Spence RJ, Noppenberger D, Palmieri TL, Greenhalgh DG, Lawless M, Voigt D, Edwards P, Warner P, Kagan R, Hatfield S, Jeng J, Crean D, Hunt J, Purdue G, Burris A, Cairns B, Kessler M, Klein RL, Baker R, Yowler C, Tutulo W, Foster K, Caruso D, Hildebrand B, Benjamin W, Villarreal C, Sanford AP, Saffle J. Effects of oxandrolone on outcome measures in the severely burned: a multicenter prospective randomized double-blind trial. *J Burn Care Res* 2006;27: 131-9; discussion 140-1.
5. Wu X, Baer LA, Wolf SE, Wade CE, Walters TJ. The impact of muscle disuse on muscle atrophy in severely burned rats. *J Surg Res* 2010;164: e243-51.
6. Walker HL, Mason AD, Jr. A standard animal burn. *J Trauma* 1968;8: 1049-51.
7. Morey-Holton ER, Globus RK. Hindlimb unloading rodent model: technical aspects. *J Appl Physiol* 2002;92: 1367-77.
8. Tou JC, Foley A, Yuan YV, Arnaud S, Wade CE, Brown M. The effect of ovariectomy combined with hindlimb unloading and reloading on the long bones of mature Sprague-Dawley rats. *Menopause* 2008;15: 494-502.
9. Linderman JK, Gosselink KL, Booth FW, Mukku VR, Grindeland RE. Resistance exercise and growth hormone as countermeasures for skeletal muscle atrophy in hindlimb- suspended rats. *Am J Physiol* 1994;267: R365-71.
10. Baer LA, Wu X, Tou JC, Johnson E, Wolf SE, Wade CE. Bone. 2013 Feb;52(2):644-50. Contributions of severe burn and disuse to bone structure and strength in rats. *Epub* 2012 Nov 7.
11. Pidcoke HF, Baer LA, Wu X, Wolf SE, Aden JK, Wade CE. Insulin effects on glucose tolerance, hypermetabolic response, and circadian-metabolic protein expression in a rat burn and disuse model. *Amy J Physiol Regul Interg Comp Physiol*. 2014 Jul 1.

11. APPENDICES

1. Project Timeline
2. Manuscripts
3. Abstracts
4. Quad Chart

1. Project Timeline

	Year 1				Year 2				Year 3				Year 4			
Progress	Q1	Q2	Q3	Q4	Q5	Q6	Q7	Q8	Q9	Q10	Q11	Q12	Q13	Q14	Q15	Q16
Task																
1	■	■														
2	■	■														
3		■	■	■	■	■	■	■	■				■	■	■	■
4		■	■	■	■	■	■	■	■				■	■	■	■
5		■	■	■	■	■	■	■					■	■	■	■
6		■	■	■	■	■	■	■					■	■	■	■
7		■	■	■	■	■	■	■	■	■	■	■	■	■	■	■
8		■	■	■	■	■	■	■	■	■	■	■	■	■	■	■
Key	■	All Dr. Wade's tasks have been completed														

2. Manuscripts

Manuscript Number:

Title: Muscle function improved in injured mice with a biological de-cellularized matrix application

Article Type: Regular Article

Keywords: mouse, muscle isometric force, porcine derived Urinary Bladder Matrix (UBM), muscle laceration injury

Corresponding Author: Dr. Juquan Song, MD

Corresponding Author's Institution: UT Southwestern Medical Center

First Author: Melody R Threlkeld, MD

Order of Authors: Melody R Threlkeld, MD; Steven E Wolf, MD; Juquan Song, MD

Suggested Reviewers: Thomas Walters
US Army Institute of Surgical Research
thomas.j.walters22.civ@mail.mil

Celeste Finnerty
University of Texas Medical Branch
ccfinner@UTMB.EDU

Marcas M Bamman
University of Alabama at Birmingham
mbamman@uab.edu

1 Muscle function improved in injured mice with a biological de-cellularized matrix
2 application

3 Melody R.S. Threlkeld, Steven E. wolf, Juquan Song*

4 Division of General and Acute Care Surgery, Department of Surgery, University of Texas
5 Southwestern Medical Center, Dallas, Texas

6 Short Title: Mouse muscle function recovery with UBM treatment

7 *Corresponding author: Juquan Song

8 Department of Surgery

9 UT Southwestern Medical Center

10 Dallas, TX 75390-9160

11 Tel.: 1-214-648-2338

12 Fax: 1-214-648-8420

13 E-mail: Juquan.Song@UTSouthwestern.edu

14 MRST is for animal experiment and muscle function test, SEW for experiment concept and
15 clinical relevance, JS experiment design and data collection

16 MRST: msaeman@gmail.com

17 SEW: swolf@UTMB.edu

18 JS: Juquan.Song@UTSouthwestern.edu

19 *Conflicts of interest and source of funding:* This work was supported by funds from the Golden
20 Charity Guild Charles R. Baxter, MD, Chair; the Department of Defense #W81XWH-13-1-0462;
21 and the National Institute for General Sciences of the National Institutes of Health under award
22 number T32GM008593. The authors have no financial or other interests construed as a conflict
23 of interest.

24 ABSTRACT: 250

25 **Introduction:** skeletal muscle injury with muscle mass loss leads to the concerns of muscle
26 function recovery later time after life threaten rescue. The novel bio-scaffold application of
27 porcine derived Urinary Bladder Matrix (UBM) is beneficial of tissue regeneration. However the
28 significance of UBM application in animal models was limited due to the treatment time. The
29 purpose of the study is to investigate whether UBM treatment 14 days after injury improves
30 muscle function recovery in injured mice. **Methods:** C57BL/6 male adult mice received bilateral
31 laceration injuries on the gastrocnemius muscle under anesthesia, following treated with 150 μ g
32 of UBM nanoparticle or vehicle injection. The treatment was applied either right after injury or
33 14 days after injury. Muscle isometric force was measured at 49 days after injury. A second
34 experiment was separately performed to investigate the effect of UBM on muscle function
35 recovery in injured mice at 49 and 90 days. **Results:** Twitch (Pt) and tetanic (Po) significantly
36 decreased about 25% in injured mice at day 49. Muscle fatigue maximum force significantly
37 increased at later time treatment compared to either vehicle treatment or UBM treatment right
38 after injury. ($p < 0.05$) The second experiment showed that Pt and Po significantly increased in
39 treated mice at day 49. However, there is no further of muscle function improvement observed in
40 injured mice with treatment at day 90. **Conclusion:** We observed muscle function recovery in
41 injured mice with UBM treatment 49 days after injury. The current model is suitable to test other
42 therapeutic strategy for muscle function improvement.

43

44 **Key words:** muscle isometric force, porcine derived Urinary Bladder Matrix (UBM), laceration
45 injury

46 **Introduction:**

47 Skeletal muscle represents the largest tissue mass in the body, with 40% to 45% of total
48 body weight providing supportive and locomotive function ¹. Loss of skeletal muscle from
49 direct injury can present debilitating effects to an individual. Later time after life threaten rescue
50 focused on function recovery and quality improvement. For those with loss of muscle from
51 direct injury, such as projectile fragments or crush injury, current management options
52 include functional free muscle transfer and the use of advanced bracing ² which have limited
53 efficiency on functional recovery. Recent reports describe functional free muscle
54 transplantation in the forearm ³ and elbow ⁴, has limitation with insufficient of function recovery.
55 Improvement in direct muscle re-growth therefore becomes a much more suitable option, if
56 possible, for patients with severe muscle injury and loss.

57 Novel regenerative medicine technologies has been applied in clinical studies of skeletal
58 muscle regeneration in trauma and burn patients ^{5 6 7}. Aside from studies of cell viability itself,
59 the extracellular environment is considered one of the most important factors related to cell
60 growth into functional tissue. Extracellular matrix provides a robust cell growth
61 microenvironment based on its structure, and contains activation factor components to
62 engender cell migration, localization, and differentiation ⁸ into functional tissue components.
63 A type of extracellular matrix derived from de-cellularized porcine urinary and bladder mucosa ⁹
64 (UBM) has been shown to improve different types of tissue regeneration *in vivo* ^{10 11}. UBM
65 contains over 90% type I, III, IV and V collagens with other components including
66 glycosaminoglycan (GAG), transforming growth factor (TGF), basic fibroblast growth factor
67 (bFGF), and vascular endothelial growth factor (VEGF). UBM provides a suitable

68 microenvironment for regeneration, and also has putative bio-active growth factors for progenitor
69 cell recruitment and propagation ¹².

70 A clinical case was shown the significant muscle mass improvement and function
71 recovery with implantation of porcine derived extracellular matrix for volumetric muscle loss
72 (VML) in a severely injured patient. In this clinical trial, muscle mass increased by 15% and
73 muscle function over 20% via leg extension torque test comparing data obtained 5 months prior
74 to UBM implantation and 9 months after ¹³. Implantation of extracellular matrix was not
75 performed until after strength was maximised through resistance training, and these
76 improvements were in addition to these. Another clinical study revealed that function
77 improvement with UBM treatment is associated with increased innervated muscle tissue islands
78 ¹⁴. However, the mechanisms of which UBM treatment improves muscle regeneration are still
79 investigated.

80 We seek a suitable animal model to address the clinical questions. Most bench studies of
81 muscle injury animal models were applied matrix treatment right after injury ^{15 16}, which are not
82 fully mimic clinical treatment and thus limit the data interpretation and translational significance.
83 In general the processing of tissue healing and recovery including injury acute inflammation,
84 subacute repair and late remodeling phases. The muscle function outcome could be altered if the
85 treatment is applied at different stages. We hypothesized that muscle function is further
86 improved when UBM is treated after the acute phase of injury. In the current study we treated
87 injured animals with UBM nanoparticle 14 days after injury, and we examined muscle isometric
88 function 49 and 90 days.

89

90 **Methods:**

91 C57BL/6 male adult mice (7 weeks old, from Jackson Laboratory, Bar Harbor, ME) were
92 acclimated one weeks in the animal facility at UTSW and then enrolled in the study. The animal
93 procedure was followed NIH guideline and the animal protocol was approved by IACUC at UT
94 Southwestern Medical Center (UTSW). Mouse was housed individually with free access of
95 water and food during the experiment.

96 Experiment 1 was to compare muscle function recovery with the treatment at the
97 different stage after injury. Twenty mice received bilateral laceration injuries procedure on the
98 gastrocnemius muscle under anesthesia, and were randomly grouped with treatment right after
99 injury (E) or 14 days (L) after injury. At each time point, injured animals were further grouped
100 with either vehicle (V, n=4) or UBM (U, n=6) treatment. Four additional animals were housed
101 paired without any procedure served as the baseline.

102 Experiment 2 was to confirm muscle function improvement with treatment over time.

103 Sixteen mice received bilateral laceration injuries procedure on the gastrocnemius muscle under
104 anesthesia, and were randomly grouped with vehicle (V, n=8) or UBM (U, n=8) treatment
105 applied 14 days later. Four animals from each group were examined for function recovery at day
106 49 and 90 after injury. Eight additional animals were housed paired without any procedure
107 served as the baseline (n=4/time point).

108 *Muscle laceration procedure* Animal was anesthetized with 2% isoflurane inhalation,
109 weighed and hair removed from both hindlimb. Mice was on prone position with aseptic
110 preparation. The skin above the gastrocnemius area was incised using a surgical blade (no. 11;
111 SteriSharps, Mansfield, MA). Gastrocnemius (GN) was blunted isolated from adjacent tissue
112 after upfolding biceps femoris and semitendinosus. GN was separated from soleus by inserting a
113 steel scalpel handle end (Brad-Parker, size 4) and two parallel full muscle thickness incisions
114 were made longitudinally in the middle of gastrocnemius with 3mm-width and 7mm-length. The

115 whole pieces of muscle was cut off with a fine scissor and leads to over 20% weight loss of
116 gastrocnemius muscle. After laceration, the skin was closed with simple interrupted suture. A
117 dose of buprenorphine SR 0.05mg/kg was given subcutaneously. Fully recovered animals were
118 housed individually at the animal facility with food and water *ad libitum* during the experiment.

119 *UBM/Vehicle treatment procedure* Animals were under anesthesia with 2% isoflurane
120 inhalation. 150 µg of UBM was suspended in 15 µl of Dulbecco's Modified Eagle Media
121 (DMEM) (ATCC, Manassas, VA) and injected intramuscularly using 1ml syringe with 23g ³/₄
122 needle (BD Bioscience, San Jose, CA). MatriStem MicroMatrix (UBM) was purchased from
123 ACell Inc (Columbia, MD). Vehicle treatment was given to animals with the same amount of
124 DMEM. Animal was fully awoken and housed at animal facility till the end of experiment.

125 *Isometric force measurement* Isometric contractile properties of the gastrocnemius
126 muscles were measured by 1305A whole animal system (Aurora Scientific, ON, Canada) and the
127 procedure described as previously ¹⁷. Under anesthesia, animal was secured on the 37°C platform
128 which is connected with a circulated water bath. The gastrocnemius muscle in left limb was
129 gently dissected free of surrounding tissue and the Achilles tendon was secured with 4-0 surgical
130 suture and attached to the lever arm of a dual mode servo muscle lever system (mod #305c,
131 Aurora Scientific, Inc). Electrodes were implanted into the distal end of severed sciatic nerve and
132 the twitch, tetanic and fatigue isometric functions of the muscle were analyzed after optimal
133 length (Lo) of the muscle was achieved. A single twitch (Pt) was stimulated with a 200 Hz
134 impulse at 10mA while the muscle was then stretched 0.2 mm every 25s. The optimal length
135 (Lo) of the muscle was reached when there was less than 2% change between twitches. The
136 isometric tetanic force (Po) was stimulated at 150 Hz with impulse duration of 0.2ms, 75 pulses
137 per train for a total of 1s. Fatigue measurement was at 40Hz with impulse duration of 0.2 ms, 14
138 pulses per train, 10 mA, for a total of 240s.

139 *Muscle sample harvest and histology processing* Animal was euthanized after *in situ*
140 muscle function test and gastrocnemius from both limbs were collected and weighed. Muscle
141 tissue were fixed in 10% neutral buffered formalin and histological processed for paraffin
142 embedding. Tissue sections (5µm) were deparaffinized and rehydrated following the standard
143 Hematoxylin & Eosin (H&E) staining procedure. The image was taken by a Nikon Eclipse Ti
144 microscope under a 10x objective using NIS-Elements v4.60 software.

145 *Statistical analysis* Statistical analysis was performed using two-way analysis of variance
146 (ANOVA) with Bonferroni post hoc tests, and paired student's t-test where appropriate. All data
147 are presented as mean ± stand error of the mean (SEM). Significance was accepted at $p < 0.05$.
148 nn

149 **Results:**

150 *Experiment 1*

151 Normalized to mouse body weight at day 0, there was not significant body weight change
152 in injured mice between treatments at day 49. We corrected tissue weight of gastrocnemius
153 muscle (at day 49) by plusing lacerated tissue weight (at day 0), then normalizing with the body
154 mass. We found that the corrected tissue weight normalized to body mass in animals was greater
155 with later treatment. The corrected tissue weight was greater in mice treated 14 days later
156 compared to those treated right after injury, ($p < 0.05$) suggesting the importance of treatment
157 time following injury. [Table 1]

158 The twitch (Pt), tetanic (Po), and fatigue isometric functions were analyzed *in situ* at day
159 49 after injury when the muscle stretched to the optimal length (Lo). Pt and Po significantly

160 decreased in injured mice at day 49 compared to normal mice. ($p < 0.05$) Lo was significantly
161 greater in late time treatment than earlier time point. ($p < 0.05$) Muscle fatigue maximum force
162 significantly increased in mice at later time treatment compared to those either with vehicle
163 treatment, or treatment right after injury. ($p < 0.05$) [Table 2]

164 *Experiment 2*

165 In the 2nd experiment, isometric force Pt and Po decreased with tissue weight loss in
166 injured mice significantly at day 49 compared to no-injured mice. ($p < 0.05$) Pt, Po, and sPo
167 significantly increased in UBM treated mice compared to vehicle treated mice. ($p < 0.05$) [Table
168 3] The results again confirmed the effect of later time treatment from Experiment 1. At day 90,
169 there was not difference of body weight and tissue weight between injured and non-injured mice.
170 In addition, there was no muscle function improvement observed in injured mice with treatment
171 at day 90. [Table 4]

172

173 DISCUSSION:

174 In the current animal model with direct muscle laceration, muscle mass loss leads to
175 muscle function impairment with over 23% of maximum tetanic force reduction in 49 days, and
176 no significant decreased muscle force was observed at 90 days after injury. We further found that
177 the nanoparticle form of UBM sped up muscle function recovery at day 49. This result was
178 confirmed from two separated experiments in the current study.

179 There are several animal models of direct injury pattern to study the muscle recovery,
180 including cryoinjury¹⁸, chemical cardiotoxin injection¹⁹, physical contusion²⁰ and sharp
181 laceration. Wu developed the massive muscle loss with laceration injury in rat model which was

182 fully described the healing time process ²¹. We chose the current model with similar laceration
183 injury to test our therapeutic strategy.

184 Merritt EK observed that injured rats with homologous extracellular matrix implantation
185 was only presented as tissue regeneration morphologic improvement but kept about 20% force
186 loss till 42 days ²². We thus designated our observational time at 49 days after injury. We didn't
187 observe the changes with treatment applied right after injury either (E-U vs. E-V). Surprisingly
188 an increased fatigue maximum force was observed in injured mice when UBM given 14 days
189 later. The result is more convincible when mice muscle function with UBM treatment was
190 repetitively improved in the second separated experiment.

191 We observed that the benefit of UBM has been diminished at day 90 and we speculated
192 that was due to biomaterial depletion and animal model self-recovery limitation. The current
193 format of UBM is nanoparticle which designs to be absorbed. UBM contains several growth
194 factors, and when UBM is decomposed with depleted of growth factors, tissue self-regenerating
195 finally covers the effect of UBM.

196 We noticed that the force value at day 90 re lower compared to other time points, and that
197 was due to the system calibration before each experiment. The animal posture and its
198 interrelationship of transducer could affected the value reading mainly. We previously noticed
199 that difference of value reading in left and right limb from one single animal because of animal
200 testing posture change related to the transducer. In this study, we measured muscle force only in
201 left limb from animals. Also, we set up a non-injury and no-treatment group as the baseline to
202 validate each single experiment.

203 In the current study, we focused on the muscle physiological improvement with isometric
204 force measurement. Beattie et al reported that UBM treatment improved tendon repair, which is

205 associated with chemotaxis of multipotential progenitor cells to wound site ²³, and this benefit
206 might be related with bioactive components released from UBM ²⁴. Though we did not focus the
207 cellular mechanism of muscle function improvement with UBM application, we speculate that
208 the time of UBM intervention could be the key because there is distinguishable cell population in
209 muscle tissue along with tissue injury-recovery period. Immune cells participate tissue wound
210 healing process, and there are two phenotypes of macrophage participating tissue regeneration ²⁵.
211 UBM application later after injury might match the time of phenotype changed macrophage or
212 monocytes, further facilitate the muscle regeneration and function improvement. The next step
213 we will investigate how UBM interact with M1 and M2 macrophage during the tissue recovery
214 period.

215 The cellular mechanism of UBM in mediating muscle cells with function recovery is
216 complicated. There are studies showing that UBM worsen co-grafted muscle cells ²⁶, or improve
217 the muscle cell presentation. Also another study showed that biological matrix not improved
218 muscle cell but jut fibroblast ²⁷. Walters' group reported multiple layers wrapped in rat right after
219 laceration improves muscle function and fibrotic tissue remodeling, but there is no evidence of
220 muscle tissue regeneration at day 28. We observed that increased myogenesis in cryo-injured
221 mice with UBM treatment ²⁸. In vitro we further found that UBM increased proliferation marker
222 PCNA expression in mouse myoblast C2C12 cell, supporting the direct effect of UBM on
223 muscle cells. [Data shown/no shown]. In the current study, tissue trichrome staining showed that
224 a prominent of fibrosis formation in muscle tissue with UBM treatment, especially treated right
225 after injury. Meanwhile the central localized myotube also were observed in UBM treatment
226 group. [Figure 1] The different outcome might be argued with different experimental settings
227 especially treatment time. We used nanoparticle form of UBM given to animals 14 days after

228 injury. The specific treatment condition could alter the interaction among different types of cells
229 involved muscle tissue regeneration.

230 In conclusion, the current study provides a reliable and clinical relevant model to
231 investigate muscle function recovery for therapeutic development. The data from the current
232 study showed that UBM nanoparticle accelerates muscle function recovery in injured mice;
233 furthermore, the limited effect of UBM demands us to optimize the therapy strategy in future.

234

235

236

237

238 ACKNOWLEDGEMENT

239

240 We thank Kevin DeSpain for supporting sample and data collection.

241 REFERENCE

- 242 1. Beatty CH, Basinger GM, Bocek RM. Differentiation of red and white fibers in muscle
243 from fetal, neonatal and infant rhesus monkeys. *J Histochem Cytochem.* 1967;15(2):93-
244 103.
- 245 2. Lin CH, Lin YT, Yeh JT, et al. Free functioning muscle transfer for lower extremity
246 posttraumatic composite structure and functional defect. *Plast Reconstr Surg.*
247 2007;119(7):2118-2126.
- 248 3. Fan C, Jiang P, Fu L, et al. Functional reconstruction of traumatic loss of flexors in
249 forearm with gastrocnemius myocutaneous flap transfer. *Microsurgery.* 2008;28(1):71-
250 75.
- 251 4. Vekris MD, Beris AE, Lykissas MG, et al. Restoration of elbow function in severe
252 brachial plexus paralysis via muscle transfers. *Injury.* 2008;39 Suppl 3:S15-22.
- 253 5. Novikova LN, Novikov LN, Kellerth JO. Biopolymers and biodegradable smart implants
254 for tissue regeneration after spinal cord injury. *Curr Opin Neurol.* 2003;16(6):711-715.
- 255 6. Schertzer JD, Lynch GS. Comparative evaluation of IGF-I gene transfer and IGF-I
256 protein administration for enhancing skeletal muscle regeneration after injury. *Gene Ther.*
257 2006;13(23):1657-1664.
- 258 7. Burd A, Ahmed K, Lam S, et al. Stem cell strategies in burns care. *Burns.*
259 2007;33(3):282-291.
- 260 8. van der Kraan PM, Buma P, van Kuppevelt T, et al. Interaction of chondrocytes,
261 extracellular matrix and growth factors: relevance for articular cartilage tissue
262 engineering. *Osteoarthritis Cartilage.* 2002;10(8):631-637.

- 263 9. Brown BN, Barnes CA, Kasick RT, et al. Surface characterization of extracellular matrix
264 scaffolds. *Biomaterials*. 2010;31(3):428-437.
- 265 10. Gilbert TW, Gilbert S, Madden M, et al. Morphologic assessment of extracellular matrix
266 scaffolds for patch tracheoplasty in a canine model. *Ann Thorac Surg*. 2008;86(3):967-
267 974; discussion 967-974.
- 268 11. Liu L, Li D, Wang Y, et al. Evaluation of the biocompatibility and mechanical properties
269 of xenogeneic (porcine) extracellular matrix (ECM) scaffold for pelvic reconstruction. *Int*
270 *Urogynecol J*. 2011;22(2):221-227.
- 271 12. Hodde JP, Record RD, Tullius RS, et al. Retention of endothelial cell adherence to
272 porcine-derived extracellular matrix after disinfection and sterilization. *Tissue Eng*.
273 2002;8(2):225-234.
- 274 13. Mase VJ, Jr., Hsu JR, Wolf SE, et al. Clinical application of an acellular biologic scaffold
275 for surgical repair of a large, traumatic quadriceps femoris muscle defect. *Orthopedics*.
276 2010;33(7):511.
- 277 14. Dziki J, Badylak S, Yabroudi M, et al. An acellular biologic scaffold treatment for
278 volumetric muscle loss: results of a 13-patient cohort study. *NPJ Regen Med*.
279 2016;1:16008.
- 280 15. Sicari BM, Rubin JP, Dearth CL, et al. An acellular biologic scaffold promotes skeletal
281 muscle formation in mice and humans with volumetric muscle loss. *Sci Transl Med*.
282 2014;6(234):234ra258.
- 283 16. Corona BT, Wu X, Ward CL, et al. The promotion of a functional fibrosis in skeletal
284 muscle with volumetric muscle loss injury following the transplantation of muscle-ECM.
285 *Biomaterials*. 2013;34(13):3324-3335.

- 286 17. Saeman MR, DeSpain K, Liu MM, et al. Severe burn increased skeletal muscle loss in
287 mdx mutant mice. *J Surg Res.* 2016;202(2):372-379.
- 288 18. Warren GL, Hulderman T, Mishra D, et al. Chemokine receptor CCR2 involvement in
289 skeletal muscle regeneration. *FASEB J.* 2005;19(3):413-415.
- 290 19. Gayraud-Morel B, Chretien F, Flamant P, et al. A role for the myogenic determination
291 gene Myf5 in adult regenerative myogenesis. *Dev Biol.* 2007;312(1):13-28.
- 292 20. Crisco JJ, Jokl P, Heinen GT, et al. A muscle contusion injury model. Biomechanics,
293 physiology, and histology. *Am J Sports Med.* 1994;22(5):702-710.
- 294 21. Wu X, Corona BT, Chen X, et al. A standardized rat model of volumetric muscle loss
295 injury for the development of tissue engineering therapies. *Biores Open Access.*
296 2012;1(6):280-290.
- 297 22. Merritt EK, Hammers DW, Tierney M, et al. Functional assessment of skeletal muscle
298 regeneration utilizing homologous extracellular matrix as scaffolding. *Tissue Eng Part A.*
299 2010;16(4):1395-1405.
- 300 23. Beattie AJ, Gilbert TW, Guyot JP, et al. Chemoattraction of progenitor cells by
301 remodeling extracellular matrix scaffolds. *Tissue Eng Part A.* 2009;15(5):1119-1125.
- 302 24. Reing JE, Zhang L, Myers-Irvin J, et al. Degradation products of extracellular matrix
303 affect cell migration and proliferation. *Tissue Eng Part A.* 2009;15(3):605-614.
- 304 25. Wynn TA, Vannella KM. Macrophages in Tissue Repair, Regeneration, and Fibrosis.
305 *Immunity.* 2016;44(3):450-462.
- 306 26. Ehrhart IC, Parker PE, Weidner WJ, et al. Coronary vascular and myocardial responses to
307 carotid body stimulation in the dog. *Am J Physiol.* 1975;229(3):754-760.

308 27. Aurora A, Roe JL, Corona BT, et al. An acellular biologic scaffold does not regenerate
309 appreciable de novo muscle tissue in rat models of volumetric muscle loss injury.

310 *Biomaterials*. 2015;67:393-407.

311 28. Song J, Hornsby P, Stanley M, et al. Porcine urinary bladder extracellular matrix
312 activates skeletal myogenesis in mouse muscle cryoinjury. *Journal of Regenerative*

313 *Medicine & Tissue Engineering*. 2014;3(3).

314

315

316

317

318

319

320

321

322

323

324

325

326

327

328 TABLE AND FIGURE LEGENDS:

329 Table 1 Animal body change and muscle tissue changes 49 days after injury

330 Δ , $p < 0.05$, late (L) vs. Earlier treatment (E); μ , $p < 0.05$, L-U vs. E-U group, two-way ANOVA.

331 TW-Gastrocnemius tissue weight; BM-body weight at day 49.

332

333 Table 2 Isometric force in mouse right gastrocnemius 49 days after injury

334 +, $p < 0.05$, vs. N-C, Student's t-test. *, $p < 0.05$, vs. E-V; Δ , $p < 0.05$, vs. E-U; ϕ , $p < 0.05$, vs. L-V,

335 two-way ANOVA. TW- tissue weight; Lo- optimal length; $\frac{1}{2}$ RT-half relaxation time; Pt- twitch

336 force; Po- tetanic force; sPo-specific tetanic force; Ft-Fatigue

337

338 Table 3 Isometric force in mouse right gastrocnemius 49 days after injury in Experiment 2

339 +, $p < 0.05$, vs. N-C; Δ $p < 0.05$, vs. V group, Student's t-test. BM- body weight; TW- tissue weight; Lo-

340 optimal length; $\frac{1}{2}$ RT-half relaxation time; Pt- twitch force; Po- tetanic force; sPo-specific tetanic force;

341 Ft-Fatigue

342

343 Table 4 Isometric force in mouse right gastrocnemius 90 days after injury in Experiment 2

344 BM- body weight; TW- tissue weight; Lo- optimal length; $\frac{1}{2}$ RT-half relaxation time; Pt- twitch force;

345 Po- tetanic force; sPo-specific tetanic force; Ft-Fatigue

346

347 Figure 1

348 Trichrome staining of mouse gastrocnemius muscle tissue. N-C: normal control; E-D: DMEM

349 treatment right after injury; E-U: UBM treatment right after injury; L-D: DMEM treatment at 14

350 days after injury; L-U: DMEM treatment at 14 days after injury.

Table 1

Treatment time after Injury	Treatment	Group (n)	Body weight change	TW (g)	TW/BM (mg/g)	Corrected TW/BM (mg/g)
No injury	No	N-C (n=5)	1.18±0.01	0.138±0.002	5.21±0.11	5.21±0.11
0 day (E)	Vehicle	E-V (n=4)	1.16±0.02	0.091±0.009	3.41±0.33	4.39±0.45
	UBM	E-U (n=6)	1.17±0.02	0.092±0.003	3.47±0.09	4.24±0.09
14 days (L)	Vehicle	L-V (n=4)	1.21±0.01	0.110±0.011	4.14±0.49	5.13±0.43
	UBM	L-U (n=6)	1.19±0.05	0.102±0.007	3.84±0.23	5.04±0.13 Δ μ

Table 2

No-injury No-treatment N-C (n=5)	Treatment at 0 day Vehicle		Treatment at 14 days Vehicle		
	E-V (n=4)	UBM		L-V (n=4)	UBM
		E-U (n=6)	L-U (n=6)		
Tissue					
weight (g)	0.152±0.010	0.143±0.009	0.122±0.005	0.124±0.007 *	0.132±0.008
Lo (cm)	1.51±0.04	1.54±0.097	1.55±0.04	1.75±0.04 *	1.54±0.05 f
½ RT (s)	0.0165±0.0016	0.0142±0.0006	0.01656±0.0008	0.0156±0.0009	0.0156±0.0009
Pt (g)	101.50±3.74	78.14±7.69 +	83.91±3.88	72.24±5.96 +	89.57±4.60
Po (g)	272.96±17.84	235.93±7.44	212.36±23.43	184.62±9.34 +	230.95±16.87
Pt/Po	0.36±0.01	0.32±0.02	0.40±0.02	0.37±0.03	0.44±0.03
sPo/PCSA	282.68±18.33	270.74±30.89	282.08±33.38	293.99±37.85	279.03±13.99
Ft-max	178.56±27.08	133.19±16.90	127.47±18.38	108.96±19.00	176.12±14.85φ Δ

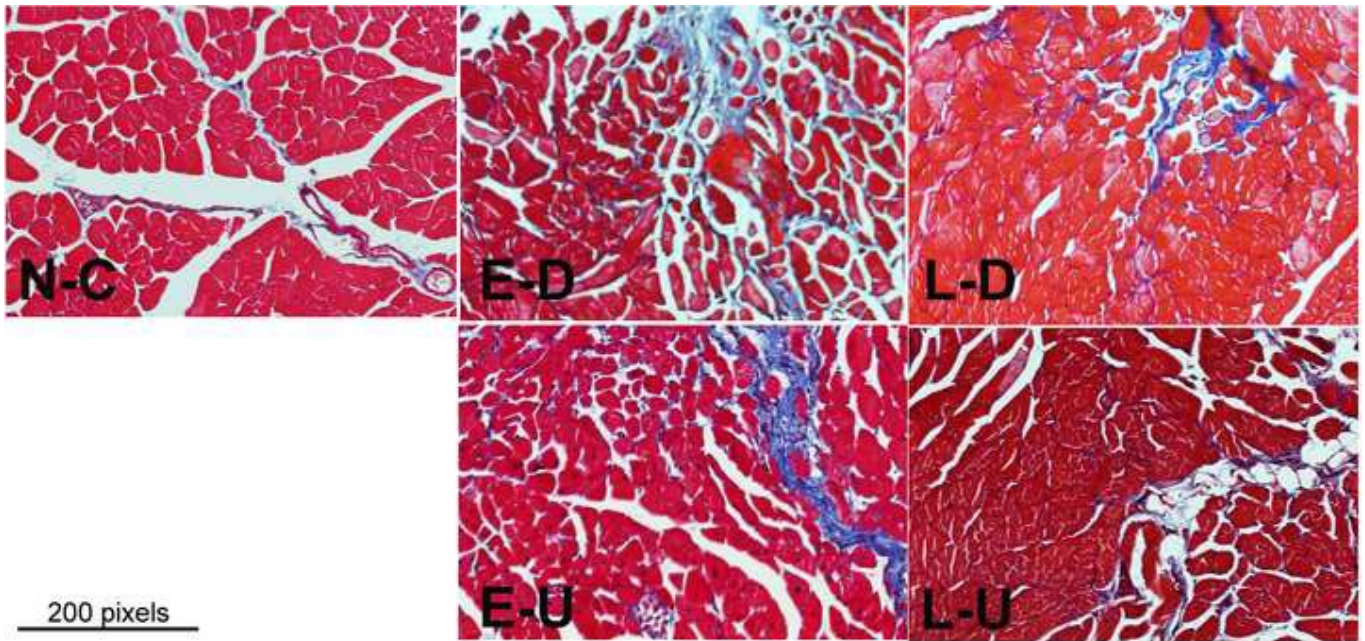
Table 3

D 49	No-injury	Treatment	
	No-treatment N-C (n=4)	Vehicle V (n=4)	UBM U (n=4)
BM (g)	27.14±0.88	25.01±0.96	26.33±0.20
TW (g)	0.171±0.007	0.143±0.001 +	0.150±0.006
TW/BM (mg/g)	6.28±0.20	5.75±0.21	5.68±0.20
Lo (cm)	1.69±0.07	1.55±0.08	1.52±0.05
½ RT (s)	0.0156±0.002	0.0142±0.001	0.0143±0.001
Pt (g)	91.39±2.84	61.21±4.18 +	82.85±7.24 Δ
Po (g)	324.52±49.54	251.25±16.53	300.16±4.29 Δ
sPo (N/cm ²)	34.06±5.21	24.36±2.05	30.86±1.83 Δ
Ft-max (g)	176.25±17.02	147.48±13.33	163.97±17.58
Ft-min (g)	8.88±0.64	9.25±4.09	8.37±3.18

Table 4

D90	No-injury	Treatment	
	No-treatment N-C (n=4)	Vehicle V (n=4)	UBM U (n=4)
BM (g)	31.41±1.17	30.11±1.17	28.84±1.46
TW (g)	0.192±0.006	0.157±0.015	0.164±0.0016
TW/BM (mg/g)	6.13±0.29	5.21±0.46	5.67±0.43
Lo (cm)	1.65±0.03	1.58±0.07	1.50±0.09
½ RT (s)	0.0141±0.0006	0.0148±0.0005	0.0132±0.0004
Pt (g)	68.59±6.14	54.24±5.20	44.59±5.92
Po (g)	175.64±31.85	163.76±42.89	154.69±45.78
sPo (N/cm ²)	20.68±2.57	14.64±3.34	16.20±4.82
Ft-max (g)	72.92±13.17	83.43±29.08	63.27±28.35
Ft-min (g)	3.42±0.65	6.16±3.56	3.06±1.34

Figure
[Click here to download high resolution image](#)



Shock. 2018 Sep; 50(3): 346–350.

Published online 2018 Aug 13. doi: 10.1097/SHK.0000000000001037 PMID: PMC6072366

PMID: 29065066

Severe Burn-Induced Inflammation and Remodeling of Achilles Tendon in a Rat Model

Paula Hernandez,* Dustin Buller,* Thomas Mitchell,* Jamie Wright,† Haixiang Liang,§ Kshitij

Manchanda,*Tre Welch,† Ryan M. Huebinger,‡ Deborah L. Carlson,‡ Steven E. Wolf,‡ and Juquan Song†

Author information Article notes Copyright and License information Disclaimer

ABSTRACT

[Go to:](#)

INTRODUCTION

Severe burn is defined as a full-thickness burn of greater than 30% of total body surface area (TBSA). It occurs at a rate of approximately 5/100,000 persons per year globally and may affect multiple organs, even those distantly located from the burn site (1). In the musculoskeletal system, severe burn induces hypercatabolism in muscle and bone due to the activation of systemic inflammation, and disuse from long immobilization periods (2–6). Muscle loss and atrophy postburn have been associated with increased levels of TNF- α (7), whereas bone mass loss has been associated with circulating TNF- α , IL-1 β , and IL-6, which are increased shortly after burn (8–10). Despite the findings of mass loss in both skeletal muscle and bone, there are limited studies on the molecular and structural effects of burn injury on tendon.

Tendon injuries are common events occurring in sports and other activities (11–13). Tendons are mostly composed of type I collagen fibrils aggregated together into fibers to provide tensile strength (14). There are also type III collagen fibrils intercalated into the collagen I fibers (14). When tendon experiences remodeling or injury, collagen III content increases, resulting in a decrease in tensile strength (15). On the contrary, metalloproteinases such as the collagenase MMP13 can cleave the collagen triple helix, creating fragments that are further degraded by gelatinases such as MMP9 (16). In addition, modulators of musculoskeletal growth and differentiation, such as TGF β 1, have been reported to coincide with scar formation and healing in tendon (17).

In this study, we hypothesize that the systemic inflammation caused by severe burn will induce molecular and structural changes in Achilles tendon that ultimately debilitate this tissue. By understanding the local changes produced in tendon, it is possible to adopt additional preventive measures to improve healing and to aid with physical therapies that target muscle and bone.

[Go to:](#)

MATERIALS AND METHODS

Animals

The animal protocol was approved by the Institutional Animal Care and Use Committee at the University of Texas Southwestern Medical Center at Dallas in accordance with the Institutional and Association for Assessment and Accreditation of Laboratory Animal Care guidelines and in accordance with NIH guidelines. All animal procedures were carried out at the UT Southwestern animal facility. A total of 40 adult male Sprague–Dawley rats (Charles Rivers), 270–300g, were acclimated in an animal facility a week before the experiment. Animals were fed a pellet diet (Harlan Teklad #2018) *ad libitum* and housed in a reversed 12-h light/dark cycle with maintained room temperature.

Burn procedure

Animals were randomly divided into five groups: control (n = 11), and 1 day (n=6), 3 days (n=6), 7 days (n=6), and 14 days (n=11) postburn. Under 2% to 4% isoflurane inhalation anesthesia, animal hair was removed from the dorsal and lateral surfaces and the animals were secured in a specifically constructed template device with opening size of 10cm length and 7cm wide (curved). Dorsal skin amounting to 40% of TBSA was exposed through the device aperture and immersed in 95°C to 100°C water for 10s. The burned animals then received intraperitoneally 4mL/kg body weight/TBSA% of lactated Ringer's solution for resuscitation immediately after injury. Animals were given analgesia intraperitoneally (buprenorphine HCl 0.05 mg/kg) immediately and 12h postburn. Control animals received sham treatment with the procedure of hair removal, anesthesia, and submersion in room temperature water. Control animals were not subjected to resuscitation procedure because injecting this amount of liquid intraperitoneally will cause cardiac failure and/or abdominal compartmentalization syndrome that would be fatal.

Tissue harvesting

Animals were euthanized with anesthetic overdose. Achilles tendons were isolated from surrounding tissue and dissected from both sides of hind limbs. The proximal ends of the Achilles tendons were disconnected at the end of the gastrocnemius, plantaris, and soleus, and the distal ends at the calcaneus. Left leg tendons of eight control rats and six burn rats for each time point (1, 3, 7, and 14 days) were stored in RNeasy Lysis Buffer (Qiagen), whereas right leg tendons were snap frozen for protein extraction. Samples were stored in -80°C for further analysis. Tendon RNA was obtained with RNeasy Universal kit (Qiagen). cDNA conversion was done with iScript kit (Bio-Rad), and qPCR with SsoFast Eva Green kit (Bio-Rad). Primers for IL-6, TNF, IL-1 β , col1a1, col3a1, MMP9, MMP13, and TGF β 1 were purchased from QuantiTect Primers (Qiagen). Gene expression was calculated using the $\Delta\Delta\text{Ct}$ method with 18s as housekeeping.

For protein extraction, tendon tissue was homogenized in RIPA buffer (Invitrogen) with proteinase inhibitor cocktail (Sigma). Protein quantification was performed with BCA assay (Pierce); 10 μg of total protein was used for Western blot. Antibodies included anti-collagen I (Abcam), anti-collagen III (Abcam), goat anti-mouse HRP (Pierce), and goat anti-rabbit HRP (Pierce), which were prepared in 2% BSA. Blots were developed with ECL (Pierce) using a CCD camera system.

Histology

Right leg Achilles tendons were dissected from three control rats and five burn rats (14 days). Parts of the calcaneus bone and gastrocnemius muscle were included. Tendons were fixed in 10% neutralized buffer formalin and decalcified with 10% formic acid. Paraffin sections of 5 μ m were processed for hematoxylin and eosin (H&E) staining, as well as Picrosirius red staining. Samples were visualized in a Nikon Eclipse Ti microscope or in an Olympus BH2-RFCA using polarized light. The image analysis for Picrosirius red was performed using ImageJ (National Institutes of Health (18)). Several regions of 320 \times 320 pixels were selected from the central area of each tendon. After converting the image into 8-bit and 256 color, the measurements of red, green, and blue colors were postprocessed in Excel. For each piece, the (green+blue)/red values were calculated and grouped as control vs. 14 days postburn, where green+blue represent more organized fibers compared with red.

Biomechanics

Three tendons from the control group and five tendons from the burn rats at 14 days postburn were dissected, leaving part of muscle and foot, and wrapped with cold PBS-soaked gauze to prevent dehydration. Sandpaper was fixed to both tendon extremities. Specimens were then clamped and tested using an Instron 5565 universal testing system (Instron Corp., Norwood, MA) equipped with a 5-kN load cell. After preconditioning using a cyclic load oscillating from 0% to 2.5% strain for 20 cycles, samples were finally pulled until failure at a crosshead speed of 6mm/min collecting force and deformation data throughout the test. Tendon material properties, ultimate tensile force, and stiffness were calculated from the force-deformation curve.

Statistics

Data are presented as mean \pm error propagation for gene expression and mean \pm standard deviation elsewhere. Data were analyzed in GraphPad Prism 7 with one-way ANOVA and Fisher LSD posthoc test, or by unpaired Student *t* test when comparing two variables ($P < 0.05$ being significant).

[Go to:](#)

RESULTS

Changes in gene expression of cytokines, MMPs, and TGF β 1 in Achilles tendon after burn

The gene expression of the proinflammatory cytokines in tendon tissue IL-1 β and IL-6 was affected by severe burn. Both increased and reached a peak level at 3 days postburn, being significantly higher compared with control group, $P < 0.05$. The expression of TNF was also higher than control but did not reach a significant level. After 7 days, all three genes decreased back to control levels (Fig. (Fig.11A)).

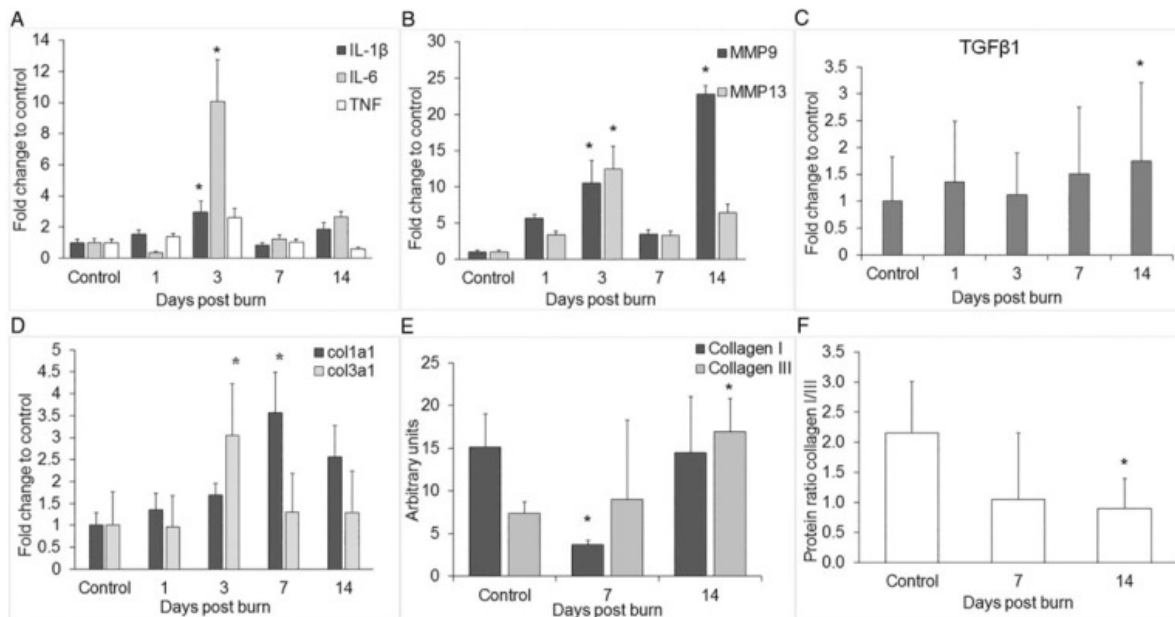


Fig. 1

Changes in expression of proinflammatory cytokines, metalloproteinases, and collagens in Achilles tendon after severe burn.

(A) Gene expression of cytokines IL-1 β , IL-6, and TNF (B) metalloproteinases MMP9 and MMP13, (C) TGF β 1 and (D) collagens col1a1 and col3a1 were examined with qPCR. (E) Protein levels of collagen I and collagen III obtained by Western blot and normalized to total protein (F). Collagen I/III protein ratio was calculated from the Western blot results. Data are shown as mean with error propagation in (A) and (B). Data are shown as mean \pm SD in (C) and (D). * P <0.05 vs. control.

We next analyzed whether the expression of the matrix metalloproteinases commonly affected in tendinopathy were altered by burn. The results showed that the expression of both MMP9 and MMP13 continually increased after the injury and reached significantly higher levels at 3 days postburn compared with the control group, pP <0.05 (Fig. (Fig.1B).1B). MMP9 showed a second significant increase at 14 days postburn by more than 20-fold compared with control, P <0.05 (Fig. (Fig.11B).

TGF β 1, which has been linked to tendon repair and healing, was also analyzed. We found a significant upregulation at day 14 postburn (P <0.05) (Fig. (Fig.11C).

Changes in collagen expression and collagen I/III ratio

The gene expression of col3a1 significantly increased at day 3 postburn, whereas col1a1 did it at day 7 postburn (Fig. (Fig.1D).1D). Protein levels of collagen I were significantly lower at day 7 postburn, P <0.05 (Fig. (Fig.1E)1E) and were restored back to control levels by day 14. Collagen III protein, on the contrary, increased significantly at day 14 postburn, P <0.05 (Fig. (Fig.1E).1E). The protein ratio of collagens I/III showed a significant decrease at day 14 postburn (Fig. (Fig.11F).

Histological and biomechanical evidence of tendon remodeling

We analyzed the control and 14-day postburn tendons stained with H&E to further investigate signs of remodeling. Tenocytes and extracellular matrix fibers were found aligned with the longitudinal axis in the control group. Most of the nuclei of tenocytes showed an elongated shape. In contrast, tendons from animals at 14 days postburn showed less parallel organization of cells and fibers, as well as hypercellularity with cell aggregation and round nuclei (Fig. (Fig.2A).2A). To observe collagen organization in more detail, tendon sections were stained with Picrosirius red and analyzed under polarized light. A representative image of a control rat showed that collagen fibers were more organized and well aligned compared with 14 days postburn, where tendon fibers showed less organization (Fig. (Fig.2B).2B). Our method of quantification of green, blue, and red colors showed that the (green+blue)/red ratio significantly decreased 14 days postburn, $P < 0.05$ (Fig. (Fig.2C).2C).

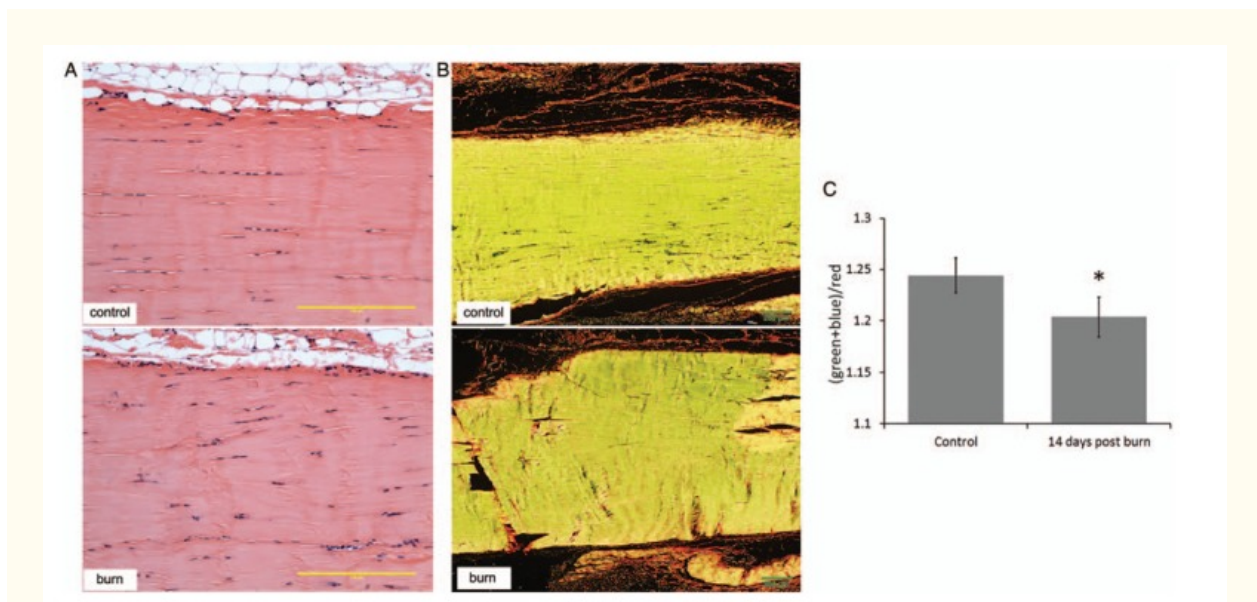
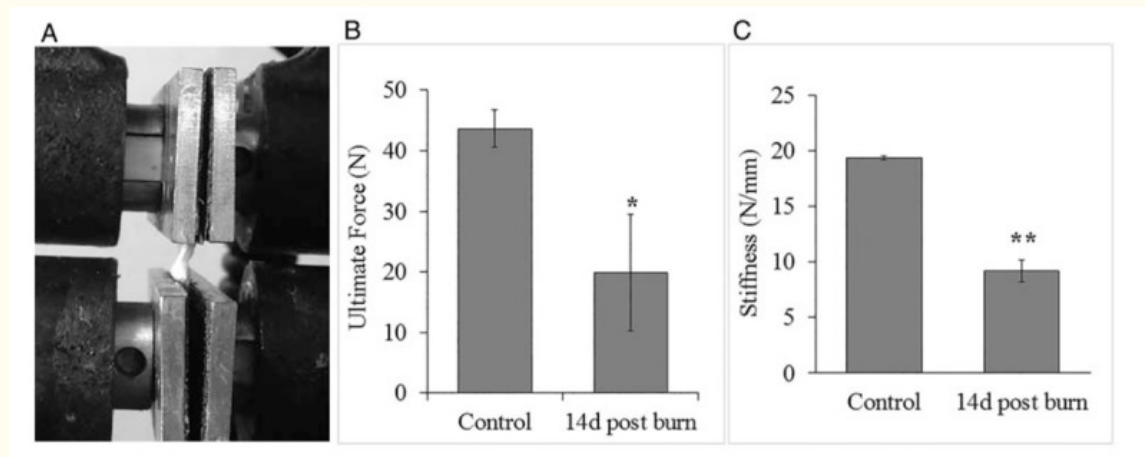


Fig. 2

Histological evidence of changes in Achilles tendon after severe burn.

(A) Tendons from control rats (upper panel) and 14-day postburn rats (lower panel) were stained with hematoxylin and eosin to show cell morphology and gross fiber organization. (B) Slides from the same tendons were used for Picrosirius red staining and analyzed with polarized light to show fiber organization of control (upper panel) vs. 14-day postburn rats (lower panel). (C) Quantification of (green + blue)/red of the Picrosirius red images under polarized light was used to determine organization of fibers. Scale bars=200 μm . * $P < 0.05$ vs. control.

To assess tendon function in parallel with histological changes, we measured the ultimate force of the left tendons of the same control and 14-day postburn rats utilized for histology (Fig. (Fig.3A).3A). Data obtained from three control rats and five burn rats showed that control tendons had a higher ultimate tensile force or maximum force before failure (Fig. (Fig.3B).3B). The average ultimate force for the control group was $43.7 \pm 3.0\text{N}$, whereas tendons of the 14-day postburn group showed an average ultimate force of less than half that of the controls at $19.9 \pm 9.7\text{N}$, $P < 0.05$.



[Fig. 3](#)

Biomechanical changes in Achilles tendon after severe burn.

(A) Example of tendon set-up for biomechanical testing. Tendons are pulled until failure. (B) Maximum load values obtained from the force-deformation curve of three control rats and five injured rats 14 days postburn. (C) Stiffness values calculated from force-deformation curves comparing no-burn vs. 14-day postburn tendons. * $P < 0.05$, ** $P < 0.001$ vs. control.

We also calculated tendon stiffness, which is the amount of measured deformation from an applied force. Control tendons had an average stiffness of 19.38 ± 0.16 N/mm that is significantly different from 14-day postburn rats with an average stiffness of 9.18 ± 0.99 N/mm, $P < 0.001$ (Fig. [\(Fig.33C\)](#)).

[Go to:](#)

DISCUSSION

In accordance with an induction of acute inflammation, we observed a significant increase in gene expression of the proinflammatory cytokines IL-1 β and IL-6 as well as the matrix metalloproteinases involved in remodeling, MMP9 and MMP13. We observed a decrease in collagen I/III protein expression, upregulation of TGF β 1, histological signs of remodeling, and a decrease in ultimate tensile strength of tendon 14 days postburn. Taken together, these results demonstrate, for the first time, the presence of inflammation and remodeling in tendon distant from the burn site after severe burn. This is consistent with similar findings in the literature for both skeletal muscle and bone ([1-4, 7](#)).

Serum levels of IL6 have been previously reported to increase rapidly after burn and stay higher than nonburn for several days ([10, 19](#)). The local increase in IL-1 β and IL-6 expression that we observed in tendons indicates an inflammatory response in this tissue. IL-6 has been suggested to also act as a growth factor by stimulating the synthesis of collagen in response to mechanical loading ([20](#)). Therefore, the rise of both IL-1 β and IL-6 levels points toward the initiation of acute inflammation in the tendon with a concomitant induction of collagen synthesis.

Previous reports have shown the involvement of IL-1 β in the upregulation of MMPs and tissue remodeling in tendon (21, 22). Even though MMPs are necessary for normal tissue homeostasis, an imbalance in the activity of these metalloproteases has been shown to be detrimental to tissue healing after injury, as an improvement of Achilles tendon repair can be obtained by the use of the nonselective MMP inhibitor, doxycycline (23). More investigation is needed to assess whether the increase in proinflammatory cytokines is mediated by tenocytes or by macrophage infiltration into the tissue after generation of the systemic response and to evaluate chronic inflammation at later time points.

Our results revealed a significant decrease in the collagen I protein level at 7 days postburn, with a subsequent increase akin to the control level by day 14. We propose that the initial decrease in collagen I can be explained by the upregulation of MMP13 and MMP9, generated by IL-1 β . Along with this, an analysis of gene expression of collagens showed that collagen III mRNA was upregulated at day 3, whereas its protein was detected elevated at day 14 postburn. Collagen I showed significantly lower protein level at day 7, together with an upregulation of its mRNA on the same time point and followed by restored protein levels similar to control by day 14 postburn. The protein ratio collagen I/III was significantly reduced by day 14. A similar shift in collagen expression at early time points has been observed for tendon-to-bone healing in rotator cuff injury (17). Analysis of gene expression of TGF β 1 showed significant upregulation at day 14. This is an important factor involved in musculoskeletal tissue differentiation that has been reported to correlate with formation of scar tissue and less organized fibers in healing tendon (17). The synthesis of collagen III protein, upregulation of TGF β 1, and the decrease in the collagen I/III protein ratio suggest an induction of scar tissue or remodeling (15). Another proinflammatory cytokine that is upregulated in rheumatic diseases and present in tendon entheses is IL-17a (24). This is produced by entheseal CD3+ lymphocytes, peripheral blood CD4+ T cells, and entheseal γ/δ T cells. We analyzed its gene expression throughout the time course, but did not find statistical significance (data not shown). This could be explained due to the chronic nature of rheumatic diseases compared with this more acute response.

Histological observations of collagen alignment and tenocyte distributions showed less tissue organization 14 days postburn compared with control. H&E staining showed less fiber alignment, cell aggregations, and even round nuclear morphology on some cells. This, together with the observation of changes in collagen composition, further indicates cellular events for tissue remodeling and possible weakening of the tendon. Collagen distribution and alignment are crucial for the transmission of forces in the tendon (14). In mature tissues, fibrils can be found parallel to the axial direction of tissue and also interwoven with the presence of a crimp pattern that provides its tensile properties (14, 15, 25). This anisotropy will derive into nonuniform strains on the cells, which can alter the cell morphology and response to differential mechanical forces. To address whether molecular changes in tissue structure will also affect its functional mechanics, the tensile force and deformation were measured. Overall, our findings showed that ultimate force and stiffness were reduced at 14 days postburn compared with controls. These biomechanical results correlate with histological findings of less organized fibers. It is possible that the initial loss in collagen I followed by an induction of synthesis of both collagens I and III results in fiber disorganization because collagen III has been previously reported as accumulated at the rupture site in tendon (15). Although previous reports have shown that Achilles tendon could react to an inflammatory event produced in surrounding tissue (26), this study is the first to report that remote systemic inflammation is capable of inducing a local inflammatory response

and remodeling in the tendon. Other models of trauma that generate systemic inflammation, such as fracture hematoma, have reported a similar pattern of circulating cytokines (27–29). Fracture hematoma with additional chest trauma has shown that systemic inflammation is capable of interfering with the normal inflammatory process on fracture healing (30). This evidence is supportive to the hypothesis that a trauma-generated systemic inflammation is potentially detrimental for soft tissues like tendon.

Severe burn patients suffer skeletal muscle and bone mass loss that can be attenuated by the introduction of physical activity. Considering the tendon as the connector and force transmitter between skeletal muscle and bone, it is essential to understand tendon's behavior in response to severe injury. Future investigation regarding the modulation of the inflammatory cascade and MMP inhibition accompanied by regulated physical therapy that allows proper tissue loading to prevent disuse, but also prevent overuse (31–35) may be promising for the improvement of recovery after severe burn and other traumatic injuries.

[Go to:](#)

Acknowledgments

The authors thank the Hofmann Fund for resident research from the Department of Orthopaedic Surgery and The Golden Charity Guild Charles R. Baxter, MD, Chair Department of Surgery fund. The authors would also like to thank The Molecular Pathology Core of UT Southwestern for processing the samples for histology and Dave Primm for his help in editing this manuscript.

[Go to:](#)

Footnotes

Contributed by

Authors' contributions: PH, JS, and SW designed the experiments and project. PH, DB, TM, JW, RH, DC, and JS performed the experiments. PH, HL, JW, KM, TW, and JS analyzed the data. All authors were involved in drafting and revising the manuscript.

Financial support: Department of Defense, grant number W81XWH-13-1-0462.

The authors report no conflicts of interest.

[Go to:](#)

REFERENCES

1. Evers LH, Bhavsar D, Mailander P. The biology of burn injury. *Exp Dermatol* 19 9:777–783, 2010. [[PubMed](#)]
2. Hart DW, Wolf SE, Chinkes DL, Gore DC, Mlcak RP, Beauford RB, Obeng MK, Lal S, Gold WF, Wolfe RR, et al. Determinants of skeletal muscle catabolism after severe burn. *Ann Surg* 232 4:455–465, 2000. [[PMC free article](#)] [[PubMed](#)]
3. Klein GL. Burn-induced bone loss: importance, mechanisms, and management. *J Burns Wounds* 5:e5, 2006. [[PMC free article](#)] [[PubMed](#)]

4. Hart DW, Wolf SE, Mlcak R, Chinkes DL, Ramzy PI, Obeng MK, Ferrando AA, Wolfe RR, Herndon DN. Persistence of muscle catabolism after severe burn. *Surgery* 128 2:312–319, 2000. [[PubMed](#)]
5. Analan PD, Leblebici B, Adam M, Sariturk C. Bone loss during the acute stage following burn injury: is it local or systemic? *West Indian Med J* 19 9:777–783, 2016.
6. Klein GL, Wolf SE, Goodman WG, Phillips WA, Herndon DN. The management of acute bone loss in severe catabolism due to burn injury. *Horm Res* 48 Suppl. 5:83–87, 1997. [[PubMed](#)]
7. Song J, Saeman MR, De Libero J, Wolf SE. Skeletal muscle loss is associated with TNF mediated insufficient skeletal myogenic activation after burn. *Shock* 44 5:479–486, 2015. [[PMC free article](#)][[PubMed](#)]
8. Tamgadge S, Shetty A, Tamgadge A, Bhalerao S, Periera T, Gotmare S. Study of polarization colors in the connective tissue wall of odontogenic cysts using picrosirius red stain. *J Orofac Sci* 7 2:119, 2015.
9. O'Halloran E, Kular J, Xu J, Wood F, Fear M. Non-severe burn injury leads to depletion of bone volume that can be ameliorated by inhibiting TNF-alpha. *Burns* 41 3:558–564, 2015. [[PubMed](#)]
10. Gauglitz GG, Song J, Herndon DN, Finnerty CC, Boehning D, Barral JM, Jeschke MG. Characterization of the inflammatory response during acute and post-acute phases after severe burn. *Shock* 30 5:503–507, 2008. [[PubMed](#)]
11. Clayton RA, Court-Brown CM. The epidemiology of musculoskeletal tendinous and ligamentous injuries. *Injury* 39 12:1338–1344, 2008. [[PubMed](#)]
12. Doral MN, Bozkurt M, Turhan E, Donmez G, Demirel M, Kaya D, Atesok K, Atay OA, Maffulli N. Achilles tendon rupture: physiotherapy and endoscopy-assisted surgical treatment of a common sports injury. *Open Access J Sports Med* 1:233–240, 2010. [[PMC free article](#)] [[PubMed](#)]
13. Riley G. Tendinopathy—from basic science to treatment. *Nat Clin Pract Rheumatol* 4 2:82–89, 2008. [[PubMed](#)]
14. Kannus P. Structure of the tendon connective tissue. *Scand J Med Sci Sports* 10:312–320, 2000. [[PubMed](#)]
15. Eriksen HA, Pajala A, Leppilahti J, Risteli J. Increased content of type III collagen at the rupture site of human Achilles tendon. *J Orthop Res* 20:1352–1357, 2002. [[PubMed](#)]
16. Riley GP, Curry V, DeGroot J, van El B, Verzijl N, Hazleman BL, Bank RA. Matrix metalloproteinase activities and their relationship with collagen remodelling in tendon pathology. *Matrix Biol* 21 2:185–195, 2002. [[PubMed](#)]
17. Galatz LM, Sandell LJ, Rothermich SY, Das R, Mastny A, Havlioglu N, Silva MJ, Thomopoulos S. Characteristics of the rat supraspinatus tendon during tendon-to-bone healing after acute injury. *J Orthop Res* 24 3:541–550, 2006. [[PubMed](#)]
18. Schindelin J, Rueden CT, Hiner MC, Eliceiri KW. The ImageJ ecosystem: an open platform for biomedical image analysis. *Mol Reprod Dev* 82 (7–8):518–529, 2015. [[PMC free article](#)] [[PubMed](#)]
19. Finnerty CC, Herndon DN, Przkora R, Pereira CT, Oliveira HM, Queiroz DM, Rocha AM, Jeschke MG. Cytokine expression profile over time in severely burned pediatric patients. *Shock* 26 1:13–19, 2006. [[PubMed](#)]
20. Andersen MB, Pingel J, Kjaer M, Langberg H. Interleukin-6: a growth factor stimulating collagen synthesis in human tendon. *J Appl Physiol (1985)* 110 6:1549–1554, 2011. [[PubMed](#)]

21. Archambault J, Tsuzaki M, Herzog W, Banes AJ. Stretch and interleukin-1 β induce matrix metalloproteinases in rabbit tendon cells in vitro. *J Orthop Res* 20 1:36–39, 2002. [[PubMed](#)]
22. Tsuzaki M, Guyton G, Garrett W, Archambault JM, Herzog W, Almekinders L, Bynum D, Yang X, Banes AJ. IL-1 beta induces COX2, MMP-1, -3 and -13, ADAMTS-4, IL-1 beta and IL-6 in human tendon cells. *J Orthop Res* 21 2:256–264, 2003. [[PubMed](#)]
23. Kessler MW, Barr J, Greenwald R, Lane LB, Dines JS, Dines DM, Drakos MC, Grande DA, Chahine NO. Enhancement of Achilles tendon repair mediated by matrix metalloproteinase inhibition via systemic administration of doxycycline. *J Orthop Res* 32 4:500–506, 2014. [[PubMed](#)]
24. Reinhardt A, Yevsa T, Worbs T, Lienenklaus S, Sandrock I, Oberdorfer L, Korn T, Weiss S, Forster R, Prinz I. Interleukin-23-dependent gamma/delta T cells produce interleukin-17 and accumulate in the enthesis, aortic valve, and ciliary body in mice. *Arthritis Rheumatol* 68 10:2476–2486, 2016. [[PubMed](#)]
25. Provenzano PP, Vanderby R., Jr Collagen fibril morphology and organization: implications for force transmission in ligament and tendon. *Matrix Biol* 25 2:71–84, 2006. [[PubMed](#)]
26. Vieira CP, Guerra Fda R, de Oliveira LP, de Almeida Mdos S, Pimentel ER. Alterations in the Achilles tendon after inflammation in surrounding tissue. *Acta Ortop Bras* 20 5:266–269, 2012. [[PMC free article](#)][[PubMed](#)]
27. Claes L, Ignatius A, Lechner R, Gebhard F, Kraus M, Baumgartel S, Recknagel S, Krischak GD. The effect of both a thoracic trauma and a soft-tissue trauma on fracture healing in a rat model. *Acta Orthop* 822:223–227, 2011. [[PMC free article](#)] [[PubMed](#)]
28. Claes L, Recknagel S, Ignatius A. Fracture healing under healthy and inflammatory conditions. *Nat Rev Rheumatol* 8 3:133–143, 2012. [[PubMed](#)]
29. Recknagel S, Bindl R, Brochhausen C, Gockelmann M, Wehner T, Schoengraf P, Huber-Lang M, Claes L, Ignatius A. Systemic inflammation induced by a thoracic trauma alters the cellular composition of the early fracture callus. *J Trauma Acute Care Surg* 74 2:531–537, 2013. [[PubMed](#)]
30. Ignatius A, Ehrnthaller C, Brenner RE, Kreja L, Schoengraf P, Lisson P, Blakytyn R, Recknagel S, Claes L, Gebhard F, et al. The anaphylatoxin receptor C5aR is present during fracture healing in rats and mediates osteoblast migration in vitro. *J Trauma* 71 4:952–960, 2011. [[PMC free article](#)] [[PubMed](#)]
31. Enwemeka CS. Inflammation, cellularity, and fibrillogenesis in regenerating tendon: implications for tendon rehabilitation. *Phys Ther* 69 10:816–825, 1989. [[PubMed](#)]
32. Hardee JP, Porter C, Sidossis LS, Borsheim E, Carson JA, Herndon DN, Suman OE. Early rehabilitative exercise training in the recovery from pediatric burn. *Med Sci Sports Exerc* 46 9:1710–1716, 2014. [[PMC free article](#)] [[PubMed](#)]
33. Godleski M, Oeffling A, Bruflat AK, Craig E, Weitzenkamp D, Lindberg G. Treating burn-associated joint contracture: results of an inpatient rehabilitation stretching protocol. *J Burn Care Res* 34 4:420–426, 2013. [[PubMed](#)]
34. Paratz JD, Stockton K, Plaza A, Muller M, Boots RJ. Intensive exercise after thermal injury improves physical, functional, and psychological outcomes. *J Trauma Acute Care Surg* 73 1:186–194, 2012. [[PubMed](#)]
35. Song J, Saeman MR, Baer LA, Cai AR, Wade CE, Wolf SE. Exercise altered the skeletal muscle microRNAs and gene expression profiles in burn rats with Hindlimb unloading. *J Burn Care Res* 38 1:11–19, 2017. [[PMC free article](#)] [[PubMed](#)]

J Burn Care Res. Author manuscript; available in PMC 2018 Jan 1.

Published in final edited form as:

J Burn Care Res. 2017 Jan-Feb; 38(1): 11–19.

doi: [10.1097/BCR.0000000000000444](https://doi.org/10.1097/BCR.0000000000000444)

PMCID: PMC5179292

NIHMSID: NIHMS811156

PMID: [27753701](https://pubmed.ncbi.nlm.nih.gov/27753701/)

Exercise Altered the Skeletal Muscle MicroRNAs and Gene Expression Profiles in Burn Rats with Hindlimb Unloading

Juquan Song, MD,^{1*} Melody R. Saeman, MD,¹ Lisa A. Baer, MS,² Anthony R. Cai, BA,¹ Charles E. Wade, PhD,² and Steven E. Wolf, MD¹

[Author information](#) [Copyright and License information](#) [Disclaimer](#)

The publisher's final edited version of this article is available at [J Burn Care Res](#)

See other articles in PMC that [cite](#) the published article.

Associated Data

[Supplementary Materials](#)

Abstract

[Go to:](#)

Introduction

Following a severe burn, patients suffer a hypercatabolic state in response to cytokine and stress hormone challenges. These stress signals, such as cortisol, catecholamine, and TNF- α , induce a catabolic/anabolic imbalance.¹ The body's flood of catabolic signals increases muscle breakdown and metabolism in muscle to call upon its role as an energy reservoir. Patients with severe burn showed 83% muscle protein degradation and a 50% increase in protein synthesis. Alongside protein degradation, skeletal muscles demonstrate a net loss of amino acids, with a 50% increased transport into the blood and a 40% decreased transport from the blood.²

Scientists explored a robust bi-phase genomic profile in response to burn and sepsis from animals and patients.³ In this multicenter study, they found that circulating leukocytes increase production of these inflammatory signals via a “genomic storm” of transcriptional changes. Genomic networks constructed for several major pathways such as inflammation and proteolysis are precisely demonstrated in burn patients.

Epigenetic changes are caused by external environmental stimulations which regulate the transcriptome but not the DNA sequence directly. Mechanisms of epigenetics include DNA methylation, histone modification microRNA (miRNA), etc. The miRNA is a conserved class of

small (20-25 bases), abundant RNA-interfering (RNAi) molecules that inhibit gene expression at the translational level. It acts by transiently binding to the 3' UTR of messenger RNA (mRNA) with partial complementarity and by blocking their translation. At least 20%-30% of protein-encoding genes in human are regulated by miRNAs, and these genes are often targeted by multiple miRNAs.⁴ Clinically, miRNAs have been studied as markers for cancer progression, which are related to tumor cell growth or death through tumor-suppressor gene silencing. miRNAs are also involved in other disease states, such as type 2 diabetes, and PTSD neural trauma injury.⁵ The alteration of miRNA profiles were related to muscle disuse and atrophy,⁶ and further affected with exercise.⁷ Particularly in the area of burn, Liang et al. previously studied the miRNA profile of cells in burned dermis and found 66 miRNAs that were significantly up- or downregulated.⁸ However, there is little information regarding the mechanism of miRNAs mediating skeletal muscle atrophy after burn.

Due to the injury, burn patients are often in bed for extended periods of time.⁹ Wu demonstrated that rat muscle function decreased after burn and hindlimb unloading in an animal model.¹⁰ We speculated that miRNA changes in skeletal muscle after burn and bed rest contribute to muscle atrophy due to its abundance and sweeping range of actions on different genes.

Exercise studies have shown to positively mitigate muscle atrophy.¹¹ In pediatric burn patients, beneficial improvement of muscle mass was achieved with a combination of aerobic and resistance exercise training.^{12,13} We recently studied the effects of resistance exercise on muscle function recovery in burn rats with hindlimb unloading.¹⁴ There was the question of whether gene expression alteration with exercise training is correlated with miRNA regulation. Therefore, we further hypothesized that exercise improves muscle pathophysiological change that is associated with epigenetics-regulated gene expression after burn and muscle disuse. The purpose of the current study was to characterize the miRNA and genomic profile in burn and hindlimb unloaded animals with exercise training.

[Go to:](#)

Methods

Forty-eight adult male Sprague-Dawley rats (Envigo [Harlan Labs], Indianapolis, IN) were used in this study. The animals' protocol was approved by the Institutional Animal Care and Use Committee at the University of Texas Health Science Center at Houston in accordance with NIH guidelines. All animal procedures were carried out at UT Houston and fully described previously.¹⁴ The experiment flow chart is presented in [Figure 1](#) and briefly addressed below.

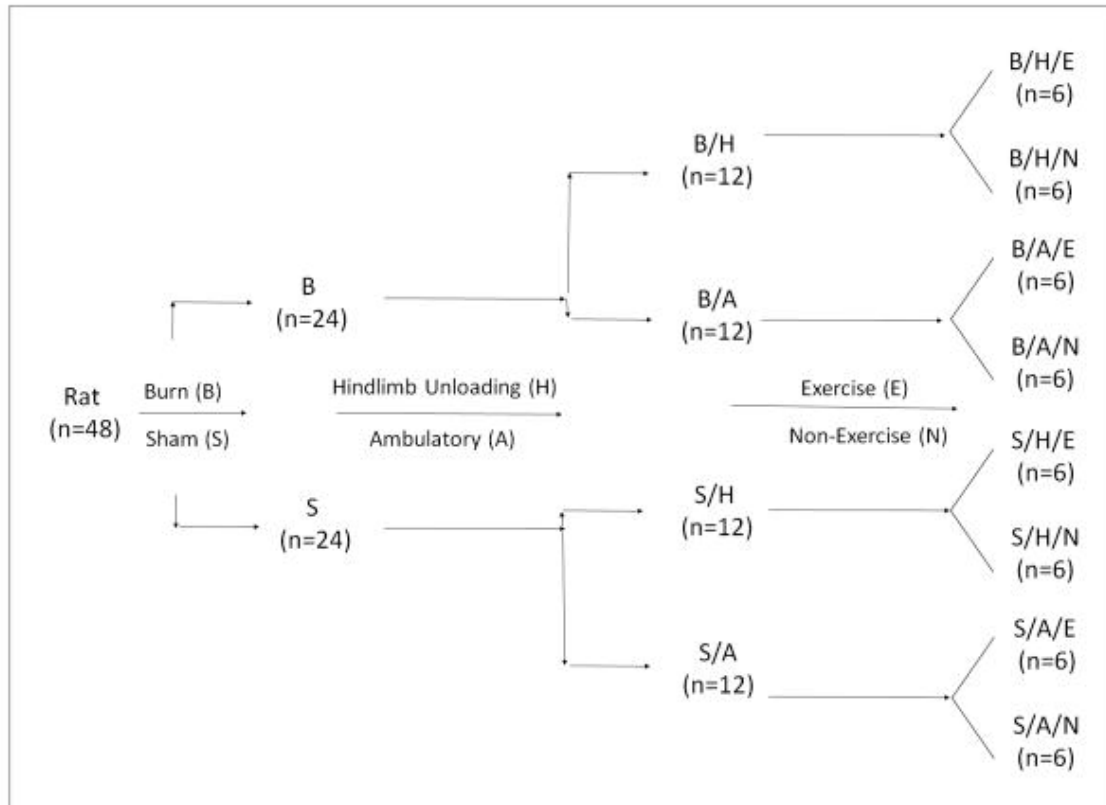


Figure 1

Flow chart of animal experiment that outlines the size of animal and the order of operation

- **Burn procedure:** All animals received a full-thickness scald burn of 40% total body surface area under 2%-4% isoflurane anesthesia. The burned animals (B) were resuscitated with 20 ml of intraperitoneal lactated Ringer's with buprenorphine for analgesia treatment. Sham animals (S) received the same procedure except for the scald burn.
- **Hindlimb unloading:** Animals were placed in a hindlimb unloading system described by Morey-Holton and Globus after burn or sham injury.¹⁵ Rats were able to freely access regular chow (Harlan Teklad #2018) and water without the hindlimbs contacting the walls of the cage. Animals in the ambulatory groups (A) were housed in similar cages but without hindlimb unloading.
- **Resistance exercise:** On the day of injury, animals were trained (E) to climb 1 meter at an 80-degree incline with tail weights five times twice daily. Weights were calculated as percent body mass of each individual rat and gradually increased in increments of 10% every few days as tolerated with a maximum weight of 50% body mass. All animals including the non-exercised group (N) were pre-trained 10 days prior to injury.

Total RNA extraction and genomic analysis

On day 14 after injury, all animals were euthanized, and the hindlimb muscles on the right were harvested and weighed. Half the plantaris tissue was immersed in RNA stabilization reagent

(Qiagen, Hilden, Germany) and stored at -80°C . Tissue samples from 3 animals in each group were pooled, and total RNA was extracted using Qiagen miRNeasy Mini Kit (Qiagen, Hilden, Germany). RNA purity was over 99%, and 1 μg of RNA sample was processed at the UT Southwestern microarray core facility for the following miRNA and gene expression measurements.

The Affymetrix miRNA 4.0 Arrays chip (Santa Clara, CA) was applied for miRNA detection. The chips' reproducibility (intra and inter-lot) is greater than 0.95. A total of 36,333 small non-coding RNA probes, including varied species and controls coated in one chip for each sample. Rat gene expression from each pooled sample was detected in triplicate using the Affymetrix Rat Gene 2.0 chip (Santa Clara, CA). The chips contains 30,429 rat gene probes. Raw signal intensity data was normalized with robust multi-array average (RMA) from the Affymetrix data bank. The raw intensity values ratio of signal intensity were background corrected, log 2 transformed, and then quantile normalized. A linear model was then fitted to the normalized data to obtain an expression measure for each probe set on each array. The linear fold change of signal data was analyzed with Affymetrix Transcriptome Analysis Console 3.0 software. Threshold filters were set as the default value for both miRNA and gene expression data analysis. The absolute linear fold change value was greater than 2. For triplicated genomic sample data analysis, a one-way between-subject ANOVA (unpaired) was further applied with significant acceptance of $p < 0.05$. The interaction of miRNA and target genes, gene ontology (GO) biological processing, and related pathways were also analyzed.

[Go to:](#)

Results

General description of miRNA and gene expressions

There were 1218 rat species miRNAs in a total of 36,333 miRNAs detected in rat muscle samples, including 728 rat mature miRNA probe sets and 490 pre-miRNA probes. Most signal intensities were lower than 2 in all groups. The highest probe signal intensity (binary log ratio) was 15.4 for miRNA-206-3p in all groups. We observed 74.5% of transcripts in the S/A/N group and 73.9% of the B/A/N group with a signal intensity of less than 2. There were 73, 79 and 80 miRNAs altered in the B/A/N, S/H/N, and B/H/N groups, respectively, compared to S/A/N group. Over 70% of the miRNAs were upregulated in response to burn and hindlimb unloading, while about 60% of miRNAs were upregulated in B/H rats with exercise training ([Figure 2 A](#)).

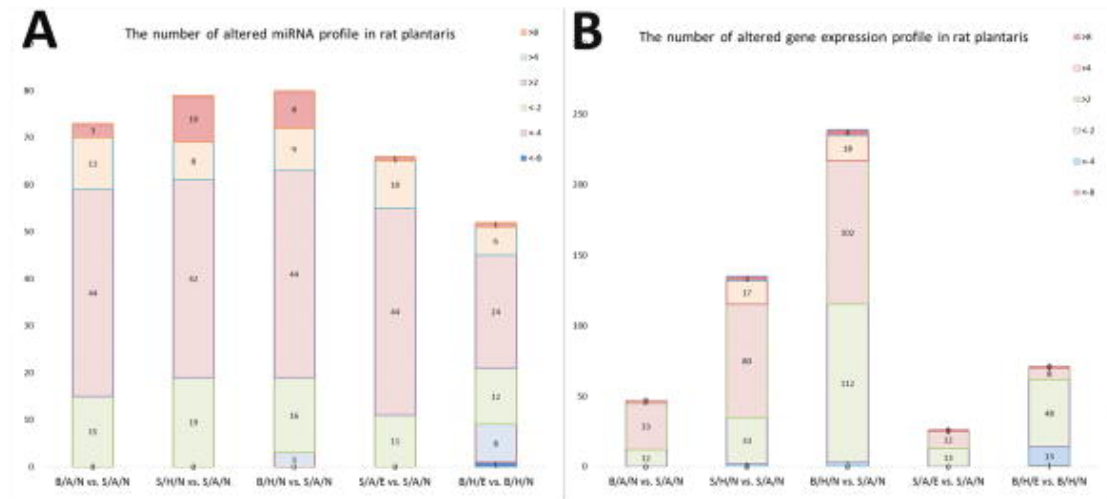


Figure 2

Stacked bar figures showing the number of miRNA (2A) and genes (2B) in rat plantaris altered in response to burn (B/A/N vs. S/A/N), hindlimb unloading (S/H/N vs. S/A/N), combination of burn and hindlimb unloading (B/H/N vs. S/A/N), exercise in normal rats (S/A/E vs. S/A/N), and exercise in burn and hindlimb unloaded rats (B/H/E vs. B/H/N).

There were 30,429 rat genes detected using the Rat Gene 2.0 chip. GAPDH (transcript cluster ID 17799923) demonstrated the greatest signal intensity (13.5 binary log ratio). Filtered by default threshold values, there were 47 and 135 genes altered in rat muscle with burn or hindlimb unloading, respectively, while 239 genes were disturbed in combined burn and hindlimb unloading rats. There were 2, 20, and 22 genes that increased greater than fourfold in the B/A, S/H, and B/H groups separately. In contrast, 62 out of 71 genes decreased in the B/H/E versus B/H/N groups ([Figure 2 B](#)).

MiRNA and gene expression profiles are distinguished in response to burn, hindlimb unloading, and exercise and described separately as follows:

The miRNA and gene expression profile in response to burn (B/A/N vs. S/A/N)

In all, 79.4% of 73 miRNAs were upregulated in burn animals. The amplitude of upregulated miRNAs was higher than that of downregulated ones. There were 14 miRNAs upregulated more than fourfold, including the 3 most upregulated miRNAs, miR-182 (12.81), miR-184 (10.50) and miR-155-5p (8.82). Fold changes were less than 3 in all 15 downregulated miRNAs. The miR-409a-3p was the most decreased (-2.95) in burn animals ([Supplemental Table 1-1](#)).

There were 47 genes changed, 12 down- and 35 upregulated, in the B/A/N group compared to the S/A/N group ([Supplemental Table 1-2](#)). Thirty-two changed genes were associated with multiple GO biological processes, and 6 signal pathways were altered. The ketone body metabolism, inflammatory response, and striated muscle contraction pathways were most activated ([Supplemental Table 1-3](#)).

In viewing the interaction network, the most upregulated miRNA, miR-182, decreased the *colla2* gene, which collaborates with downregulated miR-409-3p. MiR-182 also works with miR-193-3p and 125-b-1p to downregulate the *neu2* gene, which participates in muscle cell

differentiation. The second most upregulated miRNA, miR-184, was associated with the decreased *obp3* and *chad* genes (which are associated with GO biological processes of small molecular transportation and cartilage condensation, respectively), and also collaborates with other miRNAs (Figure 3).

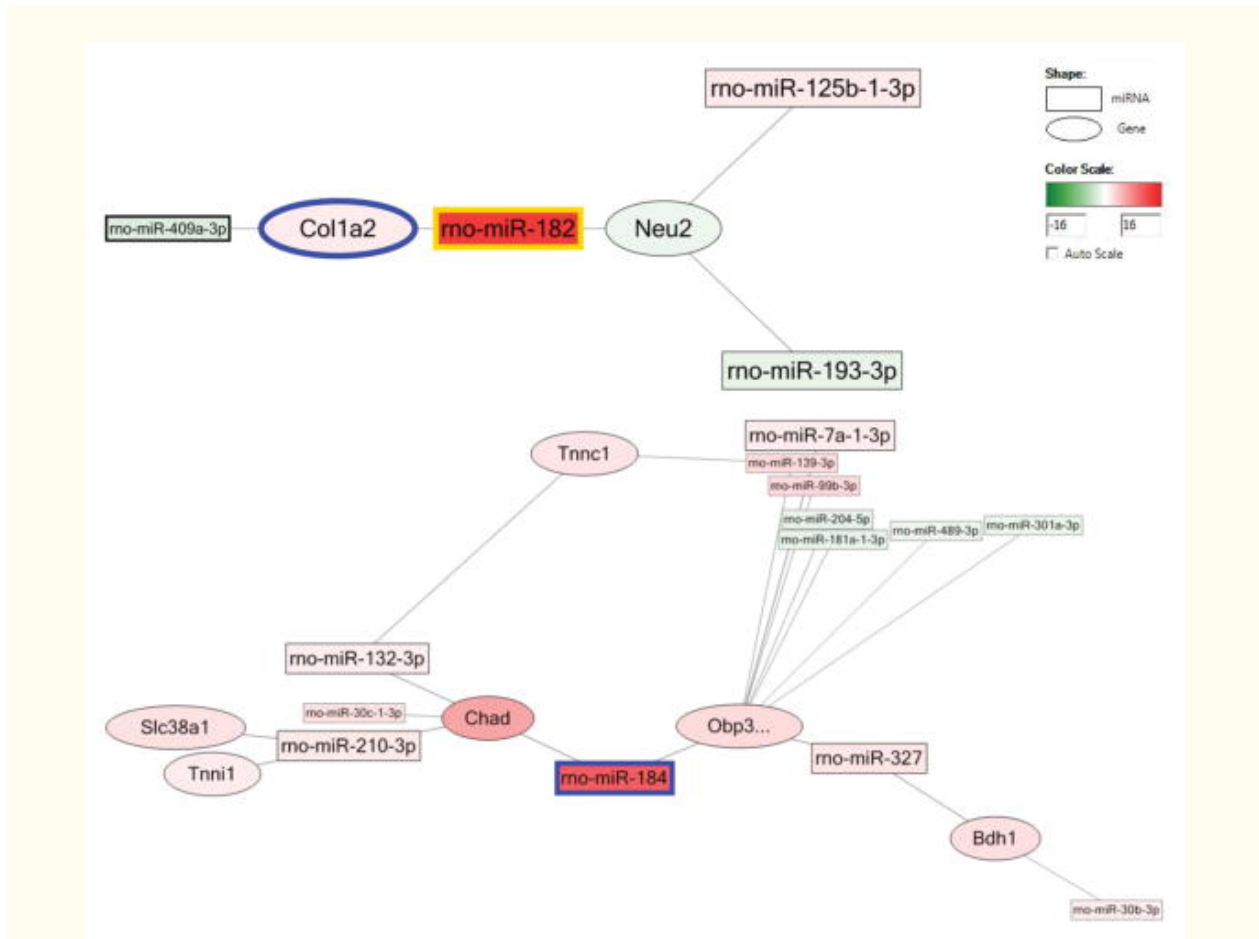


Figure 3

The network of miRNA and related genes after burn (B/A/N vs. S/A/N). Square shape stands for miRNA, oval shape stands for gene. Pseudo-color from green to red stands for fold change from -16 to 16.

The miRNA and gene expression profile in rats with hindlimb unloading (S/H/N vs. S/A/N)

There were 79 total altered miRNAs, including 19 downregulated and 60 upregulated ones. The amplitude of upregulated miRNAs was greater than that of the downregulated. Eighteen of the miRNAs' linear fold changes were upregulated over fourfold, and 10 miRNAs even changed over eight-fold; in contrast, downregulated miRNAs were all changed less than fourfold. MiR-182 (23.83), miR-184 (17.73), miR-183-5p (16.61), and miR-122-5p (14.19) were the most upregulated in the S/H/N group, and the most downregulated miRNAs included miR-489-3p (-3.54), miR-665 (-3.21), and miR-675-5p (-3.19) (Supplemental Table 2-1).

There were 135 genes, 100 up- and 35 downregulated, in rat muscle in response to hindlimb unloading. In all, 20 genes increased more than fourfold; only 2 genes decreased more than

fourfold ([Supplemental Table 2-2](#)). Seventy-nine genes had varied biological process functions involving 9 pathways, with the 3 most prominent pathways being the MAPK cascade, the blood-clotting cascade, and fatty acid synthesis ([Supplemental Table 2-3](#)).

In viewing the interaction network, a large complex network was constructed between miRNAs and genes demonstrating altered expression. The most increased miRNA, miR-182, upregulated the *clnd19* gene (for neuronal action potential propagation) in collaboration with decreased miR-489-3p. MiR-182 also worked with other miRNAs such as miR-335 and -484 to decrease the *neu2* gene (for myotube differentiation positive regulation). The second most upregulated miRNA, miR-184, worked with miR-342 and miR-484 to increase *obp3* and decrease *cib2* and *plcd4* genes, which are both for calcium ion binding ([Figure 4](#)).

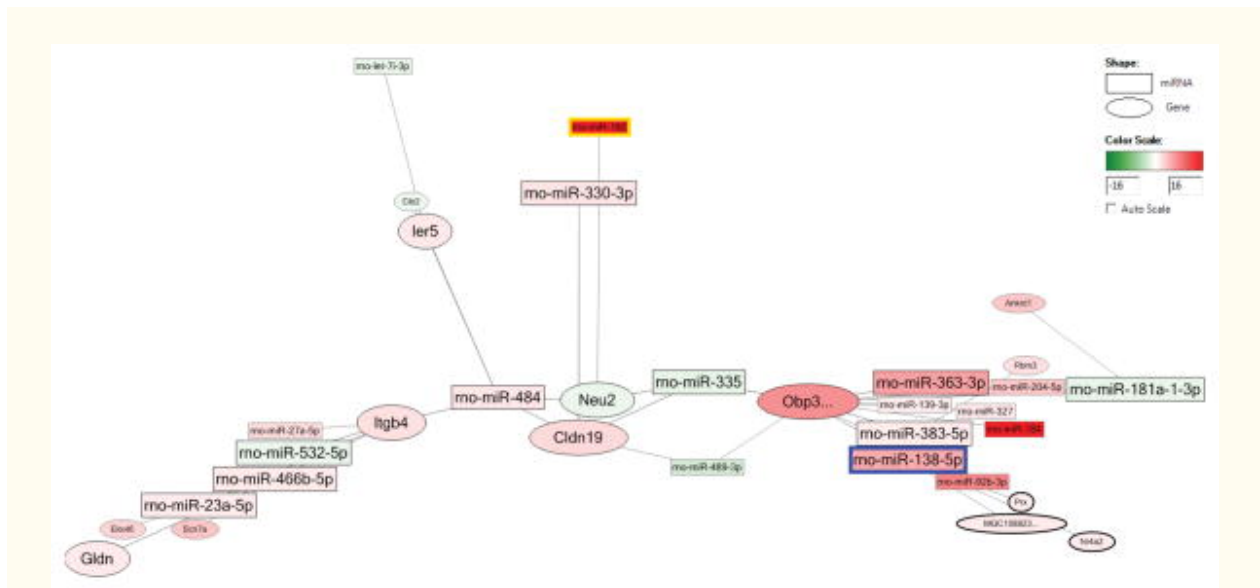


Figure 4

The network of miRNA and related genes after hindlimb unloading (S/H/N vs. S/A/N). Square shape stands for miRNA, oval shape stands for gene. Pseudo-color from green to red stands for fold change from -16 to 16.

The miRNA and gene expression profile in rats with combined burn and hindlimb unloading (B/H/N vs. S/A/N)

We found 80 miRNAs, including 61 upregulated miRNAs and 19 downregulated miRNAs, with only 3 downregulated over fourfold. There were 17 miRNAs upregulated over fourfold, and miR-182 even increased 35-fold ([Supplemental Table 3-1](#)).

There were 239 genes altered between the B/H/N versus S/A/N group. Only 3 of 115 downregulated genes changed more than fourfold, whereas there were 22 out of 124 genes upregulated more than fourfold ([Supplemental Table 3-2](#)). Overall, 165 genes related to multiple GO biological processes were involved in 14 pathways. Oxidative stress, the MAPK cascade, fatty acid synthesis, and the blood-clotting pathway were activated, and cardiovascular signaling and the p53 signal pathway were inhibited ([Supplemental Table 3-3](#)).

In viewing the interaction network, there were independent and additive effects in miRNA and gene expression levels when comparing the effects of burn and hindlimb unloading factors. While miR-409a-3p decreased 2.95-fold in B/A/N without detection in S/H/N mice, in B/H/N, miR-409a-5p decreased 2.03-fold. MiR-92b-3p only demonstrated an 8.04-fold upregulation in the S/H/N group but increased to a 9.46-fold upregulation in the B/H/N group. Most strikingly, miR-182 has an additive increased effect with combined burn and hindlimb unloading (35.35) compared to burn (12.81) and hindlimb unloading (23.82) individually. At the transcriptional level, *Fmod* only increased in burn rats but not in rats with hindlimb unloading; the *Mbp* gene increased in an opposite manner; while *Nr4a3* had an additive effect in response to the combination of burn and hindlimb unloading ([Supplemental Table 4](#)).

The miRNA and gene expression profile in rats with burn and hindlimb unloading response to exercise training (B/H/E vs. B/H/N)

There were 52 miRNAs altered, including 21 down- and 31 upregulated, in burn and hindlimb unloading rats with exercise training. There were 9 miRNAs downregulated over fourfold, while 7 were upregulated over fourfold. The most upregulated miRNAs include miR-1843-3p (8.52), miR-495 (5.92), and miR-6324 (5.78) ([Supplemental Table 5-1](#)).

In viewing the interaction network, there were 71 gene changes, with 62 downregulated genes and only 9 genes upregulated less than fourfold in transcriptional level ([Supplemental Table 5-2](#)). Overall, 54 genes partook in different biological processes and 7 pathways. The MAPK cascade, fatty acid synthesis, and the inflammation response pathway were the top 3 alleviated pathways ([Supplemental Table 5-3](#)).

We further estimated the different effect of exercise between burn rats with hindlimb unloading and sham controlled rats. In S/A/E rats, there were 66 miRNAs altered, with 11 down- and 55 upregulated. We found that miR-182 increased 10.06-fold in S/A/E. There were only 12 genes altered, with 7 upregulated and 5 downregulated. Though 9 of these genes had functions in various biological processes, no pathway change was observed in normal rats with exercise training.

[Go to:](#)

Discussion

In this study, we characterized the miRNA and gene profiles in rat plantaris under conditions of burn, hindlimb unloading, and resistance exercise. The complexity of this regulation's network is displayed at both the epigenetic and transcriptome levels. Those consequent changes of biological processing and involved signal pathways reflect muscle pathophysiological changes in response to burn and hindlimb unloading. Hyper-metabolic response ketone bodies KEGG and glucose, and inflammation response were activated after burn injury; oxidative stress, MAPK cascade, and fat acid synthesis pathways were stimulated by hindlimb unloading; and striated muscle contraction and blood clotting pathways were stimulated by both burn and hindlimb unloading. Resistance exercise altered the transcriptome profile associated with muscle structure and function improvement ([Figure 5](#)).

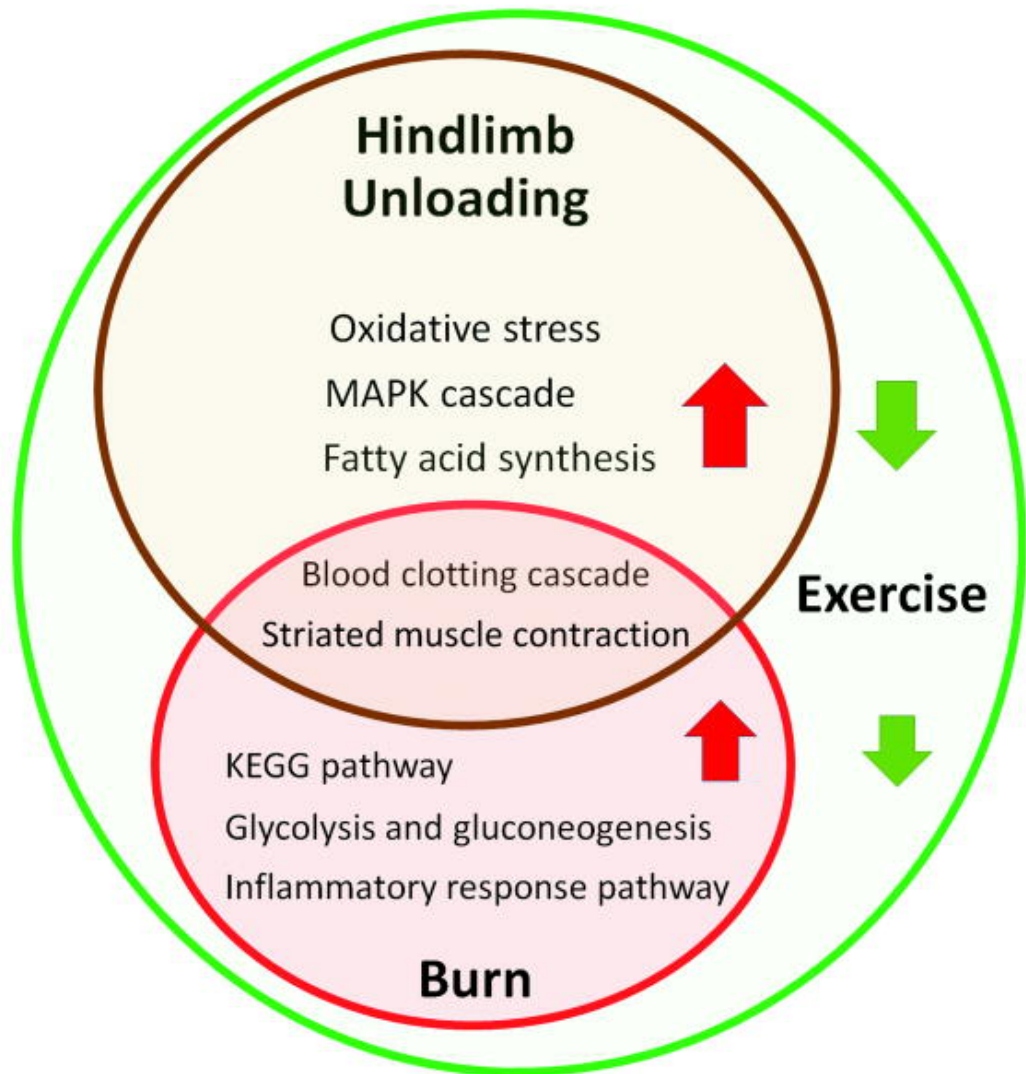


[Figure 5](#)

The scheme of affected signal pathways in response to burn, hindlimb unloading and exercise training. Red arrows indicated activated pathways. Green arrows indicates inhibited pathways.

Cells respond to the body's stress signals by making coordinated changes in gene expression. Padfield et al. reported the genomic profile in mice muscle by 3 days after burn, including muscle development and function, inflammation and acute-phase immune response, amino acid and protein synthesis, and energy metabolism pathways.¹⁶ Vemula et al. verified this, linking 28% of the changed genes to metabolism. These included genes responsible for triglyceride utilization, fatty acid import, and acute phase proteins.¹⁷ Merritt reported that the inflammatory response activated stat/NFκβ to calcium-mediated proteolysis and ubiquitin-proteasome with absence of protein synthesis inhibition.¹⁸ In addition, we found that muscle mass loss is associated with insufficient myogenesis in response to burn and that TNF-α as a pro-inflammatory cytokine plays an important role in inhibiting muscle myogenesis¹⁹. Though samples were collected 14 days after burn in the current study, we still observed increased numbers and amplitudes of gene and miRNA profile changes. Furthermore, we found those

affected genes were mainly related to the metabolic and inflammatory response signal pathways. We are therefore not surprised by Jeschke's previous report that the hypermetabolic status can even last for years in burn patients.²⁰

In human patients with bed rest, a gene profile reveals changes in energy pathways: oxidative phosphorylation, TCA cycle, organic compound usage, and carbohydrate metabolism.²¹ Bonaldo and Sandri revealed the intracellular mechanism by which hindlimb unloading activates cell apoptosis in an NF-KB dependent manner.²² In the current study, we found that burn mainly affects inflammation and metabolic pathways in rats, such as ketone bodies synthesis and degradation, inflammatory response, striated muscle contraction, and glucose metabolism; hindlimb unloading affects muscle signal pathways, including oxidative stress, MAPK cascade, fatty acid synthesis, and blood clotting cascade pathways; and *Mal*, *Hmox1* and *Btg2* genes are directly related to GO biological process of cell apoptosis. Severe burn and disuse have independent roles in body composition change.²³ Therefore, it is logically believed that burn and hindlimb unloading might activate different major pathways with distinguishable characteristic profiles.

Muscle disuse amplified muscle function impairment in severely burned rats. In plantaris, the tissue's wet weight significantly decreased in response to burn and hindlimb unloading, respectively. Normalized to body mass, the tissue weight still decreased between the ambulatory and hindlimb unloading with decreased twitch and tetanic forces.¹⁰ In our current study, we observed that muscle disuse affects more genes in rat muscle than burn, so hindlimb unloading could be more closely associated with muscle impairment and function loss than burn. Furthermore, an overlap of miRNA and gene changes were observed in burn rats with hindlimb unloading. The double factors of burn and hindlimb unloading could amplify the signal strength and extend the pathophysiological phenotype in muscle.

The current study is the first to investigate miRNA profiles related to their target genes in muscle atrophy after burn. The miRNA differs from a similar class of RNAi, short interfering RNA (siRNA), in that it does not usually cleave the complement mRNA or affect gene transcription. The importance of miRNAs has been observed in regulating skeletal myogenesis. MiRNAs are highly-enriched in skeletal muscle and participate in skeletal myogenesis and muscle regeneration.²⁴ In addition, miRNA-1 improves myogenic differentiation by inhibiting histone deacetylase 4, and miR-133a increases myoblast proliferation by repressing serum response factor.²⁵ Cardiomyocyte hypertrophy can be induced by miR-195, and miR-195 with other 4 miRNAs increased in human heart failure and upregulated during cardiac hypertrophy in vivo.²⁶

Exercise affects gene expression through miRNA changes. Following 90 minutes of exhaustive endurance exercise (forced treadmill running) in mice, miR-1 and miR-181, both thought to increase muscle differentiation and development, and miR-107, were increased.⁷ Resistance exercise training reduced anabolic signaling with gene alteration, including hypertrophic growth, protein degradation, and angiogenesis.²⁷ In another clinical study, investigators distinguished an miRNA profile from human vastus lateralis with a 5 day/week resistance exercise for 12 weeks, and speculated those miRNAs served as compensatory mechanisms.²⁸ We observed that there was a complicated network of epigenetic regulation in the current study. Not just one but several miRNAs control one single gene, and a single miRNA is also involved in multiple genes' regulation. It is therefore better to examine the whole profiles of miRNA and the related genes, and furthermore understand the protein structure and function change.

Previous studies showed that miR-182 has multiple-functions as a regulator of apoptosis, growth, and differentiation programs. Kouri reported that the injection of synthesized miR-182-based spherical nucleic acids suppressed tumor glioma burden and increased animal survival.²⁹ More interestingly, miR-182 was shown to prevent skeletal muscle atrophy by interfering with forkhead box O3 (FoxO3) mRNA. The miR-182 decreased Foxo3 expression in C2C12 with further inhibition of atrohgin-1 and ATG12.³⁰ Overall, miR-182 was the most phenomenally affected microRNA within all treatment groups in the current study. It increased 12.8- and 23.8-fold in burn and hindlimb unloading, respectively, and additively 35.5-fold in B/H/N rats. Exercise training decreased its expression 7.8-fold afterwards.

Burn causes a hypermetabolic status with a hyper-inflammation response, and muscle is a key participant in the systemic metabolic response. The current study could provide novel insight into potential target treatment at the epigenetic level. For instance, we have shown insulin resistance in animal models and burn patients.³¹ One review paper discussed the possibility of targeting miRNA to treat insulin resistance in burn patients.³²

In summary, miRNAs and transcript gene profiles in rat plantaris were affected in burn and hindlimb unloading. These changes seen in signal pathways are associated with muscle pathophysiological changes, including muscle mass loss and function impairment. The muscle improvement observed with exercise training was also observed at the gene level with miRNA and genomic pathway alterations. The current exploration of regulation networks involving epigenetics- and gene-pathophysiological changes might aide the development of future biomarkers and potential therapeutic development in patients with muscle atrophy.

[Go to:](#)

Supplementary Material

Supplemental Data File_1

SUPPLEMENTAL TABLES (separate files attached): Table 1. miRNA and gene profiles in response to burn (B/A/N vs. S/A/N)

[Click here to view.](#) (21K, docx)

Supplemental Data File_2

Table 2. miRNA and gene profiles in response to hindlimb unloading (S/H/N vs. S/A/N)

[Click here to view.](#) (26K, docx)

Supplemental Data File_3

Table 3. miRNA and gene profiles in response to the combination of burn and hindlimb unloading (B/H/N vs. S/A/N)

[Click here to view.](#) (32K, docx)

Supplemental Data File_4

Table 4. miRNA and gene comparison between burn and hindlimb unloading

[Click here to view.](#) (14K, docx)

Supplemental Data File_5

Table 5. miRNA and gene profiles in response to exercise in burn and hindlimb unloading rats (B/H/E vs. B/H/N)

[Click here to view.](#) (27K, docx)

[Go to:](#)

Acknowledgments

This work was supported by funds from the Golden Charity Guild Charles R. Baxter, MD, Chair; the Department of Defense #W81XWH-13-1-0462; and the National Institute for General Sciences of the National Institutes of Health #T32GM008593. We thank staff medical editor Dave Primm for his assistance. Authors have no financial or other interests construed as a conflict of interest.

Source of funding: This work was supported by funds from the Golden Charity Guild Charles R. Baxter, MD, Chair; the Department of Defense #W81XWH-13-1-0462; and the National Institute for General Sciences of the National Institutes of Health #T32GM008593.

[Go to:](#)

Footnotes

Author contributions: JS, MRS, and ARC contributed to data collection and analysis and manuscript preparation. LAB was for animal experiment, sample collection, and manuscript revision. CEW and SEW were integral to the concept and design of the experiment as well as the critical revision of the manuscript.

Conflicts of interest: The authors have no financial or other interests construed as a conflict of interest.

[Go to:](#)

References

1. Herndon DN, Tompkins RG. Support of the metabolic response to burn injury. *Lancet*. 2004;363(9424):1895–1902. [[PubMed](#)]
2. Biolo G, Fleming RY, Maggi SP, et al. Inverse regulation of protein turnover and amino acid transport in skeletal muscle of hypercatabolic patients. *J Clin Endocrinol Metab*. 2002;87(7):3378–3384. [[PubMed](#)]
3. Xiao W, Mindrin MN, Seok J, et al. A genomic storm in critically injured humans. *J Exp Med*. 2011;208(13):2581–2590. [[PMC free article](#)] [[PubMed](#)]
4. Liu NK, Xu XM. MicroRNA in central nervous system trauma and degenerative disorders. *Physiol Genomics*. 2011;43(10):571–580. [[PMC free article](#)] [[PubMed](#)]
5. Zovkic IB, Sweatt JD. Epigenetic mechanisms in learned fear: implications for PTSD. *Neuropsychopharmacology*. 2013;38(1):77–93. [[PMC free article](#)] [[PubMed](#)]
6. Wang XH. MicroRNA in myogenesis and muscle atrophy. *Curr Opin Clin Nutr Metab Care*. 2013;16(3):258–266. [[PMC free article](#)] [[PubMed](#)]
7. Safdar A, Abadi A, Akhtar M, et al. miRNA in the regulation of skeletal muscle adaptation to acute endurance exercise in C57Bl/6J male mice. *PLoS One*. 2009;4(5):e5610. [[PMC free article](#)] [[PubMed](#)]

8. Liang P, Lv C, Jiang B, et al. MicroRNA profiling in denatured dermis of deep burn patients. *Burns*. 2012;38(4):534–540. [[PubMed](#)]
9. Wolfe RR. Control of muscle protein breakdown: effects of activity and nutritional states. *Int J Sport Nutr Exerc Metab*. 2001;11(Suppl):S164–169. [[PubMed](#)]
10. Wu X, Baer LA, Wolf SE, et al. The impact of muscle disuse on muscle atrophy in severely burned rats. *J Surg Res*. 2010;164(2):e243–251. [[PMC free article](#)] [[PubMed](#)]
11. Ferrando AA, Tipton KD, Bamman MM, et al. Resistance exercise maintains skeletal muscle protein synthesis during bed rest. *J Appl Physiol* (1985) 1997;82(3):807–810. [[PubMed](#)]
12. Diego AM, Serghiou M, Padmanabha A, et al. Exercise training after burn injury: a survey of practice. *J Burn Care Res*. 2013;34(6):e311–317. [[PMC free article](#)] [[PubMed](#)]
13. Suman OE, Spies RJ, Celis MM, et al. Effects of a 12-wk resistance exercise program on skeletal muscle strength in children with burn injuries. *J Appl Physiol* (1985) 2001;91(3):1168–1175. [[PubMed](#)]
14. Saeman MR, DeSpain K, Liu MM, et al. Effects of exercise on soleus in severe burn and muscle disuse atrophy. *J Surg Res*. 2015;198(1):19–26. [[PMC free article](#)] [[PubMed](#)]
15. Morey-Holton ER, Globus RK. Hindlimb unloading rodent model: technical aspects. *J Appl Physiol* (1985) 2002;92(4):1367–1377. [[PubMed](#)]
16. Padfield KE, Astrakas LG, Zhang Q, et al. Burn injury causes mitochondrial dysfunction in skeletal muscle. *Proc Natl Acad Sci U S A*. 2005;102(15):5368–5373. [[PMC free article](#)] [[PubMed](#)]
17. Vemula M, Berthiaume F, Jayaraman A, et al. Expression profiling analysis of the metabolic and inflammatory changes following burn injury in rats. *Physiol Genomics*. 2004;18(1):87–98. [[PubMed](#)]
18. Merritt EK, Cross JM, Bamman MM. Inflammatory and protein metabolism signaling responses in human skeletal muscle after burn injury. *J Burn Care Res*. 2012;33(2):291–297. [[PMC free article](#)][[PubMed](#)]
19. Song J, Saeman MR, De Libero J, et al. Skeletal Muscle Loss Is Associated with Tnf Mediated Insufficient Skeletal Myogenic Activation after Burn. *Shock*. 2015 [[PMC free article](#)] [[PubMed](#)]
20. Jeschke MG, Gauglitz GG, Kulp GA, et al. Long-term persistence of the pathophysiologic response to severe burn injury. *PLoS One*. 2011;6(7):e21245. [[PMC free article](#)] [[PubMed](#)]
21. Chen YW, Gregory CM, Scarborough MT, et al. Transcriptional pathways associated with skeletal muscle disuse atrophy in humans. *Physiol Genomics*. 2007;31(3):510–520. [[PubMed](#)]
22. Bonaldo P, Sandri M. Cellular and molecular mechanisms of muscle atrophy. *Dis Model Mech*. 2013;6(1):25–39. [[PMC free article](#)] [[PubMed](#)]
23. Wade CE, Baer LA, Wu X, et al. Severe burn and disuse in the rat independently adversely impact body composition and adipokines. *Crit Care*. 2013;17(5):R225. [[PMC free article](#)] [[PubMed](#)]
24. Guller I, Russell AP. MicroRNAs in skeletal muscle: their role and regulation in development, disease and function. *J Physiol*. 2010;588(Pt 21):4075–4087. [[PMC free article](#)] [[PubMed](#)]
25. Chen JF, Mandel EM, Thomson JM, et al. The role of microRNA-1 and microRNA-133 in skeletal muscle proliferation and differentiation. *Nat Genet*. 2006;38(2):228–233. [[PMC free article](#)] [[PubMed](#)]

26. van Rooij E, Sutherland LB, Liu N, et al. A signature pattern of stress-responsive microRNAs that can evoke cardiac hypertrophy and heart failure. *Proc Natl Acad Sci U S A*. 2006;103(48):18255–18260. [[PMC free article](#)] [[PubMed](#)]
27. Nader GA, von Walden F, Liu C, et al. Resistance exercise training modulates acute gene expression during human skeletal muscle hypertrophy. *J Appl Physiol* (1985) 2014;116(6):693–702. [[PubMed](#)]
28. Davidsen PK, Gallagher IJ, Hartman JW, et al. High responders to resistance exercise training demonstrate differential regulation of skeletal muscle microRNA expression. *J Appl Physiol* (1985) 2011;110(2):309–317. [[PubMed](#)]
29. Kouri FM, Hurley LA, Daniel WL, et al. miR-182 integrates apoptosis, growth, and differentiation programs in glioblastoma. *Genes Dev*. 2015;29(7):732–745. [[PMC free article](#)] [[PubMed](#)]
30. Hudson MB, Rahnert JA, Zheng B, et al. miR-182 attenuates atrophy-related gene expression by targeting FoxO3 in skeletal muscle. *Am J Physiol Cell Physiol*. 2014;307(4):C314–319. [[PMC free article](#)][[PubMed](#)]
31. Jeschke MG, Finnerty CC, Herndon DN, et al. Severe Injury Is Associated With Insulin Resistance, Endoplasmic Reticulum Stress Response, and Unfolded Protein Response. *Ann Surg*. 2012;255(2):370–378. [[PMC free article](#)] [[PubMed](#)]
32. Yu Y, Chai J. The function of miRNAs and their potential as therapeutic targets in burn-induced insulin resistance (review) *Int J Mol Med*. 2015;35(2):305–310. [[PubMed](#)]

[J Surg Res](#). Author manuscript; available in PMC 2016 Sep 1.

Published in final edited form as:

[J Surg Res](#). 2015 Sep; 198(1): 19–26.

Published online 2015 Jun 12. doi: [10.1016/j.jss.2015.05.038](https://doi.org/10.1016/j.jss.2015.05.038)

PMCID: PMC4542145

NIHMSID: NIHMS705141

PMID: [26104324](https://pubmed.ncbi.nlm.nih.gov/26104324/)

Effects of Exercise on Soleus in Severe Burn and Muscle Disuse Atrophy

[Melody R. Saeman](#),^{a,*} [Kevin DeSpain](#),^a [Ming-Mei Liu](#),^a [Brett A. Carlson](#),^a [Juquan Song](#),^a [Lisa A.](#)

[Baer](#),^b [Charles E. Wade](#),^b and [Steven E. Wolf](#)^a

[Author information](#) [Copyright and License information](#) [Disclaimer](#)

The publisher's final edited version of this article is available at [J Surg Res](#)

See other articles in PMC that [cite](#) the published article.

Abstract

[Go to:](#)

1. Introduction

Severe burn is accompanied by a hypermetabolic state resulting in the loss of body mass [1]. Studies of protein kinetics and DEXA imaging after severe burn have shown that protein catabolism and the resulting loss of lean muscle mass continues after wound healing and can persist 9 to 12 months after injury [2]. Severe muscle loss can increase the risks of sepsis and mortality, cause prolonged recovery times, lead to longer hospitalizations, and increase costs [3]. Given limitations in movement typically present in severe burn, the majority of patients are initially bed bound, which also has been shown to contribute to muscle atrophy [4]. Studies in healthy volunteers have demonstrated that muscle loss during bed rest is exacerbated by elevated serum cortisol, a physiological response to burn; this suggests that the effects of bed rest could be worse in burn [5]. An animal model was recently created to mimic bed rest after burn by placing severely burned rats in a tail suspension system to cause hindlimb unloading. The animals are able to move around the cage freely without bearing weight on their hindlimbs, leading to disuse. This investigation found that hindlimb disuse had an additive effect on muscle atrophy with decreased muscle mass and muscle function [6]. This experiment was the first to closely model the prolonged metabolic changes with muscle atrophy and resultant decrease in function similar to the changes observed in humans after severe burn [6,7]. This newly developed model of bed rest in burn has created the opportunity to closely study treatments aimed at diminishing muscle atrophy and loss of muscle function after severe burn.

It is well established that disuse muscle atrophy can be mitigated with concurrent resistance exercise training [4,5,8-13]. Initiation of resistance exercises at the start of bed rest in healthy volunteers was shown to be protective against loss of muscle protein synthesis [12]. The use of exercise training in burn patients is variable and incompletely evaluated. Practice patterns in the rehabilitation of burn patients typically focus on range of motion, manual muscle testing, and quality of life with less emphasis on exercise training [14]. It has been documented that a combination of aerobic and resistance exercise training improves lean muscle mass in pediatric burn patients [15-17]. A study of burned adults randomized into control groups or exercise groups with supervised isokinetic leg exercise 3 times per week demonstrated a significant increase in strength [18]. These investigations of exercise training in burn patients have only evaluated its efficacy after recovery from the acute phase, typically as outpatients or 6 months after injury. No studies have evaluated the effects of exercise training during the initial acute phase of recovery. We hypothesize that early initiation of resistance training in burn with bed rest will mitigate muscle atrophy due to disuse. The aim of this study is to evaluate the effects of exercise on muscle mass and function in an animal model of burn with hindlimb unloading.

[Go to:](#)

2. Materials and Methods

Approval was granted for all procedures from the Institutional Animal Care and Use Committee (IACUC) at the University of Texas Health Science Center at Houston. All animal procedures were performed at this location. Forty-eight adult male Sprague-Dawley rats (Charles Rivers, Wilmington, MA, USA) were assigned to four groups (n = 12): sham ambulatory (S/A), burn ambulatory (B/A), sham hindlimb unloading (S/H), or burn hindlimb unloading (B/H). Animals were assigned to groups randomly after weight matching for a block design to allow for an even distribution of body mass between groups. These groups were then subdivided into exercise or no exercise (n = 6) for a total of eight groups. On arrival, animals were approximately 300g. Animals were placed in standard cages upon arrival and were then housed in specialized metabolic cages (144 in² of usable floor area) with a traction system for hindlimb unloading [11] for 5 days prior to burn procedures. Animals were fed a powder diet (Harlan Teklad #2018) *ad libitum* and housed in a reversed 12-hour light/dark cycle, to allow for exercise training during the animal's dark phase. Room temperature was maintained at 26±2 °C, with a relative humidity of 30% to 80% to simulate, as closely as possible, the ambient temperature maintained in a standard burn unit.

2.1 Thermal Injury

All animals were anesthetized with isoflurane (2-3% in 100% O₂). Each rat was shaved on the dorsal and ventral surface. Rats randomly assigned to the burn treatment groups (B/A or B/H with and without exercise) received a full-thickness scald burn of 40% total body surface area as previously described [19]. The burned animals were resuscitated with 20 ml of intraperitoneal Lactated Ringer's [20]. Animals randomized to the sham treatment groups (S/A or S/H with or without exercise) were submerged in room temperature water after shaving. All animals were given buprenorphine (0.05 mg/kg subcutaneous) at 8 hours after injury for analgesia after burn.

2.2 Hindlimb Unloading

Animals randomized to the S/H or B/H (with and without exercise) groups were placed in a tail harness and attached to a hindlimb unloading system described by Morey-Holton and Globus [11]. After animals fully recovered from anesthesia, the harness was attached to a hook and pulley traction system on top of the cage with a fish-line swivel device. The rats were positioned at a 30° head-down angle from the floor unloading the hindlimbs only. The system rides along two parallel sides of the cage and allows the animals to have 360° access within the cage and to move on an x-y axis. Rats were able to freely access food and water without their hindlimbs contacting the walls of the cage. Animals were observed for signs of distress immediately after unloading and several times a day throughout the study period. Animals in the ambulatory groups were housed in similar cages but without hindlimb unloading.

2.3 Exercise

All animals were pre-trained 10 days prior to injury. Animals were trained to climb 1 meter at an 80° incline. The 6-inch climbing lanes were covered in ½ inch plastic mesh. During the pre-training period, rats were trained daily (a.m. only) for the first 6 days and then twice daily (a.m./p.m.) once acclimated. Each session consisted of 5 climbs from bottom to top with a 10 second rest between repetitions. On the day of injury, rats were randomly assigned to exercise groups, with the exclusion of rats that outright refused to climb (n=14) during the pre-training period. After injury, weights in a plastic bag were attached with Velcro to the base of the tail during exercise. Weights were calculated as percent body mass of each rat and gradually increased by 10% every few days as tolerated with a maximum weight of 50% body mass.

2.4 Muscle Function

On day fourteen after burn or sham, all animals were anesthetized with isoflurane (2-3% in 100% O₂). The soleus and plantaris on the left leg were isolated and prepared for *in situ* isometric muscle function as previously described by Wu *et al.* [21]. The plantaris tendon was attached with a suture loop to the lever arm of a dual-mode servo muscle lever system (Aurora Scientific, Inc., model 305c). The isometric force of the plantaris muscle was then measured and recorded using the ASI muscle lever system with dynamic muscle control and analysis software (Aurora Scientific, Inc., 615A). The optimal length of the muscle was determined with a series of twitches and interval stretches. Initially, the muscle was put on 20 g of stretch. A single 200 Hz twitch was stimulated with impulse duration of 0.2 msec at 10 mA. The muscle was then stretched 0.3 mm and stimulated again with 25 seconds between stimulations. This pattern was continued until there was less than 2% change in force between twitches, indicating the optimal length (L_o) of the muscle. The length of the muscle at optimal stretch was measured with calipers. The maximum twitch (P_t) and tetanic (P_o) parameters were then measured at optimal length. Isometric tetanic function was stimulated at 150 Hz with impulse duration of 0.2 msec, 75 pulses per train, at 10 mA, for a total of 1 second. P_o was measured three times with an off-tension recovery period of 2 minutes between stimulations. This same procedure was then performed on the soleus; however, initial tension was started at 2 g of stretch. After completion of a rest period, following the third tetanic force measurement, the soleus fatigue function was measured for a total of 240 seconds at 40 Hz with impulse duration of 0.2 msec, 14 pulses per train, at 10 mA.

High-throughput Dynamic Muscle Analysis software (Aurora Scientific, Inc., 615A) was used to determine the time to peak tension (TPT) and half-relaxation time (1/2 RT) from the twitch response curves. The three tetanic force (Po) measurements were averaged. The tetanic force was converted to specific force (N/cm²) using the physiologic cross sectional area (CSA) with the formula $CSA = (\text{muscle mass} \times \cos \theta) / (\text{coefficient of muscle density} \times \text{muscle fiber length})$ [22]. The coefficient of muscle density is 1.06, and θ is the muscle fiber pennation angle of 16.4 and 3.9 for the plantaris and soleus in rats [22]. Muscle fiber length was calculated from measured muscle length at Lo using the reference ratio of 0.34 and 0.69 for plantaris and soleus in rats, respectively. Reference pennation angle, muscle density, and fiber-to-muscle length ratios were based on measurements from Eng *et al.* [22]. The fatigue minimum was considered the absolute force after 4 minutes of the fatigue function test. The fatigue index is the minimum reported as a percentage of the maximum force during the fatigue test.

2.5 Tissue Analysis

Following muscle function analysis, animals were euthanized by exsanguination. The hindlimb muscles on the right were harvested, weighed, snap frozen in liquid nitrogen, and stored at -80°C for protein analysis. The left hindlimb muscles were harvested, weighed, placed in 10% neutral-buffered formalin for 24-48 hours, and stored in 70% ethanol. Samples were paraffin embedded prior to microtome sectioning. Hematoxylin and eosin staining was performed. Quantitative analysis of soleus muscle fiber size was performed with blinded random cluster sampling of the muscle fiber cross-sectional area. Image analysis was performed using ImageJ software.

2.6 Statistical Analysis

Statistical analysis was performed with one-tailed or two-tailed Student's t-test, Mann Whitney *U* test, or three-way ANOVA using the Holm-Sidak method for pairwise multiple comparisons where appropriate using Systat Sigma Plot®. Numbers reported as mean ± SEM.

[Go to:](#)

3. Results

3.1 Animal Body Mass

We found a significant difference in animal body mass between treatment groups at day 14 ($p < 0.001$). Using pairwise multiple comparison procedures and controlling for the other treatment levels, we found that body mass was lower in the burn (284 ± 4 vs. 309 ± 5 g, $p < 0.001$), hindlimb-unloaded (283 ± 3 vs. 311 ± 5 g, $p < 0.001$), and exercise treatments (290 ± 4 vs. 303 ± 5 , $p = 0.004$). Evaluating the effects of exercise within groups showed a significantly ($p < 0.05$) lower body mass in B/A and S/A compared to no exercise with a two-tailed and one-tailed t-test, respectively (Fig.1). The decrease in body mass with exercise was not seen in the B/H and S/H groups.

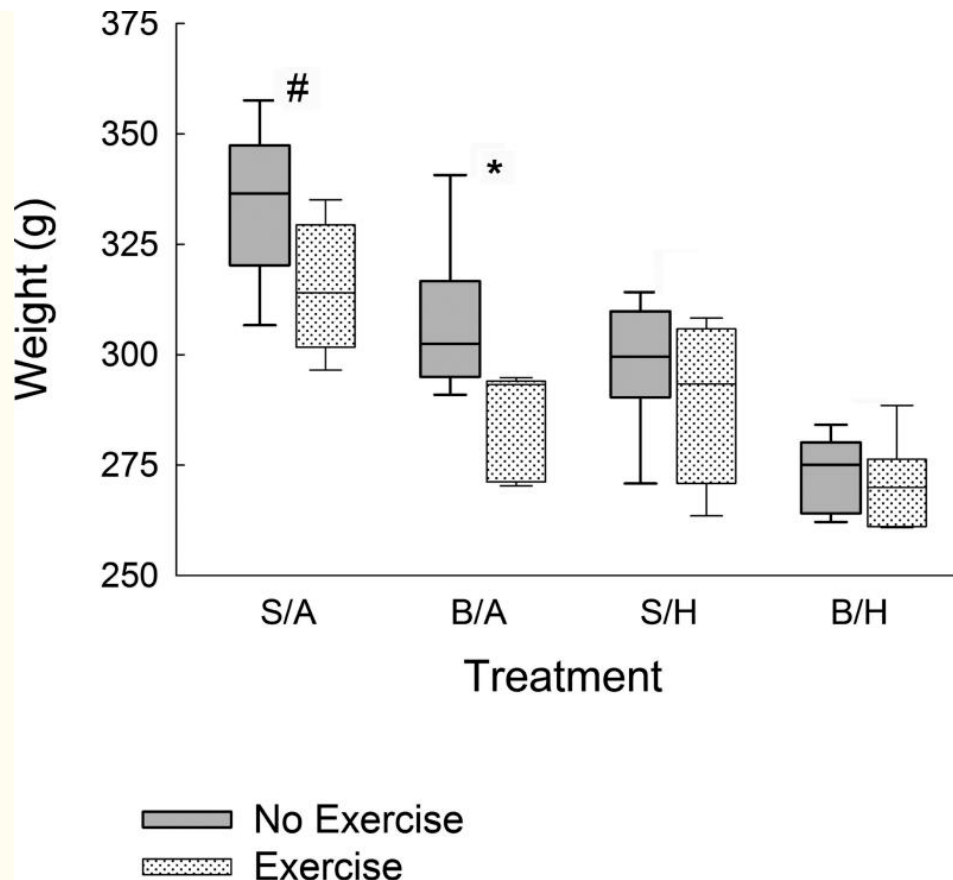


Figure 1

Animal Body Mass

Abbreviations used: S/A = sham ambulatory, B/A = burn ambulatory, S/H = sham hindlimb unloading, B/H = burn hindlimb unloading. Animals were weighed on day 14 after burn or sham. Exercise was compared to No Exercise within treatment groups. # $p < 0.05$ with one-tailed t-test and * $p < 0.05$ with two-tailed t-test. Please refer to the results section for significant differences between other factors.

3.2 Plantaris Mass and Protein Content

We found decreased right plantaris muscle mass in burn (B/A, 358 ± 11 mg) and hindlimb-unloaded (S/H, 292 ± 8 mg) compared to sham (S/A, 401 ± 14 mg); hindlimb (B/H, 293 ± 6 mg) was lower than B/A ($p < 0.01$, all comparisons). Within hindlimb unloading, there was no difference between burn and sham. There was no significant difference between groups with or without exercise. When plantaris tissue weight was normalized to body mass, a significant difference was seen only between the ambulatory and hindlimb treatments ($p < 0.001$). There was no difference in plantaris total protein content between groups. ([Table 1](#))

Table 1

Muscle Mass, Myofiber Size, and Protein Content (Right)

Group	Plantaris			Soleus			
	Wet Weight (mg)	Weight (mg) per 100g Body Mass	Protein Content (μ g)	Wet Weight (mg)	Weight (mg) per 100g Body Mass	Protein Content (μ g)	Myofiber Size (μ m ²)
No Exercise							
S/A	394 \pm 24	117 \pm 7	24.6 \pm 7.4	142 \pm 5	43 \pm 2	7.13 \pm 0.72	2187 \pm 488
B/A	365 \pm 17	119 \pm 4	24.3 \pm 2.4	122 \pm 7	40 \pm 2	2.95 \pm 0.60	2395 \pm 291
S/H	290 \pm 14	98 \pm 6	28.4 \pm 3.6	69 \pm 5	23 \pm 2	11.7 \pm 4.62	1499 \pm 89
B/H	289 \pm 9	106 \pm 3	20.3 \pm 3.7	77 \pm 7	28 \pm 3	3.82 \pm 1.67	1079 \pm 79
S/A	408 \pm 25	130 \pm 6	24.1 \pm 3.1	147 \pm 9	47 \pm 2	8.55 \pm 0.93	3739 \pm 43
Exercise							
B/A	349 \pm 13	123 \pm 5	19.8 \pm 0.7	143 \pm 7	50 \pm 2	4.24 \pm 0.75	3146 \pm 305
S/H	294 \pm 14	102 \pm 2	31.2 \pm 15	84 \pm 2	29 \pm 1	9.93 \pm 0.52	1648 \pm 130
B/H	296 \pm 10	109 \pm 4	22.9 \pm 3.0	86 \pm 4	32 \pm 2	4.59 \pm 0.93	1985 \pm 170

Abbreviations used: S/A = sham ambulatory, B/A = burn ambulatory, S/H = sham hindlimb unloading, B/H = burn hindlimb unloading. All numbers reported as mean \pm standard error of the mean. Please refer to results section for statistical significance.

3.3 Soleus Mass and Protein Content

The right soleus mass was significantly lower in hindlimb-unloaded (79 \pm 13 mg) versus ambulatory (139 \pm 19 mg, $p < 0.001$) and no exercise (103 \pm 7 mg) versus exercise (115 \pm 7, $p < 0.01$). There was no difference between burn and sham. This difference persisted when normalized to body mass. There was a significantly lower soleus whole muscle protein content in the hindlimb compared to the ambulatory groups (4.5 \pm 1.1 vs. 8.4 \pm 1.1 mg, $p < 0.05$). ([Table 1](#))

3.4 Plantaris Muscle Function

The left plantaris muscle function demonstrated a significantly lower maximum twitch force (Pt) in the hindlimb-unloaded group (89 \pm 6.5 g) versus the ambulatory group (111 \pm 6.8 g, $p < 0.05$). The absolute tetanic force (Po) was also lower in the hindlimb group (505 \pm 20 g vs. 565 \pm 21 g, $p < 0.05$). There was no significant effect in the burn or exercise treatments. There was no

significant difference between groups in the plantaris specific tetanic force (Po/CSA), the half relaxation time (1/2 RT), the time to peak tension (TPT), or the twitch to tetanic ratio (Pt/Po). We also found no difference in the plantaris physiologic cross sectional area (CSA) or optimal muscle length (Lo). ([Table 2](#))

Table 2

Plantaris Dimensions and Isometric Muscle Function (Left)

Parameter		No Exercise				Exercise			
		S/A	B/A	S/H	B/H	S/A	B/A	S/H	B/H
Muscle	Wet weight (mg)	459 ± 22	383 ± 22	341 ± 16	337 ± 13	405 ± 27	410 ± 24	347 ± 14	390 ± 61
	Lo (mm)	39 ± 0.9	39 ± 1.0	37 ± 1.1	35 ± 0.7	39 ± 1.0	40 ± 1.8	38 ± 0.8	40 ± 1.4
	PCSA (mm ²)	31 ± 0.9	26 ± 1.9	25 ± 1.4	26 ± 1.3	28 ± 2.1	29 ± 2.7	24 ± 1.1	27 ± 5.6
Twitch Force	Pt (g)	102 ± 12	117 ± 15	93 ± 7.3	89 ± 9.3	129 ± 27	97 ± 13	95 ± 11	80 ± 7.8
	TPT (ms)	28 ± 1.3	30 ± 0.9	30 ± 1.3	29 ± 1.2	30 ± 0.6	31 ± 1.0	30 ± 1.8	32 ± 0.7
	1/2 RT (ms)	18 ± 1.7	20 ± 1.0	19 ± 1.2	18 ± 1.4	18 ± 2.1	16 ± 2.1	17 ± 1.2	18 ± 1.2
	Po (g)	565 ± 42	602 ± 39	539 ± 30	517 ± 37	603 ± 72	492 ± 54	511 ± 13	452 ± 29
Tetanic Force									
	Po/CSA (N/cm ²)	18.2 ± 1.4	23.2 ± 2.3	21.9 ± 1.6	20.2 ± 1.8	20.3 ± 1.7	17.9 ± 2.3	21.4 ± 0.5	18.6 ± 2.4
		19 ± 1.7	20 ± 2.5	17 ± 0.5	17 ± 1.2	21 ± 2.1	20 ± 1.4	18 ± 1.8	18 ± 2.6
Pt/Po (%)									

Abbreviations used: S/A = sham ambulatory, B/A = burn ambulatory, S/H = sham hindlimb unloading, B/H = burn hindlimb unloading, Lo = optimal muscle length, PCSA = physiologic cross sectional area, Pt = twitch force, TPT = time to peak twitch, 1/2 RT = half relaxation time, Po = absolute tetanic force, Po/CSA = specific tetanic force, Pt/Po = twitch/tetanic ratio. All numbers reported as mean ± standard error of the mean. Please refer to results section for statistical significance.

3.5 Soleus Muscle Function

The left soleus isometric twitch force was significantly lower in the hindlimb-unloaded group (31 ± 1.5 vs. 12 ± 1.5 g, p<0.001). Compared to no exercise, the B/H exercise group had a significantly higher twitch force (14 ± 2.1 g vs. 8 ± 1.9 g, p<0.05). Across all other factors, there was no significant difference in the soleus twitch force between exercise and no exercise. There was a longer 1/2 RT in the B/A versus B/H groups (83 ± 9 ms vs. 48 ± 8 ms, p<0.05). There was a longer soleus TPT in the ambulatory versus hindlimb group (61 ± 4 ms vs. 49 ± 5 ms, p<0.05). ([Table 3](#))

Table 3

Soleus Dimensions and Isometric Muscle Function (Left)

Parameter		No Exercise				Exercise			
		S/A	B/A	S/H	B/H	S/A	B/A	S/H	B/H
Muscle	Wet weight (mg)	204 ± 16	205 ± 11	139 ± 15	174 ± 36	175 ± 13	197 ± 12	127 ± 10	114 ± 7.0
	Lo (mm)	44 ± 1.3	43 ± 2.0	39 ± 1.7	37 ± 0.4	41 ± 1.9	44 ± 2.2	40 ± 1.0	41 ± 1.1
	PCSA (mm ²)	6.3 ± 0.4	6.5 ± 0.4	5.0 ± 0.6	6.3 ± 1.4	6.0 ± 0.6	6.0 ± 0.4	4.3 ± 0.3	3.8 ± 0.4
Twitch Force	Pt (g)	31 ± 2.8	36 ± 4.4	14 ± 2.1	8.0 ± 2.0	30 ± 2.6	27 ± 2.0	11 ± 0.6	14 ± 2.1
	TPT (ms)	58 ± 8.0	66 ± 5.5	50 ± 6.6	48 ± 7.0	49 ± 11	73 ± 5.3	48 ± 14	49 ± 4.5
	1/2 RT (ms)	57 ± 12	90 ± 6.0	65 ± 11	51 ± 11	58 ± 17	80 ± 4.0	60 ± 17	45 ± 5.1
Tetanic Force	Po (g)	159 ± 18	165 ± 9.3	56 ± 4.4	42 ± 5.5	150 ± 16	118 ± 14	66 ± 8.3	54 ± 4.9
	Po/CSA (N/cm ²)	25 ± 2.8	25 ± 1.7	12 ± 2.2	7.0 ± 1.3	23 ± 2.4	20 ± 1.9	17 ± 2.0	14 ± 1.7
Pt/Po (%)		20 ± 1.4	22 ± 1.5	24 ± 6.7	19 ± 2.5	26 ± 5.2	23 ± 1.8	21 ± 3.7	26 ± 4.9
Fatigue	Minimum	105 ± 15	100 ± 10	35 ± 4.0	24 ± 2.8	76 ± 21	48 ± 16	31 ± 10	32 ± 11
	Index (%)	66 ± 5.9	69 ± 6.3	82 ± 11	76 ± 3.0	52 ± 11	37 ± 11	63 ± 6.3	58 ± 13

Abbreviations used: S/A = sham ambulatory, B/A = burn ambulatory, S/H = sham hindlimb unloading, B/H = burn hindlimb unloading, Lo = optimal muscle length, PCSA = physiologic cross sectional area, Pt = twitch force, TPT = time to peak twitch, 1/2 RT = half relaxation time, Po = absolute tetanic force, Po/CSA = specific tetanic force, Pt/Po = twitch/tetanic ratio. All numbers reported as mean ± standard error of the mean. Please refer to results section for statistical significance.

There was a significantly lower soleus tetanic force in the hindlimb-unloaded group (55 ± 5 vs. 148 ± 6 g, $p < 0.001$). B/A had a lower tetanic force in the exercise group versus no exercise (118 ± 14 vs. 165 ± 9 g, $p = 0.02$). In B/H, no difference in soleus absolute tetanic force was seen with or without exercise. All hindlimb groups had significantly lower specific tetanic force than ambulatory (12 ± 1.2 vs. 22 ± 1.3 N/cm², $p < 0.001$). The specific tetanic force in B/H was significantly higher in exercise versus no exercise (14 ± 1.7 vs. 7 ± 1.3 N/cm², $p < 0.01$); this effect was not seen in S/H or B/A groups. There was no difference in soleus Pt/Po between groups.

The soleus fatigue index was significantly lower in the ambulatory (55%) and exercise (52%) groups versus hindlimb-unloaded (69%) and no exercise (73%) groups ($p = 0.03$, $p = 0.002$ respectively). The soleus fatigue minimum was significantly lower in the hindlimb groups and in the ambulatory exercise group. The soleus CSA was significantly lower in the exercise (5.1 ± 0.3 vs. 6.1 ± 0.3 mm², $p < 0.05$) and hindlimb (4.8 ± 0.3 vs. 6.4 ± 0.3 , $p < 0.001$) compared to no exercise and ambulatory respectively.

3.6 Soleus Myofiber Size

Myofiber size of the soleus was significantly decreased in the hindlimb unloaded versus ambulatory (1552 ± 36 μm² vs. 2866 ± 38 μm², $p < 0.001$) and no exercise versus exercise (1790 ± 36 μm² vs. 2630 ± 38 μm², $p < 0.001$) groups. There was not a significant difference in soleus myofiber size between the burn and sham groups in the ambulatory animals. However, within the no exercise group, soleus myofiber size was significantly decreased in B/H compared to S/H (means reported in [Table 1](#), $p < 0.05$). Exercise had a greater impact on soleus muscle fiber size recovery in B/H compared to S/H ([Fig. 2](#)).

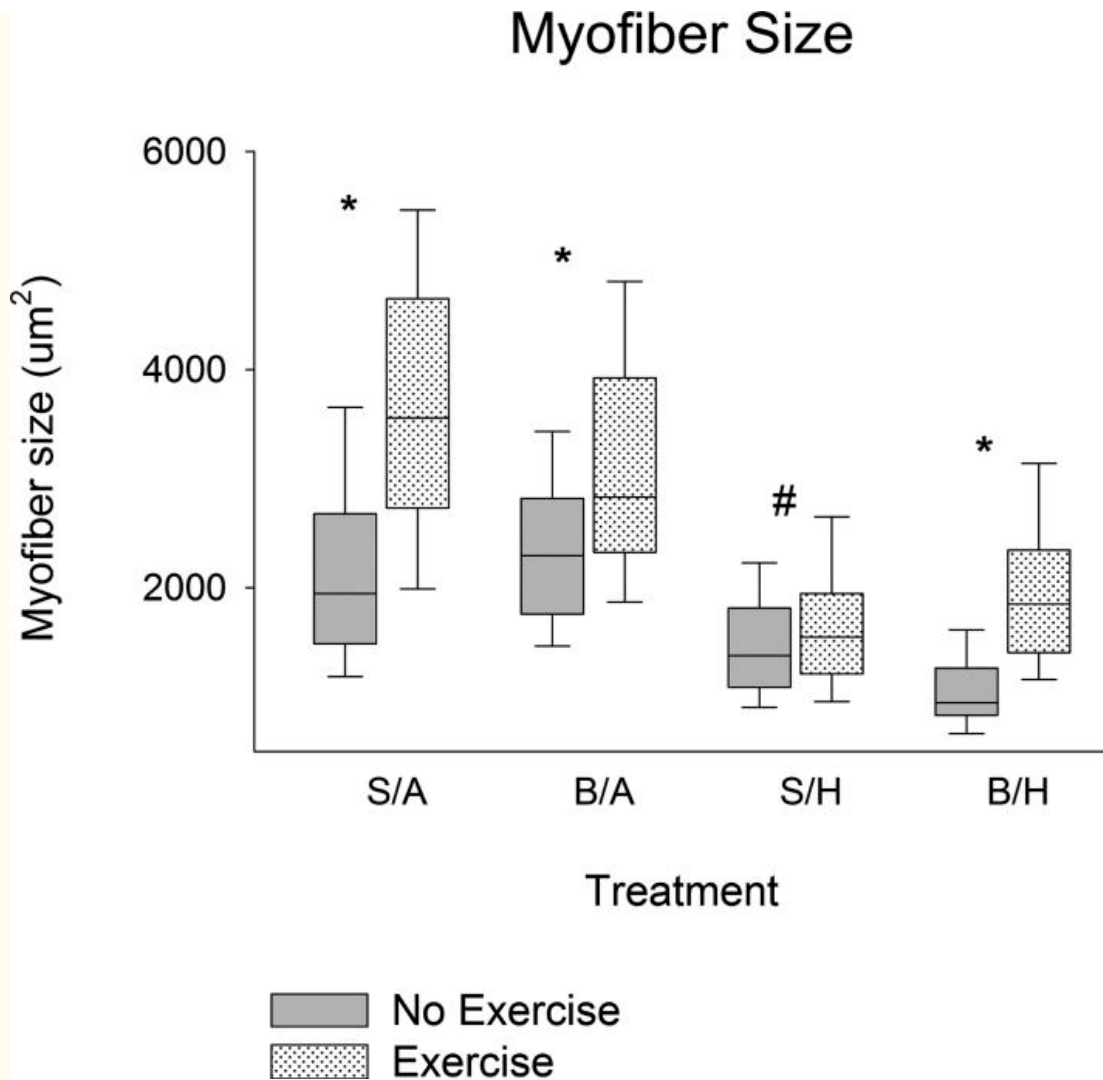


[Figure 2](#)

Soleus Myofiber Size

Abbreviations used: S/A = sham ambulatory, B/A = burn ambulatory, S/H = sham hindlimb unloading, B/H = burn hindlimb unloading. Exercise was compared to No Exercise within treatment groups. # $p < 0.05$ with one-tailed t-test and * $p < 0.001$ with two-tailed t-test. Please refer to the results section for significant differences between other factors.

[Go to:](#)

4. Discussion

In our investigation of muscle function after burn and hindlimb disuse, we found that resistance exercise in the acute recovery period significantly increased the mass, myofiber size, and function of the soleus. We did not find significant changes after exercise in the predominately fast-twitch plantaris muscle. These findings are important given that the majority of critically injured patients are subject to prolonged muscle disuse due to bed rest. This is especially true of severely burned patients, who typically require prolonged ventilation, multiple surgical procedures, and decreased mobility as a result of injury patterns.

It is established that muscle loss after burn is a result of a net increase in protein breakdown [2]. Studies in rodents have found decreased fiber size [23] with a greater impact on the fast-twitch muscle groups after burn [21]. It is also known that muscle disuse results in significant atrophy leading to a smaller fiber size with a greater effect on slow-twitch muscle groups [8]. In burn patients, it is unknown what degree of muscle atrophy is caused by disuse compared to burn alone. An animal model of thermal injury with hindlimb unloading was developed to mimic prolonged bed rest after burn. This model was found to demonstrate a closer approximation of the metabolic response and muscle atrophy after severe burn in humans [6,7]. These findings suggest that disuse is a contributing factor to the loss of muscle mass in burn patients. Many investigations have established that exercise diminishes atrophy due to muscle disuse. [4,5,8-13][14][15-17][18] Various forms of exercise have been studied in rat models of hindlimb unloading including treadmill [24], direct sciatic stimulation [25,26], isometric resistance training [25,27], flywheel resistance training [28], and climbing [29]. Dynamic resistance training in hindlimb suspension has been shown to attenuate soleus atrophy with increased mass and muscle protein [30]. Resistance training activates the PI3-AKT-mTOR pathway increasing protein synthesis [9].

Our aim was to evaluate the effects of a resistance exercise program initiated immediately following thermal injury in an animal model of muscle disuse with hindlimb unloading. We chose to evaluate a climbing protocol after burn because it is a voluntary dynamic resistance training model previously shown by Herbert *et al.* to attenuate muscle atrophy in hindlimb-unloaded rats [29,30]. We measured the change in muscle properties and function of the plantaris and soleus muscles because both are plantar flexor muscles, one predominantly fast-twitch and the other slow-twitch, respectively. Plantar flexor muscles and slow-twitch muscles have been shown to have a greater response to hindlimb unloading; whereas fast-twitch muscles have been shown to have a greater loss of mass in response to burn [10,21,31].

4.1 Animal Body Mass and Muscle Characteristics

Consistent with prior findings, animal mass was lower with burn, hindlimb unloading [25,29,32] and decreased further in B/H [6,7]. Exercise did not significantly alter body mass in the hindlimb groups [27,33,34]. B/A was found to have the greatest decrease in body mass with exercise. However, the maintenance of relative soleus and plantaris mass in this group suggests the decrease in mass is not from the loss of lean muscle.

Our findings of decreased plantaris but not soleus mass after burn are consistent with prior experiments identifying a loss of fast-twitch muscle mass after burn [6,21,35]. The plantaris mass was further reduced with hindlimb unloading, similar to findings by Wu *et al.* using this model [6]. However, we did not find a difference between the plantaris mass in S/H and B/H groups as was previously reported by Wu *et al.* [6]. It is possible that pre-training could have contributed to this difference. When the plantaris was normalized to body mass, there was only a significant decrease in the hindlimb treatments compared to ambulatory. We did not observe an effect of exercise on plantaris mass in any treatments. These findings are not surprising given that prior investigations found little effect of exercise on fast-twitch muscles in hindlimb unloading [27,29]. There was no difference in the plantaris total protein content between groups. These findings suggest that hindlimb unloading has a greater impact on plantaris mass than burn and the current exercise protocol utilized does not compensate for the loss of plantaris mass.

There was a significant decrease in the soleus absolute and normalized mass as well as protein content with hindlimb unloading consistent with prior findings [10,27,29,32]. Similarly Herbert *et al.* and other groups found exercise remediated some of the soleus muscle mass loss but did not recover to ambulatory levels in the hindlimb groups [27,29,36]. Similar to prior reports, the soleus myofiber size was decreased with hindlimb unloading [37]. We also found that the soleus myofiber size was lowest in B/H. Exercise partially recovered fiber size; this effect was greater on B/H but did not return to normal levels. Exercise increased myofiber size across all conditions.

4.2 Muscle Function

The maximum twitch and absolute tetanic forces were lower in the plantaris of the hindlimb-unloaded groups, similar to prior findings [38]. We did not observe a difference in plantaris muscle function between ambulatory burn and sham. This is similar to findings by Wu *et al.*, except that we did not appreciate a difference between B/H and S/H absolute tetanic (P_o) and the twitch/tetanic (P_t/P_o) ratio [6]. We did not identify differences in any other plantaris muscle function parameters. These findings are consistent with the changes observed in the plantaris muscle mass. The lack of changes in specific force is consistent with prior findings [6,38] and suggests that decline in plantaris function is related to a decrease in quantity of muscle tissue predominantly as a result of hindlimb unloading. Exercise did not appear to impact muscle atrophy from hindlimb disuse in the plantaris. Prior experiments have shown a mild improvement in muscle function of fast-twitch muscle groups with exercise training during hindlimb suspension [27,29,33]. It is possible that we did not see an effect on the plantaris with exercise training due to differences in duration, frequency, and type of training.

The soleus demonstrated lower twitch force in the hindlimb-unloaded groups as previously reported [6,10,27,29,38]. Exercise increased the twitch force only in the burn hindlimb group but not to control levels. The increased speed to peak (TPT) and relaxation time ($1/2 RT$) observed in the soleus of hindlimb groups is similar to prior findings and could reflect an increased relative proportion of fast-twitch fibers [6,38].

The absolute and specific tetanic soleus forces were lower across all hindlimb groups consistent with prior findings [6,10,27,32]. The soleus specific tetanic force was doubled with exercise in the burn hindlimb treatment only; however, this increase was not sufficient to return to ambulatory levels. Prior studies of exercise in hindlimb unloading have demonstrated variable results, but many did show improvement in the soleus [27]. The lack of improvement in the S/H group after exercise suggests that a more rigorous regimen could be used and may demonstrate an even larger change in the B/H group. There was no difference in the twitch to tetanic ratio (P_t/P_o) across treatments; this is in contrast to prior findings by Wu *et al.* [6]. A possible explanation for the differences in P_t/P_o could be differences in the protocol of isometric muscle function testing such as sequential instead of simultaneous muscle testing and a truncated protocol to obtain L_o . This difference in protocols could have led to altered muscle ATP levels between the two methods at the time of tetanic force testing. Also the pre-training period could have created a protective effect accounting for differences in our findings.

The soleus fatigue index observed in the hindlimb-unloaded group was higher than the ambulatory group, but the minimum force after 4 minutes was significantly lower than the ambulatory groups. The fatigue index in the exercise hindlimb groups was similar to ambulatory

levels. The alteration in the contraction times and fatigue properties is suggestive of a change in the relative fiber types in the soleus muscle with hindlimb unloading. We did find a relatively increased percentage of fast-twitch fibers in the soleus muscle after hindlimb unloading. Exercise in B/H further increased the ratio of fast-twitch fibers (data not shown). The soleus is known to have a decrease in the percentage of slow-twitch fibers with unloading [32], and our histological and functional findings suggest that resistance exercise does not diminish the loss of slow-twitch fibers.

[Go to:](#)

5. Conclusions

Consistent with prior investigations of this burn animal model, we found that hindlimb unloading contributed to the loss of muscle mass, myofiber size, and function in severe burn [6]. We have shown that exercise did not impact changes in the plantaris characteristics or muscle function in this model. We did demonstrate some changes in the soleus with an exercise regimen; however, this did not result in a return to normal levels of function. We found that exercise increased soleus force only in the burn hindlimb group. Exercise remediated the loss of muscle mass from hindlimb unloading across groups but was not fully compensatory. Similarly, exercise correlated with an increase in soleus myofiber size across all treatments, with the greatest impact on the burn hindlimb group. These findings suggest that resistance exercise can be protective in sparing some muscle function in burn injury with muscle disuse. Exercise appears to have an increased compensatory effect on hindlimb unloading in the presence of burn. Our histological and functional findings in the soleus suggest that resistance exercise increases myofiber size but does not prevent the loss of slow-twitch fibers. Our current findings suggest that resistance training does not completely ameliorate the loss of function and will likely need to be part of a regimen aimed at reducing muscle atrophy. Further investigations with exercise regimens that include aerobic and/or pharmacological components are needed.

[Go to:](#)

Acknowledgements

We would like to acknowledge Mary A. Wallace for her assistance.

The authors report no proprietary or commercial interest in any product mentioned or concept discussed in this article. Research reported in this publication was supported by the Department of Defense grant number CDMRP W81XWH-13-1-048 and the National Institute for General Sciences of the National Institutes of Health under award number T32GM008593.

[Go to:](#)

Footnotes

Publisher's Disclaimer: This is a PDF file of an unedited manuscript that has been accepted for publication. As a service to our customers we are providing this early version of the manuscript. The manuscript will undergo copyediting, typesetting, and review of the resulting proof before it is published in

its final citable form. Please note that during the production process errors may be discovered which could affect the content, and all legal disclaimers that apply to the journal pertain.

The authors listed above have made substantial contributions to the preparation of this manuscript. Melody R. Saeman contributed to this work through data acquisition, data analysis, and data interpretation as well as drafting and preparing the manuscript. Kevin DeSpain, Ming-Mei Liu, and Brett A. Carlson assisted with data acquisition. Lisa A. Baer and Juquan Song were involved with conceptual and experimental design; data acquisition and analysis; and revision of the manuscript. Charles E. Wade was integral to the concept and design of the experiment; the critical revision of the manuscript for important intellectual content; and the final approval of the version to be published. Steven E. Wolf contributed to the concept, design, and draft of the manuscript.

[Go to:](#)

References

1. Newsome TW, Mason AD, Jr., Pruitt BA., Jr. Weight loss following thermal injury. *Ann Surg.* 1973 Aug;178(2):215–7. [[PMC free article](#)] [[PubMed](#)]
2. Hart DW, Wolf SE, Mlcak R, et al. Persistence of muscle catabolism after severe burn. *Surgery.* 2000 Aug;128(2):312–9. [[PubMed](#)]
3. McClave SA, Mitoraj TE, Thielmeier KA, Greenburg RA. Differentiating subtypes (hypoalbuminemic vs marasmic) of protein-calorie malnutrition: incidence and clinical significance in a university hospital setting. *JPEN J Parenter Enteral Nutr.* 1992 Jul-Aug;16(4):337–42. [[PubMed](#)]
4. Wolfe RR. Control of muscle protein breakdown: effects of activity and nutritional states. *Int J Sport Nutr Exerc Metab.* 2001 Dec;11(Suppl):S164–9. [[PubMed](#)]
5. Ferrando AA, Stuart CA, Sheffield-Moore M, Wolfe RR. Inactivity amplifies the catabolic response of skeletal muscle to cortisol. *J Clin Endocrinol Metab.* 1999 Oct;84(10):3515–21. [[PubMed](#)]
6. Wu X, Baer LA, Wolf SE, Wade CE, Walters TJ. The impact of muscle disuse on muscle atrophy in severely burned rats. *J Surg Res.* 2010 Dec;164(2):e243–51. [[PMC free article](#)] [[PubMed](#)]
7. Wade CE, Baer LA, Wu X, Silliman DT, Walters TJ, Wolf SE. Severe burn and disuse in the rat independently adversely impact body composition and adipokines. *Crit Care.* 2013;17(5):R225. [[PMC free article](#)] [[PubMed](#)]
8. Baldwin KM, Haddad F, Pandorf CE, Roy RR, Edgerton VR. Alterations in muscle mass and contractile phenotype in response to unloading models: role of transcriptional/pretranslational mechanisms. *Front Physiol.* 2013;4:284. [[PMC free article](#)] [[PubMed](#)]
9. Brooks NE, Myburgh KH. Skeletal muscle wasting with disuse atrophy is multi dimensional: the response and interaction of myonuclei, satellite cells and signaling pathways. *Front Physiol.* 2014;5:99. [[PMC free article](#)] [[PubMed](#)]
10. Winiarski AM, Roy RR, Alford EK, Chiang PC, Edgerton VR. Mechanical properties of rat skeletal muscle after hind limb suspension. *Exp Neurol.* 1987 Jun;96(3):650–60. [[PubMed](#)]

11. Morey-Holton ER, Globus RK. Hindlimb unloading rodent model: technical aspects. *J Appl Physiol* (1985) 2002 Apr;92(4):1367–77. [[PubMed](#)]
12. Ferrando AA, Tipton KD, Bamman MM, Wolfe RR. Resistance exercise maintains skeletal muscle protein synthesis during bed rest. *J Appl Physiol* (1985) 1997 Mar;82(3):807–10. [[PubMed](#)]
13. Hart DW, Wolf SE, Chinkes DL, et al. Determinants of skeletal muscle catabolism after severe burn. *Ann Surg*. 2000;232(4):455–65. 10. [[PMC free article](#)] [[PubMed](#)]
14. Diego AM, Serghiou M, Padmanabha A, Porro LJ, Herndon DN, Suman OE. Exercise training after burn injury: a survey of practice. *J Burn Care Res*. 2013 Nov-Dec;34(6):e311–7. [[PMC free article](#)][[PubMed](#)]
15. Suman OE, Spies RJ, Celis MM, Mlcak RP, Herndon DN. Effects of a 12-wk resistance exercise program on skeletal muscle strength in children with burn injuries. *J Appl Physiol* (1985) 2001 Sep;91(3):1168–75. [[PubMed](#)]
16. Hardee JP, Porter C, Sidossis LS, et al. Early rehabilitative exercise training in the recovery from pediatric burn. *Med Sci Sports Exerc*. 2014 Sep;46(9):1710–6. [[PMC free article](#)] [[PubMed](#)]
17. Al-Mousawi AM, Williams FN, Mlcak RP, Jeschke MG, Herndon DN, Suman OE. Effects of exercise training on resting energy expenditure and lean mass during pediatric burn rehabilitation. *J Burn Care Res*. 2010 May-Jun;31(3):400–8. [[PMC free article](#)] [[PubMed](#)]
18. Ebid AA, Omar MT, Abd El Baky AM. Effect of 12-week isokinetic training on muscle strength in adult with healed thermal burn. *Burns*. 2012 Feb;38(1):61–8. [[PubMed](#)]
19. Walker HL, Mason AD., Jr. A standard animal burn. *J Trauma*. 1968 Nov;8(6):1049–51. [[PubMed](#)]
20. Pruitt BA. Fluid resuscitation of the extensively burned patients. *Ann Chir Plast*. 1979;24(3):268–72. [[PubMed](#)]
21. Wu X, Wolf SE, Walters TJ. Muscle contractile properties in severely burned rats. *Burns*. 2010 Sep;36(6):905–11. [[PMC free article](#)] [[PubMed](#)]
22. Eng CM, Smallwood LH, Rainiero MP, Lahey M, Ward SR, Lieber RL. Scaling of muscle architecture and fiber types in the rat hindlimb. *J Exp Biol*. 2008 Jul;211(Pt 14):2336–45. [[PubMed](#)]
23. Quintana HT, Bortolin JA, da Silva NT, et al. Temporal study following burn injury in young rats is associated with skeletal muscle atrophy, inflammation and altered myogenic regulatory factors. *Inflamm Res*. 2014 Nov 21; [[PubMed](#)]
24. Kim JH, Thompson LV. Differential effects of mild therapeutic exercise during a period of inactivity on power generation in soleus type I single fibers with age. *J Appl Physiol* (1985) 2012 May;112(10):1752–61. [[PMC free article](#)] [[PubMed](#)]
25. Haddad F, Adams GR, Bodell PW, Baldwin KM. Isometric resistance exercise fails to counteract skeletal muscle atrophy processes during the initial stages of unloading. *J Appl Physiol* (1985) 2006 Feb;100(2):433–41. [[PubMed](#)]
26. Adams GR, Haddad F, Bodell PW, Tran PD, Baldwin KM. Combined isometric, concentric, and eccentric resistance exercise prevents unloading-induced muscle atrophy in rats. *J Appl Physiol* (1985) 2007 Nov;103(5):1644–54. [[PubMed](#)]
27. Hurst JE, Fitts RH. Hindlimb unloading-induced muscle atrophy and loss of function: protective effect of isometric exercise. *J Appl Physiol* (1985) 2003 Oct;95(4):1405–17. [[PubMed](#)]

28. Dupont-Versteegden EE, Fluckey JD, Knox M, Gaddy D, Peterson CA. Effect of flywheel-based resistance exercise on processes contributing to muscle atrophy during unloading in adult rats. *J Appl Physiol* (1985) 2006 Jul;101(1):202–12. [[PubMed](#)]
29. Herbert ME, Roy RR, Edgerton VR. Influence of one-week hindlimb suspension and intermittent high load exercise on rat muscles. *Exp Neurol*. 1988 Nov;102(2):190–8. [[PubMed](#)]
30. Cholewa J, Guimaraes-Ferreira L, da Silva Teixeira T, et al. Basic models modeling resistance training: an update for basic scientists interested in study skeletal muscle hypertrophy. *J Cell Physiol*. 2014 Sep;229(9):1148–56. [[PubMed](#)]
31. Desplanches D, Mayet MH, Sempore B, Flandrois R. Structural and functional responses to prolonged hindlimb suspension in rat muscle. *J Appl Physiol* (1985) 1987 Aug;63(2):558–63. [[PubMed](#)]
32. Thomason DB, Booth FW. Atrophy of the soleus muscle by hindlimb unweighting. *J Appl Physiol* (1985) 1990;68(1):1–12. 01. [[PubMed](#)]
33. Linderman JK, Gosselink KL, Booth FW, Mukku VR, Grindeland RE. Resistance exercise and growth hormone as countermeasures for skeletal muscle atrophy in hindlimb-suspended rats. *Am J Physiol*. 1994 Aug;267(2 Pt 2):R365–71. [[PubMed](#)]
34. Fluckey JD, Dupont-Versteegden EE, Knox M, Gaddy D, Tesch PA, Peterson CA. Insulin facilitation of muscle protein synthesis following resistance exercise in hindlimb-suspended rats is independent of a rapamycin-sensitive pathway. *Am J Physiol Endocrinol Metab*. 2004 Dec;287(6):E1070–5. [[PubMed](#)]
35. Fang CH, James HJ, Ogle C, Fischer JE, Hasselgren PO. Influence of burn injury on protein metabolism in different types of skeletal muscle and the role of glucocorticoids. *J Am Coll Surg*. 1995 Jan;180(1):33–42. [[PubMed](#)]
36. Fluckey JD, Dupont-Versteegden EE, Montague DC, et al. A rat resistance exercise regimen attenuates losses of musculoskeletal mass during hindlimb suspension. *Acta Physiol Scand*. 2002 Dec;176(4):293–300. [[PubMed](#)]
37. Riley DA, Bain JL, Romatowski JG, Fitts RH. Skeletal muscle fiber atrophy: altered thin filament density changes slow fiber force and shortening velocity. *Am J Physiol Cell Physiol*. 2005 Feb;288(2):C360–5. [[PubMed](#)]
38. Diffie GM, Caiozzo VJ, Herrick RE, Baldwin KM. Contractile and biochemical properties of rat soleus and plantaris after hindlimb suspension. *Am J Physiol*. 1991;260(3 Pt 1):528–34. 03. [[PubMed](#)]

3. Abstracts

Effects of Resistance Exercise on Caloric Intake and Body Mass in Rats Following Burn and Disuse

Baer LA, Song J, Wolf SE, Wade CE

Introduction: The treatment and recovery of patients with severe traumatic injuries is impacted by a pronounced increase in metabolism. Injury induces a systemic catabolic response with increased energy expenditure and loss of body mass. The ability to resume normal activities is compromised due to inactivity associated with bed rest and the catabolic response due to burn injury. Exercise and nutritional interventions have been used independently with limited success. Using a combined severe burn and hindlimb unloading rodent model with no exercise, hypermetabolism was observed associated with a significantly reduced body mass combined with increased food intake. The purpose of this study was to determine if body mass and caloric intake are affected by daily resistance exercise following burn and disuse.

Methods: Male, Sprague-Dawley rats were randomized into four groups: Sham Ambulatory (SA), Burn Ambulatory (BA), Sham/Hindlimb unloaded (SH) and Burn/Hindlimb unloaded (BH), with daily resistance exercise (EX) or no exercise (NEX) (N=6/group). Rats were introduced to resistance exercise by adding weight to each tail during repetitive ladder climbing ten days prior to injury. Rats were then weight-matched into treatment groups, either daily exercise or no-exercise. Statistical analysis using ANOVA with significance at $p < 0.05$.

Results: No differences in body mass were observed between any groups at the time of injury. At day 14, NEX-SA and NEX-BA body mass were significantly greater than EX-SA and EX-BA, but no differences in SH or BH. BH rats were significantly smaller than other treatment groups. Compared to other treatment groups, there was a significant increase in average kcals consumed over the last 5 days in BH, irrespective of exercise. No other differences in food intake between NEX and EX within each treatment group were observed.

Conclusions: Disuse showed no significant changes in body mass due to exercise. Irrespective of exercise, BH demonstrated a hypermetabolic response with increased caloric intake in conjunction with significantly reduced body mass. Burn injury, accompanied by long-term disuse results in complex metabolic changes early after the initial injury. With disuse, exercise did not affect body mass and alterations in caloric intake were independent of exercise. Different underlying factors seem to be influencing the acute metabolic changes offering opportunities for early intervention resulting in positive long-term outcomes.

Grant Information: US Army MRMC CDMRP W81XWH-13-1-0489

	SA	BA	SH	BH
D14 Body Mass (g)				
NEX	336±7	307±7	305±6	282±4 [¥]
EX	319±6*	287±5*	294±7	278±4 [¥]
Caloric Intake (kcal/100g BM/day)				
NEX	20.5±0.8	21.3±0.4	21.7±0.6	22.1±0.9 [¥]
EX	19.7±0.4	21.0±0.6	20.2±0.5	23.0±0.9 [¥]

Exercise Alleviates Skeletal Muscle Protein Loss After Severe Burn and Hindlimb Disuse

Carlson BA, Song J, Saeman MR, DeSpain K, Baer LA, Wade CE, Wolf SE

Introduction: Muscle atrophy is common after severe burn which is associated with muscle disuse. In a rat model of hindlimb unloading after burn supports the contention that bedrest contributes significantly to catabolism and muscle atrophy. The aim of our study was to evaluate whether exercise mitigates the protein content loss in this animal model.

Methods: Forty-eight Sprague-Dawley male adult rats were randomly assigned to burn ambulatory (BA), burn hindlimb unloading (BH), sham ambulatory (SA), or sham hindlimb unloading (SH). Rats received a full thickness scald burn of 40% total body surface area (TBSA) or sham, and were allowed to ambulate or placed in a tail traction system for hindlimb unloading. Half of them were trained to exercise twice a day; another group had no exercise. On day 14 skeletal muscles in hind limb were harvested for tissue weight. Muscle proteins were extracted from rat gastrocnemius media (GM), soleus (SL) and plantaris (PL) following T-PER Tissue protein extraction procedure (Thermo Fisher Scientific). Protein concentration was measured with DC Protein Assay (Bio-Rad Laboratories Inc.). Statistical analysis was performed with Sigma Plot using three-way ANOVA. Significance was accepted with $p < 0.05$.

Results: Muscle tissue wet weight in rat GM, SL, PL significantly decreased after hindlimb unloading; only PL and GM (but not the SL) had significantly decreased protein content in rats 14 days after burn without hindlimb unloading. The ratio of soleus to body mass significantly increased with exercise treatment in rats ($p < 0.001$). There was significant protein content loss in SL in rats with HLU ($p = 0.001$), and protein yield in GM significantly increased in rats with exercise training ($p = 0.003$). (Table 1) Western blotting results showed that the absorbance ratio of desmin to GAPDH in tissue lysate from GM significantly decreased in BH group ($p < 0.05$), which was attenuated with exercise as there was no difference between BH and SA groups after exercise.

Summary: Skeletal muscle mass loss was significantly affected by hind limb immobilization. Exercise increased protein yield in rat GM muscle. Western blot data confirmed muscle specific protein loss was alleviated in the GM through exercise treatment in severe burn rats with hind limb unloading.

Applicability of Research to Practice: The current study demonstrates the benefit of physical therapy in burn victims with muscle disused atrophy

Skeletal Muscle Fiber Type Changes in Severe Burn Rats with Muscle Disuse Atrophy

Song J, Baer LA, Saeman MR, Liu MM, Carlson B, Wolf HE, DeSpain K, Wade CE, Wolf SE

Introduction: Muscle atrophy is common in severe burned patients with limited movement. In a rat model of hindlimb unloading after burn supports the contention that bedrest in the severe burn contributes significantly to muscle atrophy. The aim of our study was to evaluate if exercise in the setting of bedrest affected myofiber type in this burned animal model.

Methods: Male rats were assigned to four treatments: sham ambulatory (SA), sham hindlimb unloading (SH), burn ambulatory (BA), or burn hindlimb unloading (BH). Rats received 40% total body surface area (TBSA) scald burn or sham. Animals grouped to either ambulate or were placed in a tail traction system for hindlimb unloading. Within each treatment half of rats (n=6 per group) performed twice daily exercises of climbing 1 meter with 5 repetitions (EX) with the others did not exercise (NX). On day 14 skeletal muscles in hind limb were harvested. Myofiber type in plantaris (PL) and soleus (SL) muscles were determined using Immunohistochemistry methods (IHC) staining with anti-myosin heavy chain (MHC) Slow, type I and Fast, Type II antibodies (Sigma Aldrich, MO). The positive stained myofiber number was counted blinded to treatment under light microscopy at 10 x magnification. Statistical analysis was performed with Sigma Plot using 3-way ANOVA method, and significance was accepted by $p < 0.05$.

Results: Type I MHC myofiber was predominate in the soleus with only 11.4% type II myofibers in the sham ambulatory group. Burn had no effect on myofiber type, while the number of type II myofibers increased significantly in the soleus 14 days after hind limb unloading ($p=0.004$). No significant change in soleus myofiber type was found between exercise and non-exercise groups. Type II MHC myofiber was predominant (91±1.2 %) in the plantaris. the interior of the muscle on cross-section had significantly decreased type I fibers after burn ($p=0.047$); no difference was found after HLU or exercise.

Summary: Following severe burn, muscle immobilization increased the proportion of fast twitch myofiber in the soleus, while the burn injury had more effect on the predominately fast-twitch plantaris. No effect of exercise on myofiber type change in both PL and SL muscle was observed. Changes in myofiber type may occur independently due to injury or disuse, and do not responds to exercise training. Myofiber type distribution might be related with metabolic changes in burn patients and muscle disused dystrophy.

External Funding support: US Army MRMC CDMRP, NIH T32 Training Grant

The Effects of Exercise on Soleus Function in Severe Burn with Muscle Disuse Atrophy

Saeman MR, DeSpain K, Liu M, Carlson B, Baer LA, Song J, Wade CE, Wolf SE.

Introduction: Muscle loss is a known sequela of severe burn and critical illness that increases the risk of complications such as sepsis and prolonged recovery time. A prior study in a rat model of hindlimb unloading after burn supports that bedrest contributes significantly to muscle atrophy. The aim of our study was to evaluate if exercise mitigates the loss of muscle in this animal model.

Methods: Two groups of 24 Sprague-Dawley rats were randomly assigned to burn ambulatory (B/A), burn hindlimb unloading (B/H), sham ambulatory (S/A), or sham hindlimb unloading (S/H). One group was trained to perform twice daily weighted resistance climbing of 1 meter with 5 repetitions; the other group had no exercise. Rats received a full thickness scald burn of 40% total body surface area or sham and were allowed to ambulate or were placed in a tail traction system for hindlimb unloading. On day 14 in situ isometric forces were measured on the left soleus muscle. Statistical analysis was performed with Sigma Plot using Student's t-test, Mann Whitney, or ANOVA with Holm-Sidak method where appropriate.

Results: The soleus wet weight was lower in the hindlimb (144 mg) and the exercise (136 mg) versus the ambulatory (190 mg, $p < 0.001$), and no exercise (180 mg, $p = 0.01$) groups. There was no difference in weights between burn and sham. Twitch was significantly lower in the hindlimb group: 31 vs 12 g ($p < 0.001$). Compared to no exercise, the B/H exercise group had a significantly higher twitch force 14 vs. 8 g ($p = 0.04$). Across all other factors there was no significant difference in the twitch between exercise and no exercise. There was a significantly lower tetanic force in the hindlimb group: 55 vs 148 g ($p < 0.001$). B/A had a lower tetanic force in the exercise group versus no exercise: 118 vs 165g ($p = 0.02$). In B/H no difference in tetanic force was seen with or without exercise. All hindlimb groups had significantly lower specific tetanic force than ambulatory: 12 vs. 22 N/cm² ($p < 0.001$). The specific tetanic force in B/H was significantly higher in exercise versus no exercise: 14 vs. 7 N/cm² ($p = 0.008$). Fatigue index was significantly lower in the ambulatory (55%) and exercise (52%) groups versus hindlimb (69%) and no exercise (73%) groups ($p = 0.03$, $p = 0.002$ respectively). Muscle function of all groups included in table.

Conclusion: Hindlimb unloading is a

significant factor in muscle atrophy with or without burn. Exercise increased soleus twitch and specific force in this model. However, there was a surprising decrease in muscle mass with exercise in all groups and a decrease in the fatigue index. These findings suggest that exercise contributes to a functional muscle change in a model of disuse and critical illness.

Soleus Weight and Isometric Contractile Function								
	No Exercise				Exercise			
	BA	BH	SA	SH	BA	BH	SA	SH
Muscle Weight (mg)	200 (10)	170 (40)	210 (20)	140 (40)	190 (10)	110 (10)	190 (10)	120 (4)
Twitch Force (g)	36 (4.4)	8 (2.0)	31 (2.8)	14 (2.1)	27 (2.0)	14 (2.1)	30 (2.6)	11 (0.6)
Tetanic Force (g)	165 (9)	42 (5)	159 (18)	56 (4)	118 (14)	54 (5)	150 (16)	66 (8)
Specific Force (N/cm ²)	25 (2)	7 (1)	25 (3)	12 (2)	20 (2)	14 (2)	23 (2)	17 (2)
Fatigue Index (%)	69 (6)	76 (3)	66 (6)	82 (11)	37 (11)	58 (13)	52 (11)	63 (6)
Data are expressed as mean (SEM)								
BA: Burn Ambulatory; BH: Burn Hindlimb; SA: Sham Ambulatory; SH: Sham Hindlimb								
Specific Force calculated from maximum tetanic force (N)/ physiological cross sectional area (cm ²)								
Fatigue Index: (minimum force at 4 minutes/maximum force) x 100								

Plantaris microRNA and Target Gene Profile After Exercise Training in an Animal Model of Hindlimb Unloading and Severe Burn

Saeman MR, Song J, Baer LA, DeSpain K, Wade C, Wolf SE

Muscle atrophy in severe burn is exacerbated with bed rest. Exercise is known to ameliorate disuse atrophy. MicroRNAs (miRNAs) are small non-coding RNAs that regulate post-transcriptional gene expression. The study aim was to investigate if exercise alters the muscle epigenetic profile in burn with bed rest using a clinically relevant animal model. Male Sprague-Dawley rats received 40% total body surface area (TBSA) scald burn and were placed in a hindlimb unloading traction system. Half (n=6) exercised twice daily by climbing 1 meter 5 times (EX) the others did not exercise (NX). On day 14, plantaris was harvested and stored in RNA later at -80°C. Samples from each group were pooled. Total RNA was extracted with Qiagen miRNeasy Mini kit. MicroRNA profiles were measured using Affymetrix miRNA 4.0 Array chips at our institutional microarray core facility. One chip, including 363,353 small non-coding RNA probes with varied species and controls, was used per sample. Chip reproducibility (intra and interlot) was greater than 0.95. Genomic profile was examined from RNA samples running with Affymetric Rat gene 2.0 ST arrays. Raw data was normalized with Robust Multi-array Average (RMA). Data was analyzed with Transcriptome Analysis Console (TAC 2.0). In each group 36,222 miRNAs were detected; 1,218 miRNAs were *rattus norvegicus*. 623 miRNAs were upregulated and 587 were down regulated in exercise. 31 probes increased over 2 fold and 21 probes decreased over 2 fold with exercise. Of these, 6 upregulated and 7 down regulated miRNAs corresponded with target gene profile changes (Table). All gene expression except *Rrm2* was down regulated. Type I collagen gene was associated with several miRNAs. Down regulation of mir-182, mir-92b-3p and up-regulation of mir 409a-3p together inhibits *Col1a2* expression; mir-138-5p inhibits *Col1a1* expression. Exercise in disuse atrophy after burn altered the miRNA profile with down regulation of target genes. Mechanisms of miRNA regulation are complicated. Redundant epigenetic pathways provide flexibility to adapt to injury. Targeting miRNA could be useful as a therapeutic approach.

Plantaris microRNA and Target Gene Profile After Exercise Training in an Animal Model of Bed Rest and Severe Burn

Saeman MR, Song J, Baer LA, DeSpain K, Wade C, Wolf SE

Muscle atrophy in severe burn is exacerbated with bed rest. Exercise is known to ameliorate disuse atrophy. MicroRNAs (miRNAs) are small non-coding RNAs that regulate post-transcriptional gene expression. The study aim was to investigate if exercise alters the muscle epigenetic profile in burn with bed rest using a clinically relevant animal model. Male Sprague-Dawley rats received 40% total body surface area (TBSA) scald burn and were placed in a hindlimb unloading traction system. Half (n=6) exercised twice daily by climbing 1 meter 5 times (EX) the others did not exercise (NX). On day 14, plantaris was harvested and stored in RNA later at -80°C. Samples from each group were pooled. Total RNA was extracted with Qiagen miRNeasy Mini kit. MicroRNA profiles were measured using Affymetrix miRNA 4.0 Array chips at our institutional microarray core facility. One chip, including 363,353 small non-coding RNA probes with varied species and controls, was used per sample. Chip reproducibility (intra and interlot) was greater than 0.95. Genomic profile was examined from RNA samples running with Affymetric Rat gene 2.0 ST arrays. Raw data was normalized with Robust Multi-array Average (RMA). Data was analyzed with Transcriptome Analysis Console (TAC 2.0). In each group 36,222 miRNAs were detected; 1,218 miRNAs were *rattus norvegicus*. 623 miRNAs were upregulated and 587 were down regulated in exercise. 31 probes increased over 2 fold and 21 probes decreased over 2 fold with exercise. Of these, 6 upregulated and 7 down regulated miRNAs corresponded with target gene profile changes (Table). All gene expression except *Rrm2* was down regulated. Type I collagen gene was associated with several miRNAs. Down regulation of mir-182, mir-92b-3p and up-regulation of mir 409a-3p together inhibits *Colla2* expression; mir-138-5p inhibits *Colla1* expression. Exercise in disuse atrophy after burn altered the miRNA profile with down regulation of target genes. Mechanisms of miRNA regulation are complicated. Redundant epigenetic pathways provide flexibility to adapt to injury. Targeting miRNA could be useful as a therapeutic approach.

Muscle microRNA Profile Alteration Following Severe Burn

Song J, Saeman MR, DeSpain K, Baer L, Wade C, Wolf SE

Introduction: Injury causes systemic epigenetic changes associated with clinical outcomes. MicroRNAs (miRNAs) are a class of small non-coding RNAs that function in RNA silencing and post-transcriptional regulation of gene expression. Muscle is significantly involved in the metabolic response after severe burn; however, the miRNA profile in this state is unknown. The aim of the study is to outline the microRNA profile in response to severe burn in an animal model.

Methods: Twelve male Sprague-Dawley rats were randomly assigned to sham and burn groups. Rats received 40% total body surface area (TBSA) scald burn or sham. On day 14, hindlimb skeletal muscles were harvested. plantaris tissue samples from three animals were pooled in each treatment group for total RNA extraction. The microRNA profile of each biological sample was measured using Affymetrix miRNA 4.0 Arrays chips at our institutional microarray core facility. Each chip contained a total of 36,353 small non-coding RNA probes, and the chip reproducibility is greater than 0.95. The raw data signal intensity **was normalized with Robust Multi-array Average (RMA)**. Data was analyzed with Transcriptome Analysis Console (TAC 2.0) software.

Results: A total of 36,222 miRNAs were detected in each grouped sample, of these 1,218 *rattus norvegicus* miRNAs probes were identified. The highest probe signal intensity (binary log ratio) was 16 for miRNA-206-3p in both groups. There were 74.5% transcripts in the sham group and 73.9% in the burn group, with a signal intensity less than 2. We identified 703 (57.7%) up-regulated miRNAs and 515 (42.3%) down-regulated miRNAs in the burn group compared to sham. Among the up-regulated profiles, 8 miRNAs were increased over 5 fold. All of the down-regulated miRNAs were within a -3 fold change (table1). MiR-182 was the most up-regulated miRNA following burn. It increased 12.81 linear fold (log ratio 6.14 in BA, 2.46 in SA). It inhibits *Colla2 gene* (for type I collagen) and promotes *NEU2 gene* (for Sialidase-2). MiR-409a-3p was the most down-regulated miRNA in response to burn (-2.95 fold change). Interestingly, it functions with miRNA-182 to inhibit muscle *Colla2 gene* expression after burn.

Conclusion: In summary, we describe the miRNA profile in muscle 14 days after burn. Up-regulation predominated in response to burn. The interaction network between epigenetics and genomic profile confirmed with biological response is under investigation.

Burn and Disuse with Resistance Exercise Effects on Fibroblast Growth Factor-21 and eNOS in Rats

Baer LA, Song J, Stanford KI, Wolf SE, Wade CE

Severe burn and disuse cause metabolic alterations associated with changes in fat metabolism, with exercise showing a similar effect. Using our rodent model of burn and disuse with resistance exercise, circulating FGF-21 and eNOS protein content were measured. Rats randomized into Sham Ambulatory (SA), Burn Ambulatory (BA), Sham/Hindlimb unloaded (SH) and Burn/Hindlimb unloaded (BH), with (EX) or without (NEX) daily exercise. BH rats were significantly smaller. Burn rat groups had the greatest reduction in subcutaneous adipose fat. FGF-21 was higher in EX-SA compared NEX-SA, but showed no differences within other groups. In comparison, eNOS showed an upregulation in burn rats compared to SA, showing a burn effect. It seems that the injury state may be overriding exercise and may be causing other shifts to occur. This increase may be associated with improved glucose metabolism and mitochondrial function, indicating a previously unrecognized role for resistance exercise and improved adipose tissue function. (US Army MRMC W81XWH-13-1-0489)

Effects of Resistance Exercise and Daily Insulin on Body Mass, Food Intake, Fat Mass and Total Hindlimb Muscle Mass in Rats Following Burn and Disuse

Baer LA, Song J, Wolf SE, Wade CE

Introduction: Treatment and recovery of patients with severe traumatic injuries is impacted by an increase in metabolism. Injury induces a systemic catabolic response with increased energy expenditure and loss of body mass. After burn injury, the ability to resume normal activities is compromised due to inactivity associated with bed rest as well as the catabolic response. Exercise and nutritional interventions have been used independently with limited success. The purpose of this study was to determine following burn and disuse how body mass, food intake and total hindlimb muscle mass are affected by a combination of daily resistance exercise and daily insulin.

Methods: Male, Sprague-Dawley rats were randomized into four groups: Burn/Hindlimb unloaded (BH) with daily resistance exercise (EX) or no exercise (NEX) and vehicle control (VEH) or insulin-treated (INS). Daily resistance exercise began ten days prior to injury by adding weight to the tail during repetitive ladder climbing. Rats were then weight-matched into treatment groups, either daily exercise or no-exercise, VEH or INS. Body mass, food intake was collected daily throughout the study. Fat mass and total hindlimb muscle (TA+EDL+Plantaris+Soleus+Medial and Lateral Gastroc) mass was measured on D14. Data are mean±SEM and an ANOVA was used with significance at $p<0.05$.

Results: No differences in body mass were observed between any groups at the time of injury or day 14. Exercise caused a significant increase in mean food over the last 5 days independent of daily insulin. Fat mass was not different between any of the groups. Exercise significantly increased total muscle mass irrespective of insulin. Total hindlimb muscle mass was further increased with the combination of daily insulin and exercise.

Conclusions: Exercise independently and with insulin elicited a significant increase in food. However, the increase in food intake did not result in differences between treatment groups in either body mass or fat mass, supporting a hypermetabolic effect. Muscle wasting was reduced with daily exercise. When daily exercise was combined with daily insulin, there was a greater attenuation of muscle wasting, suggesting the combination of exercise and insulin may be a contributing factor in reversing wasting as a result of burn injury. Different underlying factors seem to be influencing the acute metabolic changes offering possible opportunities for combinations of early interventions resulting in positive long-term outcomes.

Applicability of Research to Practice: The combination of exercise and pharmacological agents immediately following severe injury is anticipated to improve long-term outcome.

Exercise Treatment Reversed Micro RNA Profile in Burn Rats with Hindlimb Unloading

Cai R, Song J, Kumar PB, Sehat AJ, Saeman MR, Baer LA, Wade CE, Wolf SE

Introduction: Micro RNA (miRNA) is a class of non-coding RNA that regulates gene expression by silencing messenger RNA. Burn induces muscle breakdown that is made worse by bed rest, while exercise has been found to alleviate this muscle atrophy. We hypothesize that the alteration of miRNA and target gene profiles contributes to skeletal muscle mass loss after burn, and exercise reverses the muscle atrophy. The purpose of our study was to characterize the miRNA profile correlated to gene expression in an animal model for burn and disuse, as well as miRNA changes seen with exercise.

Methods: Forty-eight Sprague-Dawley rats were randomly assigned to sham ambulatory (SA), burn ambulatory (BA), sham hindlimb unloading (SH), and burn hindlimb unloading (BH) groups. Rats received 40% total body surface area scald burns or sham treatment, and they were placed in hindlimb unloading by tail harness, a model for bed rest, or ambulatory. Half of each group received twice daily resistance exercise for eight total groups (n=6 per group). After the 14-day treatment period, the plantaris muscles were harvested for miRNA and genomic data analysis.

Results: Our results show that compared to the SA group, BA and SH independently upregulate 3- to 4-fold more miRNAs and genes than they downregulate. miRNA-182, -187-3p, and -155-5p rank among the most upregulated. Comparing the combination of B and H (BH) to SA reveals that miRNA-182, miRNA-187-3p, and gene Nr4a3 receive additive contributions from B and H. With exercise, miRNA-182 increased 10.06-fold, and miRNA-138-1-3p decreased 2.14-fold. In comparison, exercise in the BH group strongly downregulated miRNA-182 7.04-fold and miR-138-1-3p 6.57-fold. In a similar fashion, exercise upregulated genes Chad and Cpxm2 in SA, then downregulated them in BH.

Conclusions: Burn and disuse additive contributions to miRNA and gene changes may explain the additional muscle atrophy burn patients experience with bed rest. Furthermore, exercise demonstrates a greater downregulation of miRNA and genes in BH compared to the SA group. Applicability of Research to Practice: Elucidating specific miRNAs' roles in muscle atrophy secondary to burn and bed rest opens the possibility of new markers and treatments targets.

Combined Effects of Oxandrolone and Exercise on Muscle Function Recovery in Rats with Severe Burn and Hindlimb Unloading

Song J, DeSpain K, Baer L, Wade CE, Wolf SE

Introduction: Muscle mass loss and function impairment worsens with restricted mobility in severe burn patients. We previously showed exercise training improved muscle function recovery in severely burned rats with hindlimb unloading. The aim of the study was to evaluate if the combination of daily oxandrolone with resistance exercise mitigates the loss of muscle function in this animal model.

Methods: Twenty Four Sprague-Dawley rats received a full thickness 40% total body surface area (TBSA) burn and were randomly assigned to vehicle (corn oil) without exercise (V/NEX), oxandrolone (0.1mg/kg/day) without exercise (O/NEX), vehicle with exercise (V/Ex), or oxandrolone with exercise (O/Ex) (n=6/group). All animals were placed in a tail traction system for hindlimb unloading to mimic bed rest after burn. The exercise groups completed resistance training twice a day. On day 14 *in situ* isometric forces of the left plantaris and soleus muscles were measured by using the ASI muscle lever system with dynamic muscle control and analysis software (Aurora Scientific, Inc). Fatigue measurement was only performed in the soleus. Statistical analysis was performed with Sigma Plot using Student's t-test or ANOVA where appropriate.

Results: Tetanic (Po) muscle function were significantly elevated in the plantaris with exercise (p=0.038), but not with oxandrolone treatment alone. Fatigue index (FI) was lower and integration was significantly elevated in the soleus after exercise (p<0.05) with or without oxandrolone treatment [Table1]. A generalized estimating equation linear regression model was applied to further analyze data of fatigue in the soleus. Results showed that average max force was achieved in the soleus either with oxandrolone treatment or resistance exercise independently. The max force for the O/Ex group was significantly higher than that for the V/NEX group (p=0.01).

Conclusion: Resistance exercise improves muscle function in burned rats with hindlimb unloading. Oxandrolone treatment increases strength in the soleus, but is not additive to the effects of exercise.

Support: DOD funding W81XWH-13-1-0462

Table 1

Plantaris	NEX		Ex		Soleus	NEX		Ex	
	V	O	V	O		V	O	V	O
Tissue weight (g)/100g BM	0.119±0.015	0.133±0.013	0.122±0.019	0.133±0.011	Tissue weight (g)/100g BM	0.028±0.010	0.032±0.006	0.034±0.003	0.037±0.006
Lo (mm)	22.2±1.8	22.2±2.5	22.3±1.1	22.3±1.2	Lo (mm)	21.8±2.4	22.0±3.0	21.4±3.4	20.8±0.8
1/2 RT (s)	0.0166±0.001	0.0169±0.001	0.0187±0.001	0.0165±0.001	Pt (g)	47.8±29.4	52.3±14.1	64.9±39.8	48.8±11.2
Pt (g)	98.0±13.4	115.8±27.1	112.4±22.5	105.9±11.5	Po (g)	113.5±69.9	126.0±49.9	106.3±18.6	124.1±17.8
Po (g)	426.7±137.6	469.1±47.2	489.7±58.1	555.4±45.4*	FI	26.4±11.8%	27.2±13.0%	15.6±7.7%	16.1±6.4%*
Po/ Pt	4.29±1.01	4.17±0.70	4.48±0.94	5.31±0.55	Fatigue(max)	79.9 ± 45.6	95.1 ± 36.4	100.2 ± 13.5	104.7 ± 11.3
sPt(N/cm2)	6.79±0.80	8.97±2.97	7.85±1.45	8.19±1.02	Integration	4837.4±2608.6	4830.8±2371.4	6614.2±1864.5	7985.4±727*
sPo(N/cm2)	29.69±10.06	35.21±7.44	34.73±6.98	38.25±11.78	sPt(N/cm2)	9.69 ± 5.55	10.81 ± 4.50	14.05 ± 8.33	9.52 ± 1.74

*, p<0.05, exercise vs. non exercise, two way ANOVA; presented as mean±SD	sPo(N/cm2)	22.67 ± 14.04	29.08 ± 13.79	23.41 ± 6.09	24.46 ± 4.14
---	------------	---------------	---------------	--------------	--------------

Combined Effects of Insulin and Exercise on Muscle Function in Severe Burn

Saeman MR, DeSpain K, Song J, Baer LA, Wade CE, Wolf SE

Introduction: Muscle loss is a known sequela of severe burn and critical illness that increases the risk of complications such as sepsis and prolonged recovery time. A prior study in a rat model of hindlimb unloading after burn supports that bedrest contributes significantly to muscle atrophy. The aim of our study was to evaluate if exercise combined with insulin in the immediate recovery period mitigates the loss of muscle function in this animal model.

Methods: Twenty Four Sprague-Dawley rats received a full thickness 40% total body surface area (TBSA) burn and were randomly assigned (n=6) to vehicle without exercise (V/No), insulin (pro zinc 40U daily) without exercise (I/No), vehicle with exercise (V/Ex), or insulin with exercise (I/Ex). All animals were placed in a tail traction system for hindlimb unloading to mimic bed rest immediately following burn. The exercise group was trained to perform twice daily weighted resistance climbing of 1 meter with 5 repetitions. On day 14 *in situ* isometric forces of the left soleus and plantaris muscles were measured. Fatigue measurement was performed in only the soleus. Statistical analysis was performed with Sigma Plot using Student's t-test or ANOVA where appropriate.

Results: There was no significant change in animal body mass between treatments. The physiological cross sectional area (PCSA) of the plantaris increased with combined insulin and exercise. The tetanic (Po) and twitch (Pt) muscle functions were significantly elevated in the plantaris of I/Ex. However, there was no change in the tetanic force when normalized to PCSA (Po/CSA). The soleus had significant elevation of Po, Pt, Po/CSA, fatigue maximum, and fatigue minimum in I/Ex. Please refer to the table for specific values and significance.

Conclusion: Insulin and resistance exercise have a positive combined effect on the hindlimb muscle function in this model of critical illness. The plantaris muscle demonstrated increased physiological cross sectional area with increased force suggesting a net increase in muscle fibers as the cause of this change. The soleus demonstrated a change in the specific force of the muscle and fatigue functions indicating a change in the composition of muscle fiber types.

Muscle Dimensions and Isometric Muscle Function

Parameter	Plantaris		Soleus	
	No Exercise	Exercise	No Exercise	Exercise
	Vehicle Insulin	Vehicle Insulin	Vehicle Insulin	Vehicle Insulin
Muscle Wet weight (mg)	332 ± 18 329 ± 9	348 ± 6.3 354 ± 14	119 ± 2 143 ± 23	151 ± 32 131 ± 7
Lo (mm)	35 ± 2 31 ± 0.3	32 ± 1 32 ± 1	33 ± 1.4 29 ± 0.4	31 ± 0.9 30 ± 0.4
PCSA (mm ²)	27 ± 3 30 ± 2	30 ± 2 #31 ± 2	5.0 ± 0.2 6.9 ± 2.3	6.7 ± 1.3 6.0 ± 0.3
Twitch Force Pt (g)	89 ± 9 85 ± 3	92 ± 2 †102 ± 8	10 ± 2 10 ± 2	14 ± 2 *18 ± 1
Tetanic Force Po (g)	430 ± 31 459 ± 12	508 ± 14 †522 ± 17	38 ± 8 38 ± 9	59 ± 5 *69 ± 5
Po/CSA (N/cm ²)	16 ± 2 15 ± 2	16 ± 1 17 ± 1	7.4 ± 2 7.0 ± 1	10 ± 2 †12 ± 1
Pt/Po (%)	21 ± 1 19 ± 1	18 ± 0.4 20 ± 1	26 ± 1 24 ± 2	24 ± 2 26 ± 2
Fatigue Maximum (g)	— —	— —	33 ± 6 34 ± 9	53 ± 4 *64 ± 4
Minimum (g)	— —	— —	27 ± 6 27 ± 6	†46 ± 4 *54 ± 4
Index (%)	— —	— —	81 ± 7 84 ± 5	87 ± 5 84 ± 5

Lo = optimal muscle length * vs. No Exercise (ANOVA, p<0.05)

PCSA = Physiological Cross Sectional Area † vs. Vehicle No Exercise (ANOVA, p<0.05)

Po/CSA = Tetanic force normalized to PCSA # vs. Vehicle No Exercise (one-tailed t-test p<0.05)

Pt/Po (%) = Ratio of twitch to tetanic force ‡ vs. Other groups combined (two-tailed t-test, p=0.05) Fatigue Index = Ratio of fatigue minimum to maximum

Resistance Exercise Effects on Body Mass, Free Fatty Acid Concentration and Fatty Acid Metabolism in sqWAT Following Burn and Disuse in Rats

Baer LA, Stanford KI, Song J, Wolf SE, Wade CE

Introduction: Severe burn induces a catabolic response with increased energy expenditure and loss of body and white adipose tissue (WAT) mass. Burn induces WAT lipolysis, increasing intracellular free fatty acid (FFA) turnover, but despite increased lipolysis, circulating FFA can either increase or decrease. The ability to resume normal activities after burn injury is compromised due to the catabolic response and inactivity associated with bed rest. Exercise, improves insulin sensitivity and decreases circulating FFA, likely due to adaptations in adipose tissue. We investigated how resistance exercise in a combined rodent model of burn and disuse affects circulating FFA, WAT mass and expression of genes involved in fatty acid transport and metabolism.

Methods: Male SD rats randomized into 8 groups: Sham/Amb (SA), Burn/Amb (BA), Sham Unloaded (SH), Burn Unloaded (BH) with (EX) or without (NEX) exercise. Daily resistance exercise by repetitive ladder climbing. Body mass was collected daily throughout the study. Blood was collected and subcutaneous white adipose tissue (sqWAT) was collected on D14. Circulating FFAs were measured in plasma. Enzymatic pathways of fatty acid metabolism were measured in 84 key genes.

Results: Significant decrease in body mass in SAEX and BAEX vs. SANEX and BANEX. Exercise significantly reduced circulating FFA and sqWAT in SA, BA, and BH. SHNEX & BHNEX had a decrease in expression of sqWAT genes involved in fatty acid metabolism compared to SANEX & BANEX. Exercise increased expression of sqWAT genes in fatty acid metabolism (SAEX, BAEX vs. SANEX, BANEX). Exercise restored genes involved fatty acid metabolism to that of SANEX. Overall, hindlimb unloading decreased genes involved in sqWAT fatty acid metabolism, while the expression was increased with burn injury. In all cases, resistance exercise restored expression of genes involved in fatty acid metabolism to that of the SANEX.

Conclusions: Burn injury with disuse is affected by exercise. Exercise reduced body mass in ambulatory groups, but maintained body mass when combined with unloading. Reductions in circulating FFAs is an indication of possible intracellular breakdown. Alterations in fatty acid metabolism gene expression are often associated with metabolic syndrome, resultants of burn injury and disuse. Fatty acid metabolism in sqWAT is decreased by both burn and unloading, independently and in combination, however, with the incorporation of daily resistance exercise, it appears to be restored. Gene pathway data may help to shed some light on molecular changes that may be occurring and these data suggest the incorporation of a daily exercise program may be an effective treatment resulting in positive long-term outcomes.

Grant Information: US Army MPMC CDMRP W81XWH-13-1-0489.

	SA	BA	SH	BH
D14 Body Mass (g) (n=6/group)				
NEX	334±7	306±4	298±6	273±3 [‡]
EX	315±6	265±5	289±7	270±4 [‡]
Free Fatty Acid (nmol/L) (n=6/group)				
NEX	2.45±0.17	1.74±0.16	1.89±0.23	1.62±0.09 [‡]

EX	1.89±0.14 [‡]	1.59±0.20	2.06±0.38	1.39±0.09 [‡]
sqWAT Fat Mass (n=6/grp)				
NEX	1.97±0.18	1.47±0.16	1.32±0.17	1.18±0.07 [‡]
EX	1.59±0.14	1.08±0.11	1.31±0.12	1.02±0.11 [‡]

Mean ± SEM; [‡] p<0.05 from SANE

Moderate Resistance Exercise Improves the Metabolic Profile of Adipose Tissue in a Model of Disuse

Baer LA, Harris J, Sindeldecker D, Song J, Wolf S, Stanford KI, Wade CE

Treatment of trauma and several other maladies requires patient immobilization and restriction of physical activity, which can result in impaired metabolic health. In contrast to physical immobilization, physical activity and exercise improves metabolic health. Using a rodent model of disuse (hindlimb unloading) combined with resistance exercise, we determined if moderate resistance exercise could negate the effects of disuse on the metabolic profile of white adipose tissue (WAT). Male rats were assigned to four groups 1) Ambulatory No Exercise (ANE); 2) Ambulatory Exercise (AE); 3) Hindlimb Unloaded No Exercise (HUNE); 4) Hindlimb Unloaded Exercise (HUE). All rats completed a 10-day pre-training resistance exercise regiment prior to random group assignments. HUNE and HUE animals were placed in a tail traction system with their hindlimbs unloaded and were followed for 14 days. Animals designated to AE or HUE groups exercised for 14 days. At day 14, plasma and tissue samples were collected and analyzed. Resistance exercise resulted in a decrease in body mass in the ambulatory animals (AE vs. ANE), and hindlimb unloading significantly decreased body mass compared to ambulatory animals (HUNE and HUE vs. ANE and AE), but there was no additive effect of exercise on body mass (HUNE vs. HUE). Hindlimb unloading reduced hindlimb muscle mass (ANE and AE vs. HUNE and HUE), and resistance exercise partially restored soleus mass in the hindlimb unloaded animals (HUNE vs. HUE). Total white adipose tissue mass (WAT), perigonadal WAT (pgWAT) mass, and subcutaneous WAT (scWAT) mass and adipocyte size were significantly reduced in response to both exercise and hindlimb unloading. Expression of genes and proteins in scWAT involved in fatty acid oxidation and glucose metabolism were significantly increased with exercise (ANE vs. AE), reduced with hindlimb unloading (ANE vs. HUNE), and restored with exercise in the hindlimb unloaded animals (HUNE vs. HUE). In conclusion, these data indicate that moderate resistance exercise improves the metabolic profile of both pgWAT and scWAT in both the ambulatory state and in an animal model of disuse, providing a novel therapeutic benefit for the bed rest patients.

Support or Funding Information

US Army MRMC CDMRP W81XWH-13-1-0489

Transcriptomic Profile Alterations in Burn/Hindlimb Unloaded Rats with Insulin and Exercise Combination Treatment

Song J, Baer LA, Saeman MR, Wade CE, Wolf SE

We previously demonstrated changes in miRNA related gene profiles in burn and hindlimb unloaded (B/H) rats. We also found that exercise training reversed those gene profiles which was principally related to diminished oxidative stress and inflammatory signaling. Insulin treatment has also shown positive effects in burns; we recently observed that insulin additively improved muscle function when combined with exercise treatment in burn and hindlimb unloaded rats. We wondered whether transcriptome profiles reflect skeletal muscle pathophysiological changes in this event. Twenty-four Sprague-Dawley rats received a full thickness 40% total body surface area (TBSA) burn and placed in a tail traction system for hindlimb unloading to mimic bed rest immediately following burn. Half were trained to perform twice daily weighted resistance climbing of 1 meter with 5 repetitions, while the other half was not. Six rats the exercise and no exercise groups received insulin injection subcutaneously (5 U/kg daily). On day 14 plantaris muscles were harvested and tissues were grouped for RNA extraction and genomic data analysis applied with Affymetrix Analysis Console 3.0 software. With threshold for absolute fold change greater than 2, we found 59, 48 and 93 miRNAs altered in rat muscle with insulin, exercise, and combination treatment respectively; miR-499-5p was the most increased with 15 fold in the combination group. For gene expression, we found 122, 119 and 170 changes in insulin, exercise and combination treatment respectively. Act1, Sln, Tecr1 were the most upregulated, and Mbp, Pmp2, Mpz were the most down-regulated genes with exercise and insulin treatment. Wikipathway analysis showed that striated muscle contraction pathways were improved with both exercise and insulin treatment, and directly correlated with the muscle function improvement. Meanwhile, TGF beta and TLR signaling pathways were inhibited with both treatments. In conclusion, exercise and insulin contribute additively to miRNA and gene expression changes after burn and immobilization, and reflect physiologic muscular improvement. The finding of the study identifies the specific pathway signals affected by insulin and exercise.

Effects of the Combination of Daily Insulin Plus Resistance Exercise During the Unloading and Reloading Phases Following Burn and Disuse in Rats on Body Mass, Food Intake and Fat Mass

Baer LA, Nutall K, Burchfield J, Vincent S, Stanford KI, Song J, Wolf SE, Wade CE

Introduction: Treatment and recovery of patients with severe traumatic injuries is impacted by an increase in metabolism. After burn injury, the ability to resume normal activities is compromised due to inactivity associated with bed rest as well as the catabolic response. Following discharge, a major goal is the ability to execute a long-term recovery plan. Previously we found daily exercise combined with SQ insulin improved body mass loss during the unloading period. The purpose of this study was to determine immediately following burn and disuse injury how a combination of daily resistance exercise and daily insulin injections during the unloading phase followed by daily resistance exercise during the reloading phase affects body and fat mass and food intake.

Methods: Male, Sprague-Dawley rats were used. Injury was induced by a 40% TBSA burn injury and hindlimb unloaded immediately following injury. Rats were weight-matched into either saline vehicle (VEH; N=12) or insulin (INS; 5U/kg; N=12) for 14 days with daily resistance exercise. Daily resistance exercise was completed prior and following injury by adding weight to the tail during repetitive ladder climbing (5 climbs, 2X/days). Following removal from unloading at 14 days, rats were re-distributed within the original VEH or INS to exercise (EX; N=6) or no exercise (NEX; N=6) for 14 days. Body mass and food intake was collected daily throughout the study. Fat mass was collected at the end of the study.

Results: No differences in body mass were observed between any groups at the time of injury or day 14. Daily insulin showed a decrease in mean food intake over the last 5 days of the unloading phase with no differences in body mass. During the reloading phase, a steady increase in body mass was shown in all groups, however, INS, irrespective of exercise had a greater body mass increase. In addition, mean food intake was significantly increased in the INS + EX group during the reloading phase. Fat mass was not different between any of the groups.

Conclusions: During the unloading phase, daily exercise with insulin elicited a decrease in food intake, however, the decrease in food intake did not result in differences between treatment groups in either body mass or fat mass, possibly showing additional mechanisms are causing overall metabolic changes. Possible metabolic changes during the reloading phase, indicate improvements may be occurring following removal from disuse. Different underlying factors seem to be influencing the acute metabolic changes offering possible opportunities for combinations of early interventions resulting in positive long-term outcomes.

Applicability of Research to Practice: An exercise program may improve metabolic health following discharge.

Insulin and Exercise Combination Therapy Recovers Muscle Function in a Burn and Disuse Rat Model by Activating Protein Synthesis and Inhibiting Proteolysis

Geng C, Karbhari N, Song J, Baer L, Wolf SE, Wade C

Introduction Burn injuries bring about a hypermetabolic state that results in a loss of muscle mass and function. Like burns, disuse of muscle also results in muscle loss. Resistance exercise and insulin have individually been shown to attenuate burn and disuse induced muscle atrophy, though neither is fully compensatory. To date, there is no data on the efficacy of insulin and exercise as a combination therapy to recover muscle mass and function. This project investigates the molecular mechanisms behind musculoskeletal pathophysiological improvements in a burn and disuse rat model given these treatments. Muscle function, protein synthesis/proteolysis pathway protein levels, and genomic profiles are examined.

Methods. 24 Sprague-Dawley rats received full thickness 40% total body surface area burns and hindlimb unloading and were randomly grouped into vehicle without exercise (V/N), pro zinc 5U/kg of insulin without exercise (I/N), vehicle with exercise (V/E), and insulin with exercise (I/E) groups. 14 days after injury, hindlimb muscle function was measured and muscle tissues were harvested for genomic profile and western blot analysis.

Results. The isometric force including tetanic (Po) and twitch (Pt) were significantly elevated in the plantaris of I/E rats. The soleus also had significant elevation of Po, Pt, fatigue maximum, and fatigue minimum in I/E rats. Affymetrix transcriptome analysis determined that 70, 62, and 116 genes were upregulated more than 2 fold in insulin, exercise, and combination treatment, respectively. Western blots showed that pPDK 1, which activates AKT activity, was significantly increased in all treatment groups compared to control. . p-AKT S473 was significantly increased in the combination group eEF2 controls the elongation step in translation and was increased in the exercise and combination. Muscle RING-finger protein-1(MuRF-1), an E3 ubiquitin ligase, was reduced in the combination group.

Conclusions Insulin and resistance exercise have a positive combined effect on muscle function recovery. Signal pathway examination showed that the combination treatment decreased protein degradation and increased protein synthesis. The observed changes at the transcriptional and protein levels are supported by muscle function improvements.

Applicability of Research. to Practice Muscle loss is a sequela of burn and disuse that increases cost and risk of complications. By identifying the molecular basis of these changes, treatments that target critical proteins can be developed to mitigate muscle loss and improve patient outcomes.

A Long-Term of Resistant Exercise Decreased Rat Muscle Function in Fast Twitch Myofiber Dominated Plantaris

Song J, DeSpain K, Baer L, Burchfield J, Nutall K, Vincent S, Wade C, Wolf SE

Introduction: We previously showed muscle function was impaired with hindlimb unloading in burned rats which was alleviated by insulin treatment and resistance exercise. In the current study, we investigated the role of continued resistance exercise to further improve function in a model designed to mimic the late recovery period akin to the rehabilitation phase in patients.

Methods: Twenty-four Sprague-Dawley rats received a full thickness 40% total body surface area (TBSA) burn and hindlimb unloading (HLU) to mimic severe burn with muscle disuse. All animals underwent exercise training twice a day with 5 climbs per training session. Resistance exercise was achieved by adding weight to the base of the tail and increased every 3 days. All rats were given a subcutaneous injection of either saline or pro zinc insulin 5U/kg daily. On day 14, all rats were removed from HLU and all injections stopped. Then, rats within each treatment group were separated into no exercise (NEX) and exercise (EX) groups (n=6 per group) for an additional 14 days. On day 28, in situ isometric forces of the left soleus and plantaris muscles were measured. Values are presented as mean \pm SD. Statistical analysis was by two-way ANOVA.

Results: Plantaris isometric twitch tension force (Pt) and muscle optimal length (Lo) significantly decreased with exercise treatment for 28 days (149.40 \pm 16.95g NEX vs Pt: 131.99 \pm 17.84g EX) (p=0.028); (39.42 \pm 1.77mm NEX vs Lo: 37.08 \pm 1.99mm EX) (p=0.008). However, soleus tetanic force (Po) increased significantly in those treated with insulin previously with or without continued exercise (183.01 \pm 33.33g vehicle vs 220.61 \pm 26.01g insulin) (p=0.01). Further, the ratio of single twitch force to maximal tetanic force (Pt/Po) significantly decreased in the soleus with exercise treatment (0.32 \pm 0.08 NEX vs. 0.26 \pm 0.02 EX) (p=0.037).

Conclusions: In our previous study, we found the combination of insulin treatment and exercise after burn and hindlimb unloading improved muscle function in both plantaris and soleus. In the current study, the effect of previous insulin treatment further augments improvements at 28 days after injury in slow twitch muscle. However, continued resistance exercise actually decreased muscle isometric force in the fast twitch myofiber dominated plantaris with no change in the slow-twitch soleus. The decrease in Pt/Po ratio in slow-twitch myofiber dominated soleus suggests a myofiber type change in response to continued resistance exercise.

Applicability of Research to Practice: The current study provides evidence of appropriate type of exercise in burn patient rehabilitation.

Molecular and Structural Changes in Intervertebral Discs Following Severe Burn in Rats

Hernandez P, Fa A, Mitchell T, Buller D, Huebinger R, Van Hal M, Wolf SE, Song J

Introduction: Intervertebral discs (IVD) connect to the spinal vertebrae. IVD impairment and dysgenesis are clinically relevant to pain management and movement restriction. Severe burn disrupts skeletomuscular metabolic status. IVD response following severe burn is currently unknown. Transient receptor potential cation channel subfamily V member 4 (TRVP4) protein is a Ca^{2+} -permeable, nonselective cation channel which has been recently reported to be elevated in human disc degeneration. The aim of this study is to investigate the role of TRVP4 in rat IVDs following thermal injury.

Methods: Under a UTSW IACUC approved protocol, 40 adult male Sprague-Dawley rats were examined in this study. Animals received 40% of total body surface area (TBSA) scald burn with the standard procedure under anesthesia and randomly grouped: Control (n = 11), 1 day (n = 6), 3 days (n = 6), 7 days (n = 6), and 14 days (n = 11) post burn. Total RNA was extracted from whole IVDs and analyzed for expression of IL-6, TNF, IL-1 β , MMP9, MMP13 and TRPV4 by qPCR. Lumbar IVD was also fixed for histological analysis. Data are presented as mean \pm standard deviation. Data were analyzed in GraphPad Prism 7 with one-way ANOVA and Fisher's LSD post hoc test, or by unpaired Student's t test when comparing two variables, ($p < 0.05$ being significant).

Results: Gene expressions of IL-6, TNF and IL-1 β were not altered in rat IVD after burn. ILMMP9 and MMP13 gene expression showed a significant upregulation in thoracic IVD at day 1 after burn. Histological analysis of lumbar IVD showed an increase in nucleus pulposus (NP) height in discs at days 1 and 3 after burn compared to control discs, indicating tissue swelling following thermal injury. The gene expression of the calcium-permeant channel TRPV4, activated by osmotic changes, showed a significant upregulation in both thoracic and lumbar IVD at day 3 after burn.

Summary: Local response of IVD was observed with the increased height of NP and the increased gene expression of MMP9 and MMP13. The elevation of TRPV4 gene expression after burn indicates local mechanical/osmotic changes in IVDs. Future investigations will focus on the acute structural changes and if these alterations lead to late degeneration of the IVDs in the current animal model.

Clinical relevant: Patients start experiencing back pain and disc degeneration long after trauma occurs, it is crucial to understand the early events occurring at the cellular level in IVD triggered by trauma.

Acknowledgements: Funded by Hofmann funds for Resident research from the Department of Orthopaedic Surgery. TM and DB were funded by UT Southwestern Summer Research program. Baxter Surgery Department Funding. DOD- W81XWH13-1-0462

Vascular Smooth Muscle Dysfunction After Burn

DeSpain K, Song J, Rosenfeld CR, Wolf S

Introduction: Hypotension is a major complication after large surface area burns. Increased systemic vascular permeability causes hypovolemic shock in server burn patients. Historically the volumetric loss of fluid through leaking capillaries has been treated by replacement with fluids. However important, this is not the sole answer and often times the patient remains hypotensive. We proposed to determine if this hypotensive condition was solely due to fluid loss during the leaky vessel condition seen after burn, or if there were other contributing factors. The purpose of study is to investigate the physiological profile of vascular smooth muscle in response to severe burn.

Methods: Adults Sprague-Dawley male rats were enrolled in the study. 34 rats received a 40% total body surface area (TBSA) scald burn and fluid resuscitation using the Parkland formula ($V = 4\text{mL} \times \text{TBSA} \% \times \text{kg}$). At time points of 6 hrs, 24 hrs, 3 days, 7 days and 14 days post burn, animals were euthanized and endothelial intact carotid arteries were dissected for ex vivo test in organ baths containing 37°C PBS. The force measurement of artery ring were collected under the Optimal length (L_0) as the vessels were exposed to the vasoconstrictors Norepinephrine (NE) and Angiotensin II (AngII), and vasodilator Acetylcholine (ACh) consequently. Force was measured in grams and converted to Stress (N/m^2) taking into account L_0 and the weight of the vessel (grams).

Results: A cumulative dose response was used for NE ($10^{-8}\text{M} - 10^{-5}\text{M}$) and on average at each dose there was a 50% decrease in stress generated by the vascular smooth muscle (VSM) at 6hrs ($P=0.012$). We saw a very similar response to a single dose of AngII (10^{-7}M) in that there was a 70% decrease in stress generated at 6hrs ($P<0.001$). The arteries were precontracted with NE 10^{-5}M , allowed to reach a steady state and then were exposed to a cumulative dose response of ACh ($10^{-7}\text{M} - 10^{-4}\text{M}$). The 3 day, 7 day and 14 day arteries relaxed (specify for the force change) significantly more than the 6hr post burn arteries ($P=0.001$).

Conclusion: In this study we have shown that at 6 hrs after burn there is a significant decrease in responsiveness to both Norepinephrine, which works through adrenergic receptor, and Angiotensin II, which works through the angiotensin type II receptor. At 24 hrs after burn, these responses have returned to control levels. Acetylcholine binds to a receptor on the cell membrane of the vascular smooth muscle endothelial cell. This causes the endothelial cell to generate nitric oxide (NO) through the activation of the nitric oxide synthase (NOS) pathway. The newly created NO diffuses into the VSM and initiates dilation. We administered ACh into the baths to determine if this NOS pathway also may contribute to a hypotensive state after burn. This could explain why one may see persistent hypotension days after burn possibly through an increase in NOS activity.

Applicability of Research to Practice: We believe that this study will help physicians understand the mechanism related to the hypotensive phenomena seen in patients after burn and how to treat that patient through the administration of pressors to attain a normotensive status.

5. Quad Chart

Combination Therapies for the Mitigation of Musculoskeletal Pathologic Damage in a Novel Model of Severe Injury and Disuse

OR120033/OR120033P1 Award Number W81XWH-13-1-0489/W81XWH-13-1-0462

PI: Charles Wade, PhD and Juquan Song, MD Org: UTHealth, Houston, UTSouthwestern, Dallas/UTMB, Galveston Award Amount: \$1,081,066

Study/Product Aim(s)

- Aim 1: Characterize the effect of resistance exercise on muscle and bone health in a validated model of burn and disuse.
- Aim 2: Evaluate the effect of resistance exercise in combination with currently used pharmacological therapies (insulin or oxandrolone) on muscle and bone health in a validated model of burn and disuse.
- Aim 3: Determine the interrelationship between muscle and bone after re-ambulation following pharmacological interventions and exercise.

Approach

A 40% TBSA severe burn will be induced followed by disuse for 14 days. Rats will be assigned to vehicle or drug treatment and further into exercise or no exercise groups. We will examine effects of re-ambulation with or without further resistance exercise after the 14 days. Blood and select organs, muscles and bones will be removed and weighed for testing of mechanical properties, typing, bone morphology, mineral content, and microarchitecture measurements.

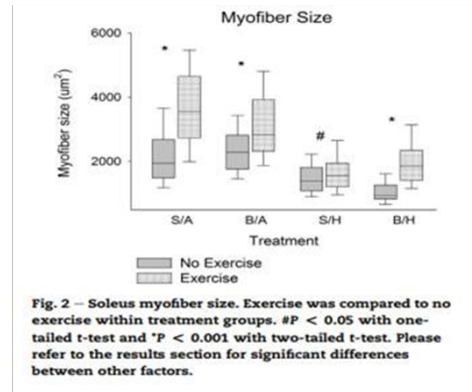


Fig. 2 – Soleus myofiber size. Exercise was compared to no exercise within treatment groups. *P < 0.05 with one-tailed t-test and *P < 0.001 with two-tailed t-test. Please refer to the results section for significant differences between other factors.

Timeline and Cost*

Activities CY	14	15	16/17	18/19
Aim 1 – Burn/Disuse + Exercise	█			
Aim 2 – Burn/Disuse + Exercise + Pharmacological Therapy		█		
Aim 3 – Burn/Disuse + Exercise + Pharmacological Therapy + Exercise				█
Estimated Budget (\$K)	\$399	\$348	\$278	\$56

* Combined Institutional Budgets

Goals/Milestones for Current Award Year

CY14 Goals

- ✓ Obtain all animal approvals and order supplies
- ✓ Aim 1 animal experiments and sample collections
- ✓ Complete muscle function testing, uCTs and bone testing
- ✓ Complete ELISAs

CY15/16 Goal

- ✓ Aim 2 animal experiments and sample collections
- ✓ Complete muscle function testing, ELISAs, uCTs and bone testing

CY17/18 Goal

- ✓ Aim 3 animal experiments and sample collections
- *Complete muscle function testing, ELISAs, uCTs and bone testing (*In Process*)
- *Complete data analysis (*In Process*)
- *Submission of final results manuscript (*In Process*)

Comments/Challenges/Issues/Concerns

- ✓ Requested and received no-cost extension for FY17/18 to complete AIM3

Budget Expenditure to Date

- \$ 664,759.34 Final Expenditures for UTHealth
- *UTMB has outstanding expenditures

*Outstanding UTMB Goals/Budget

Updated: 9 Jan 2019